Order Number 8821060

Laser Raman scattering by sensitizing dyes adsorbed on substrates

Akpabli, Cornelius Kwami, Ph.D.

City University of New York, 1988

U·M·I
300 N. Zeeb Rd.
Ann Arbor, MI 48106

LASER RAMAN SCATTERING BY SENSITIZING DYES ADSORBED ON SUBSTRATES

by

CORNELIUS KWAMI AKPABLI

A dissertation submitted to the Graduate Faculty in Chemistry in partial fulfillment of the requirements for the degree of Doctor of Philosophy, The City University of New York.

1988

This manuscript has been read accepted for the Graduate Faculty in Chemistry in satisfaction of the dissertation requirement for the degree of Doctor of Philosophy.

April 21, 1988
Date

Daniel L. Akins
Chair of Examining Committee

4/21/88
Date

Executive Officer

Daniel L. Akins

Supervisory Committee

The City University of New York

ABSTRACT

LASER RAMAN SCATTERING BY SENSITIZING DYES ADSORBED ON SUBSTRATES

by

Cornelius Kwami Akpabli

Adviser: Professor Daniel L. Akins

A Raman scattering enhancement theory based on the formation of molecular vibro-excitonic levels, developed to account for aggregating dyes, is described. Enhanced Raman scattering of 1,1'-diethyl-2,2'-cyanine and five other cyanine dyes adsorbed on some substrate electrodes have been studied. The excitation wavelength dependence of the Raman scattering; the surface potential, the supporting electrolyte, the electrode pretreatment and the pH effects on the Raman scattering intensity and the intrinsic enhancement dependence on the number of molecules in the aggregate are experimentally investigated. The theoretical model presents a unified picture of the enhancement effect and is found to be consistent with the experimental findings. Electrode pretreatment is found not to be a prerequisite for these dyes to give enhanced Raman scattering, but KI as the supporting electrolyte and silver as the substrate are found to give optimum spectra; surface potential and pH also affect the relative Raman intensities. All these findings are supported by uv/vis spectroscopy. The relative enhancement of Raman bands of these dyes adsorbed on silver electrodes

for which the surface potential is varied suggests that a resonance can be tuned by variation of surface potential. The relative intensities of Raman bands obtained indicate that the adsorption-desorption kinetics are affected by the surface potential and pH of the solution. A resonance effect on the Raman scattering intensity is also found when the exciting laser radiation's frequency approaches the aggregate absorption band of the adsorbed dye. When incident excitation is close to resonance with the J-aggregate absorption, Raman bands which are due to Franck-Condon overlap between intramolecular modes of the molecules in the aggregate and intermolecular lattice modes of the aggregate, and which are attributable to the A-term of Albrecht's polarizability expression, appear in addition to the bands attributed to the B-term present in the nonresonant case. Bands assigned to the A-term have been used as internal Raman standards to normalize the surface concentration, thereby isolating the electric potential dependence of Raman bands assigned to the B-term. Stark-effect shifting of the J-aggregate band has been used to explain the voltage dependence of concentration normalized Raman band intensities for 2,2'-cyanine and 4,4'-cyanine.

DEDICATION

Dedicated to loving memories of my father and mother, who both were there to bid me farewell when I left home to pursue my studies for the doctorate, but would not be there to welcome me home. My father, Fofo Akpabli Bese Honu, passed away as a true son of Ahliha-masi-dzo nine months after I left home; my devoted mother, Nanye Alorwuso Hodor, who made such great sacrifices, also departed for the eternal life when I had a few months more to complete the dissertation. If I deserve any honor, with them I share that honor.

ACKNOWLEDGEMENTS

Gratitude is expressed to my adviser, Professor D. L. Akins, for all the help and encouragement he has given me. I am very grateful to him for all the resources and discussions he has provided in solving and understanding many research issues. I thank Mrs. Barbara Alexander for the part she played in the typing of the dissertation.

My gratitude is also expressed to the Fulbright Commission and the Institute of International Education for their sponsorship through all the years I spent in pursuit of the Ph.D. degree at the City University of New York. I am also grateful to the Association of African Universities and the African Exchange Program of the City College of New York, for their help and the interest they have shown. In addition, I am very grateful to the University of Ghana, Legon, Ghana, who had to extend my leave on two occasions.

Finally, but not least, the kindness and patience of my family back in Ghana, who had to do without me these turbulent five years, deserve high commendation. I am very grateful to them for their deep understanding to bear the pains of my long absence. God's grace, care, and guidance are things taken for granted and they abound through his loving kindness, and without him nothing could be initiated and be accomplished. To God, therefore, all thanks and gratitude are due.

TABLE OF CONTENTS

PAGE

LIST OF TABLE

TABLE PAGE

LIST OF FIGURES

FIGURES CONTINUED PAGE

FIGURES CONTINUED PAGE

FIGURES CONTINUED PAGE

FIGURES CONTINUED PAGE

CHAPTER 1

INTRODUCTION

1.1 GENERAL CONSIDERATIONS

Until recently, Raman scattering has been primarily a valuable, supplemental laboratory technique in studies of the structure of individual molecules and the nature of coupling interactions between molecules and atoms (e.g., in the solid state). However, the advent of laser sources, better optical instruments and detection techniques have revolutionized Raman scattering research, enabling Raman scattering techniques to become a basic spectroscopic research method, leading to dramatic qualitative and quantitative capabilities in many scientific and technological fields.

In particular, the application of Raman scattering techniques (both spontaneous and nonlinear) to interfacial probing is of substantial current interest. Also, interest has been shown in applying Raman scattering to a variety of other areas such as fluid mechanics, combustion technology, industrial process control, chemical laser diagnostics, and atmospheric pollution monitoring.

Application of Raman scattering to interfacial phenomena is a natural application of the technique and has many diagnostic applications which are currently attracting large amounts of research effort. The research reported here was aimed at applying Raman scattering to the study of molecular

surface structure and the dynamics of aggregated dyes adsorbed on solid surfaces, and to explore the theoretical implications and explanations of our experimental findings.

The application of Raman scattering as a probe technique for interfacial studies (especially solid/liquid interfacial studies) has become necessary because of the limitations of the more conventional probes, for example, infrared absorption is handicaped in its applications because of sampling difficulties and because most of the systems involve aqueous solutions which lead to significant background absorption. Several other techniques, such as ultraviolet photoemission spectroscopy (UPS), low energy electron diffraction (LEED), and electron energy loss spectroscopy (EELS) have been applied in the investigation of solid/gas interfaces (1). A great wealth of insight has been derived from such techniques despite the low information content of several of the measurements as well as weak signals (usually) due to insufficient surface concentration of the important species. With increasing sophistication and advances in instrumental technology, other techniques such as Fourier Transform IR (FTIR) and electrochemically modulated infrared spectroscopy (EMIRS) (2) have become useful in providing insight into surface mechanisms (of reactions) and structures in solid/liquid systems.

With regards to specificity, the spectral shift of Raman-scattered light is equal to a vibrational or rotational frequency of the observed molecule. Since these frequencies are different for different molecules and change with their level of molecular excitation, it is possible to identify each line in a Raman spectrum with a particular type of molecule and its level of

excitation. In Raman scattering each molecule has at least one allowed Raman band, in contrast to infrared absorption, which is not sensitive to molecules without a permanent dipole moment.

Infrared absorption technique is applicable to almost any kind of sample but some materials like intractable polymers, single crystals, and aqueous solutions are quite difficult to handle. With Raman spectroscopy sample preparation is remarkably simple and the capability for using glass or quartz cells is a marked advantage. Its principal limitation is with highly colored or fluorescing materials.

The intrinsic weakness of the Raman effect is that Raman line intensities are about 10^{-6} the intensity of the exciting line, and the scattering cross sections are typically three orders of magnitude smaller that of Rayleigh scattering cross sections and roughly ten to sixteen orders of magnitude smaller than cross sections for unquenched fluorescence. This necessitates the use of dilute solutions and the use of an intense monochomatic light source (e.g. a laser source).

The rapid expansion of the field of Raman scattering research and applications was marked by the observation of enhanced signals from Raman scattering of molecules on noble metal surfaces. The technique was seen right from the very beginning to have the advantage of acquiring more detailed molecular vibrational information for processes occurring at general interfaces, and to give a better resolution of surface structure and environment. This can be appreciated by noting that several reviews have been published recently, for example, that of Birke et al. (3). The use of a temporally instaneous phenomenon, like Raman scattering, to study the

structure of surfaces, dynamics of surface changes, and the kinetics of surface reactions promises to improve the current technologies in a variety of areas, including catalytic conversion, photoelectrochemical and photovoltaic devices, electrophotographic devices, photographic film and semiconductor processing.

Since surface-enhanced Raman scattering is still a young area of study, interests by researchers and theorists have focused on the phenomenon itself. The effect is becoming better understood theoretically. The present theories are mainly centered around two mechanisms - electrodynamical and chemical. In Chapter 3, these theories will be briefly discussed and it will be shown that they cannot adequately account for the phenomenon involving aggregated molecules, hence the need for a new theory involving excitonic concepts.

Chapter 2 will be devoted to the discussion of the sensitizing dyes used in the investigations. Chapter 4 presents the experimental sections while the results are presented in Chapter 5. Chapter 6 contains a discussion of the results and conclusions. What follows in the rest of this introductory chapter is the discussion of the Raman effect itself and some of the Raman techniques.

1.2 THE NATURE OF THE RAMAN EFFECT

Raman spectroscopy is one of the spectroscopic methods based upon light scattering phenomena. In a more general sense, spectroscopy itself is the absorption or emission of radiation as a function of energy (frequency or

wavelength) occurring when an atom or a molecule changes its energy state as a consequence of its interaction with radiation. This gives the spectrum from which the nature of the discrete energy levels of the atom or molecule may be deduced by application of quantum mechanics. For molecules, this may enable the determination of molecular structure by knowing the nature of the forces holding the nuclei together. Information on individual molecules can form the basis for calculation or help predict the bulk chemical and physical properties of matter.

Many of the old and familiar spectroscopic methods like ultraviolet, visible, infrared absorption and emission, nuclear magnetic resonance, electron spin resonance, fluorescence, X-ray fluoresence, Mossbauer spectroscopy, etc., are essentially resonance methods. Raman spectroscopy is an inelastic scattering phenomenon. It does not involve absorption or emission from the energy levels directly but rather from some intermediate real or virtual state. In this case a quantum change made to the incident photon energy or frequency upon scattering, as a result of its interaction with the sample, is related to the energy levels of the atomic or molecular system. While infrared spectroscopy is performed with infrared radiation, the Raman effect is more general and can be, in principle, observed with any excitation frequency.

The Raman effect was first predicted from theoretical considerations by A. Smeka in 1923 (4), but it was not until 1928 that the effect was observed by C. V. Raman (5) in India almost coincidentaly with the observation by G. Landsberg and L. Mandelstant (6) in the Soviet Union. It was considered a significant discovery at a time when a lot of interest had been generated in

the inelastic phenomena caused by the earlier discovery of the Compton effect. The effect was named after Raman and he was awarded the Nobel Prize in 1930, just two years after his publication.

The Raman effect is usually observed in the presence of comparatively stronger scattering phenomena. If a beam of highly collimated and monochromatic light from a highpowered source is passed through a sample, three kinds of scattering can usually be observed. The weak scattering of the incident light due to dust particles or inhomogeneities in the medium is known as the Tyndall scattering which occurs at the same frequency as the source. The elastic Rayleigh effect, caused by polarization of the medium, is weaker than Tyndal scattering but still at the same frequency as the source. The third scattering, Raman scattering, inelastic and several orders-of- magnitude weaker than the Rayleigh scattering, occurs at frequencies different from that of the source.

If Raman scattering from a sample is analyzed by passing it through a spectrometer, the scattered energy will be found at definite frequencies above and below that of the incident beam. The incident frequency will be found to be modified and the modifying agent turns out to be the frequencies associated with the normal modes of vibration of the molecules . These may be molecular rotational or vibrational modes of a gas, lattice modes of a crystal, etc. In Raman spectroscopy, it is the difference between the frequencies of the Raman line and that of the source, i.e. the frequency shift, that is of interest, not the absolute frequencies of the scattered radiation.

Although the intensity of the scattered light (the bands in the spectrum) strongly depends on the frequency of the exciting light, the shapes and positions of the Raman bands do not. This is illustrated in Fig. 5-15 where a set of spectra of 2,2'-cyanine observed with different frequencies was shown.

Raman spectroscopy, since its discovery, has been periodically rejuvenated by advances in instrumentation. In addition to many text books of which some are referenced (7-10) many times in this book, there are numerous reviews (3,11-13) which are written on different aspects of the subject and can serve as valuable references. What follows in this introduction is a brief discussion of only those Raman techniques which are vital to the studies reported in this thesis.

1.2.1 Normal Raman Techniques

What has been described so far for Raman spectroscopy is essentially the normal Raman effect. It is purely the inelastic scattering of photons usually in the visible range from molecules in the gaseous, liquid, solution or crystal phase. When an incident photon with energy not equal to any of the electronic transition energies of the target molecule (thus eliminating absorption) collides with the target molecule, energy exchange takes place between the photon and the molecule which is put, for example, into an excited vibrational state if it is the molecule which gains energy. The scattered photon then leaves with reduced energy and hence a lower frequency which appears in the spectrum, at a frequency lower than the Rayleigh line, as a Raman Stokes line. A molecule in a vibrationally excited

state may give a quantum of energy to the photon which then leaves with a higher frequency and appears at the higher frequency region in the spectrum as an anti-Stokes line, which is normally weaker than the Stokes line under normal conditions. The ratio of Stokes to anti-Stokes intensities is governed by the temperature, with which it varies according to Boltzmann's energy dependency.

The normal Raman effect is "non-resonant" phenomena where no absorption of the photon is involved and the effect is not dominated by one transition moment as happens in the resonant methods. It is especially good for colorless substances which do not absorb in the visible region of the electromagnetic spectrum.

1.2.2 Resonance Raman Effect.

In 1960, thirty-two years after the discovery of the Raman effect, a paper by P. P. Shorygin and L. L. Krushinsky (14) was published in which the expression "resonance Raman spectra" appeared, probably for the first time in the literature, and in 1962 there was a paper published by Shorygin (15) in which he described the resonance Raman effect. This was followed by several articles (11,12,16,17) on both theory and practice of the effect.

Although vibrational or rotational states are generally involved, electronic states have also been implicated in Raman spectroscopy. When the energy of the exciting photon is close to an electronic transition energy of the target molecule, i.e. close to resonant absorption in the sample, a situation leading to enhanced scattering is observed. The signal from the

inelastic Raman scattering will be higher than what would have been observed if the excitation energy is out of resonance. This is the resonance Raman effect, in which one or few transition moments dominate the scattering probability. Since in circumstances like this, not only fluorescence becomes a problem in acquiring a spectrum but absorption of the scattered radiation also becomes large, leading to sample degradation and therefore one has to normally perform the experiment on very dilute solutions to realize the resonance Raman effect.

The effect is frequently difficult to separate from fluorescence in both practice and theory. In a review article, J. Behringer (12) outlines the differences and similarities between the two phenomena and how to distinguish one from the other. With fluorescence there is resonant absorption and the system is excited to a high electronic state for a measurable life time of about 10^{-8} seconds, followed by resonant emission, bringing the system to either the same lower state (resonance fluorescence) or a different one. Raman scattering processes involve excited state life times on the order of a vibrational period, typically less than 10^{-12} seconds, and the scattering system stays in the same electronic state. Line widths of fluorescence lines are typically on the order of 1-3 cm^{-1}, while that of Raman lines can be much less than 1 cm^{-1}.

Simplified energy level diagrams are shown in Fig. 1-1 illustrating the Raman effects and the fluorescence for a simple diatomic molecule. Apart from the reabsorption of the scattered light by the sample, resonance Raman spectroscopy is limited to molecules which must absorb at the frequency of the source photons. Many small molecules of interest do not absorb visible

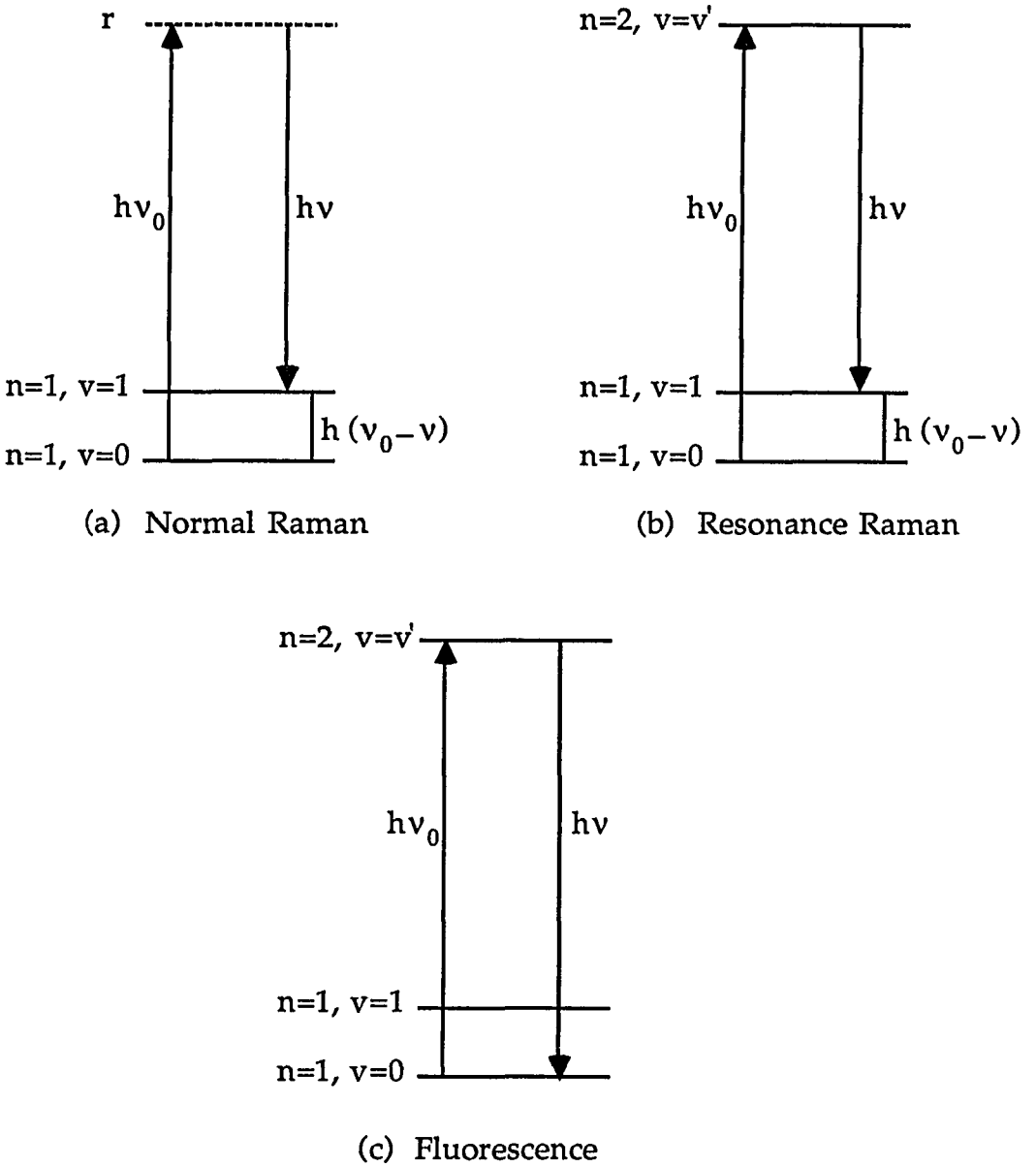

Fig. 1-1: Fundamental processes of (a) normal Raman scattering, (b) resonance Raman, and (c) fluorescence (resonance). In (a) the virtual state is represented by the dashed line.

light. Nevertheless, it was for some time the only known technique in which stronger Raman signals could be obtained from a number of molecules until the discovery of Surface-enhanced Raman scattering in 1975.

A wealth of structural data on molecules have been obtained from the resonance Raman effect which has been used for molecules of biological significance (18), where the increase in scattering cross section permits recording Raman spectra of species near normal physiological concentrations, which may be quite low. Resonance Raman is a particularly selective tool which makes it not only useful in analytical chemistry, but also suitable for studying photoreactive systems, and many researchers (19-22) find it useful in their studies of the photosynthetic cycle of bacteriorhodopsin.

1.2.3 Surface-Enhanced Raman Scattering (SERS)

Surface-enhanced Raman scattering (SERS) is a spectroscopic technique which is used to obtain information on vibrations of molecules adsorbed at metal surfaces analogously to that which has been extensively employed for molecules in solids, liquids or gases using normal resonance Raman spectrosocpy. SERS has received much more attention in recent years and has become a useful tool with a considerable potential for studying molecules adsorbed on solid substrates (23).

Surface-enhanced Raman scattering is a physical phenomenon that was unnoticed when first encountered in 1975. The effect was first obtained

from molecules adsorbed on silver metal working electrodes of electrochemical cells by Martin Fleischmann and colleagues (24) at the University of Southampton, U.K., and since has become a useful method for electrode/electrolyte interfacial studies. Studies done by Fleishmann and his coworkers (25) in 1974 led to enhancement of Raman spectrum obtained from a monolayer of pyridine adsorbed on a silver surface. These studies opened up a new field of scientific inquiry and has drawn many inquisitive workers.

Fleishmann et al. (25) in their publication had reported a normal Raman spectrum with a good signal-to-noise ratio obtained from a roughened electrode surface, thereby, they thought, increasing the surface area enough to have a sufficient number of molecules in the beam. It was recognized afterwards by other workers who independently observed and reported the enhancement effect (26,27) that the effect was a new physical phenomenon. The intensity of the Raman spectrum of pyridine was enhanced by a factor of five to six orders of magnitude over what could be expected from the scattering cross section of the isolated molecule (i.e., normal Raman scattering). The observation of this anomalously intense Raman scattering led to the name "surface-enhanced Raman scattering" (SERS). The explanation of surface-enhanced Raman scattering is now under extensive experimental and theoretical investigation by chemists and physicists around the world.

In SERS the magnitude of the enhancement is relatively independent of the identity of the adsorbed molecule but not of the metal surface. There is sufficient evidence that the coinage metals of Group IB give SERS to some

extent, but silver exhibits the strongest enhanced scattering effect and has received more attention (28-37). For both copper and gold, better results were obtained with laser excitation in the red end of the visible spectrum (38-41).

The effect is not limited to electrochemical systems alone. It was observed at a metal/gas interface (42), at metal island film/liquid interfaces (43), at metal/ultra high vacuum interfaces (44-48]) at solid/solid interfaces (49,50), and at silver and gold metal sol/liquid interfaces (51-55). The effect was also reported for nickel supported on silica in an atmosphere of carbon monoxide and hydrogen (56).

The observation of SERS in a diversity of interfacial systems allows the study of some of the systems which are normally difficult to study with most spectroscopic techniques, thus leading to the understanding of such systems, which are the focus of a great deal of current research. Several review articles have come up with detailed experimental techniques (1,3,13,57,58), and a number of theories have been advanced to explain the enhancement (59-66).

Colaboration between research and theory has now made it clear that the SERS phenomenon cannot be explained by a single enhancement mechanism. The widely accepted view is that both chemical and electrodynamic interactions play fundamental roles in the enhancement mechanism (57,67,68). The electrodynamic theories attribute enhancement to the effect of roughness and structures that support and enhance electrodynamic fields (58,69), while the chemical mechanisms and their theories are based on the presence of resonances between the exciting

radiation and quantum states created by coupling between quantum states of the adsorbed species and the quantum states of the substrate (62,63,67,70).

1.2.4 Aggregation Enhanced Raman Scattering (AERS)

Working with cyanine dyes adsorbed on colloidal silver and silver electrodes (36,54,55,71), we have found that the enhancement properties exhibited by these systems differ substantially from those noted by others. The primary explanation, for this observation, advanced from our laboratory (72) is associated with the somewhat unique properties exhibited by cyanine dyes aggregating on surfaces to form ordered macrostructures (73), and the increased polarizability of such structures. The enhancement is attributed to the formation by the aggregate structures in the ground and excited states; the latter leading to exciton band formation. The theory embodying this explanation is one of the subjects of Chapter 3.

1.3 BASIC REQUIREMENTS FOR RAMAN WORK

In the basic Raman experimental set up, the sample under examination is irradiated by a suitable monochromatic source, and the Raman spectrum is observed by use of a system comprised of a monochomator, detector, and recorder. Fig. 1-2 shows a block diagram of a simplified modern Raman spectrometer. The first major requirement is a suitable intense source which provides monochromatic light for exciting the sample. The light from the source is further filtered by passing it through a filter or grating before it reaches the sample. The collection of the scattered light is shown at the usual viewing angle of 90° to the direction of the incident light. A series of lenses serve to collimate the weak scattered light which is then passed through the entrance slit of a monochromator. From the monochromator the spectrum is usually recorded with the aid of a photomultiplier detector. A diode array detector is also available in our laboratory for detection. After the signal is passed through an amplifier/descriminator or pulse shaper, it is then recorded and stored in the computer. The spectrum is a plot of intensity versus frequency.

1.3.1 Sources.

Until the advent of lasers, the most commonly used device for producing intense monochromatic radiation was the low-pressure mercury discharge lamp; sources like this are accompanied by numerous difficulties (7,10). Soon after the first realization of a ruby laser in 1960 by T. H. Maiman (74), there was hope that lasers could solve most of the problems associated

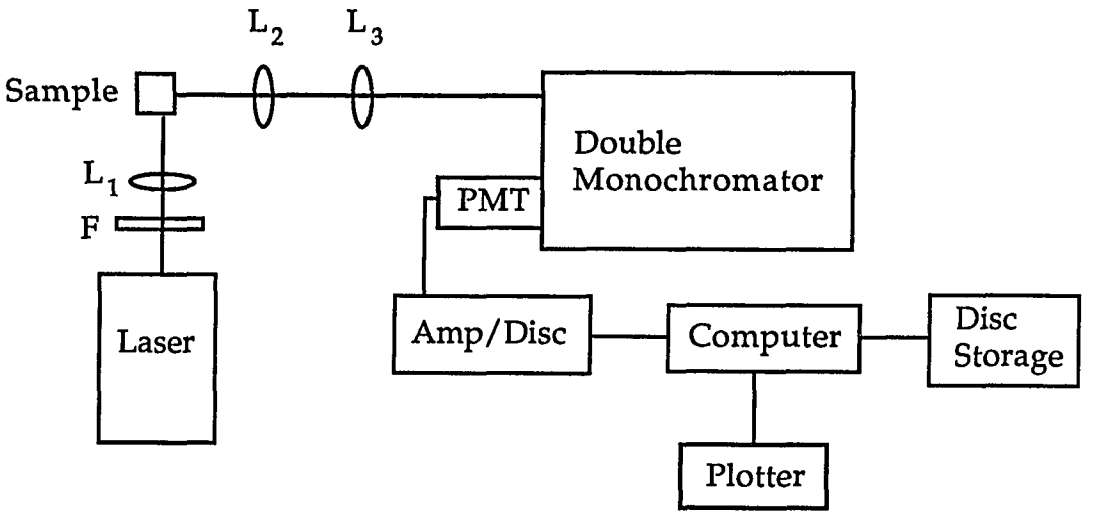

Fig. 1-2: Block diagram of a simple computer interfaced laser Raman spectrometer. The L's are focusing lenses and F is a laser line filter.

with mercury lamp sources. Certainly one of the most important scientific tools discovered since the discovery of the photographic plate in 1950 has been the laser.

Since the basic physics of lasers is by now well covered in many general texts on physics and optics it is not included here. The laser is an electromagnetic oscillator that derives its energy directly from simulated excitation of matter. The excitation often takes place in the internal quantum states of atoms or molecules but recently it has become possible to utilize free electrons for laser operation.

Lasers provide intense, monochromatic light with well-defined phase relationships. Most solid and gaseous state lasers which are somewhat restricted to chemical applications produce photons at a fixed wavelength, while the dye lasers, which operate mainly in the visible and near ultraviolet, and F-center lasers and tunable diodes, which operate in the infrared, can be tuned continuously over a certain wavelength range.

The output of a laser falls within a narrow bandwidth, thus producing very nearly monochromatic photons. The laser output can also be produced in a very short time, of the order of picoseconds, making it suitable for kinetic measurements on time scales impossible to achieve by other techniques. The continuous-wave (cw) lasers are more common for more general applications. Some have very high powers, e.g., 24 KW from a carbon dioxide laser.

It is therefore not surprising that since the advent of lasers, many applications have been made of them in the fields of science and

technology. Spectroscopy is one of the many techniques where much progress is a direct result of the introduction of lasers. By 1965 many instrument manufacturers like Perkin-Elmer, Cary Instruments, Coderg, and Spex, started to develop laser-powered spectrometers.

The helium-neon source provides an ideal Raman source for a 632.8 nm line with power up to 100-200 mW, while the higher power ionized argon, krypton, neon and nitrogen devices are suitable for operation at a considerable number of wavelengths and can be used to pump dye lasers. With tunable dye lasers one can have flexibility in the visible region. Pulsed lasers like the neodymium yttrium-aluminum garnet (YAG) or ruby lasers are also suitable for Raman work.

1.3.2 Sampling and Focusing Optics

The effort put into the selection and arrangement of pre-slit optics will determine the quality of the spectrum to be recorded. A particular experiment may demand its own unique sampling system and pre-slit optics to ensure that not only the sample has the maximum illumination but also that much of the scattered light is efficiently collected and passed to the entrance slit of the monochromator.

Raman spectra can easily be recorded on gases, liquids, and solids. Gases demand higher powered lasers and more complex sampling apparatus (75,76). Liquids may be examined in ordinary glass cuvettes or in sealed ampules, tubing, or capillaries, depending on the amount of the sample available. Since water is a poor scatterer it is frequently used as a solvent for

Raman spectral measurements. For easily decomposable systems, a flow through cell may be necessary. One such cell has been described for observation of liquid samples without realignment (77).

Delicate solid state samples can be tapped into an open-ended cavity or into a glass capillary tube while fibres, block specimens, and films can be studied directly without any special preparation.

In the setting of the sampling systems and the optics, three basic geometries are used.

1. The 90 degree scattering system, used by the majority of workers, involves the laser beam propagating normal to the direction in which the scattered light is collected.

2. The 180 degree system is a backscattering geometry where the beam is travelling away from the slit. It can be designed to allow rotation and cooling of the sample simultaneously (78).

3. In the zero degree (forward scattering) system where the laser beam is directed at the slit, it is necessary to place a small mirror before the slit to reflect the laser beam away from the monochromator.

1.3.3 Monochromators

Monochromators with very high discrimination are necessary for Raman work. First generation laser-excited instruments used monochromators with gratings that were ruled instead of the glass-prism

dispersion monochromators in use before them. They were originally based on a single monochromator function but by 1961, instruments using a double monochromator (e.g. the Cary 81) had been made commercially available. Higher order monochromators were thought necessary to improve discrimination and to improve signal-to-noise ratios.

Holographic gratings which are much improved are now available which provide significant improvement in signal-to-noise ratios. The stray light rejection achieved in new instruments which now use concave holographic gratings in addition to the conventional plane gratings is sufficiently good that Raman spectra can be obtained with a single monochromator with higher through-put.

A monochromator's efficiency, with regard to its energy transmission, is a function (amongst other things) of the slit height and focal length (79). This makes instruments with high slits desirable provided they can be effectively illuminated.

1.3.4 Detectors, Amplifier and Recorders

In the beginning the photographic plate was the means by which most Raman spectra were detected and recorded. Although the method was simple and cheap, the processing was too time consuming which made it unsuitable for routine spectrocopy.

A photomultiplier tube, of which the RCA C31034 or the Hamamatsu 928 are typical examples, has been developed featuring a Ga-As or multi-

alkali photocathode surface to be used in the photoelectric detection. They have a high absolute quantum efficiency, and give constant response over the entire visible spectrum. The most recent ones were developed with extremely low dark current to improve detection of weak Raman bands. Cooling of detectors can be beneficial in enhancing their signal-to-noise ratios, particularly at red wavelengths, though there has been controversy over this assertion (10,11,80,81).

In the earliest Raman instruments, d.c. amplification methods were used. At present there are a number of other amplification systems in use. In one type, called synchronous or lock-in amplification, the optical beam is interrupted before it reaches the detector at low audiofrequency, and the a.c. signal from the detector is amplified by a phase-sensitive amplifier, filtered to remove noise, and rectified to produce an output d.c. potential proportional to the intensity of the radiation to be detected.

In the photon counting systems, an energy sorter or "discriminator" is inserted after the detector to allow the pulses due to the optical signal to pass to another device which converts the pulse energies to a constant value, followed by rectification of the signal to produce a d.c. voltage output porportional to the number of photons per second arriving at the photomultiplier.

Raman instruments are now routinely being interfaced to minicomputers and to microprocessors. This has many advantages. Signal averaging is made possible through the use of long intergration times and data can be saved, processed and plotted at a convenient time.

CHAPTER 2

SENSITIZING DYES

2.1 INTRODUCTION

Nature is beautiful; she is colorful and can make or change colors to make herself attractive. The colored matter of nature has always attracted man's interest, and in very early times he found ways of extracting dyes and using them for coloring clothing, for painting, etc. Dyes obtained in this way are termed natural. An example of one of the earliest ones is natural indigo, known as early as 2000 B.C., which was obtained from the leaves of various species of "indigofera" plants and applied by means of a fermentation vat.

The extraction of natural dyes became a substantial industry which flourished until the latter half of the 19th century when that industry was gradually supplanted by one based on synthetic dyes. The natural dyes have almost completely been replaced by synthetic dyes in large scale operations because the extractions are usually unsuitable for a large-scale production, the products lack uniformity, and their colorfast properties are inadequate. However, with the belief that Nature's products are invariably superior to man's, the natural dyes are often preferred by some workers in handicraft (82,83).

Long after the natural dyes had been abandoned commercially they retained the interest of chemists who have carried out a great deal of work on the determination of their structures. Their efforts led to synthetic equivalents of some of the natural dyes, such as indigo and alizarin, which were commercially manufactured.

The foundation of the synthetic dye industry was laid in 1856, when Sir William Perkin, in the course of attempts to synthesize quinine by the addition of oxygen to allyltoluidine, studied the action of potassium dichromate on aniline sulfate, and discovered Mauveine (84) (originally called Aniline Purple or Tyrian Purple), the first synthetic dye to be manufactered and used for práctical dyeing in the textile industry. One of the earliest synthetic dyes, Rosolic, which was prepared earlier by Runge in 1834 but was not manufactured until after 1861, was used chiefly in the form of a red lake for wallpaper printing (85).

Research on synthetic dyes was pursued in many laboratories, and soon other basic dyes were discovered and manufactured in England, France, and Germany. Dyes like oxazines, thiazines, acridines, xanthenes, and azo dyes were produced (86).

In the same year that Perkin discovered Mauveine, C. H. Williams discovered Cyanine (or Quinoline) Blue which was valueless as a dye on account of the very poor fastness of the shades, but his work led, half a century later, to the synthesis of a whole series of photographic spectral sensitizers which are the main subject of this chapter.

With the simultaneous and largely inter-dependent progress made during the last hundred years in dyestuff chemistry and in organic chemistry, synthetic dyes have been prepared in bewildering number and variety, and the possibilities of further synthesis are unlimited.

By 1963 there were at least 3,000 (87) dyes employed by the textile and other color using industries. The third edition of the Color Index (88) in 1971 listed 7898 generic names of individual dyes and pigments over half of which were dyes with known structures. The most important note is that many of the dyes mentioned in the Color Index are

obsolete, while many more new dyes with improved properties have been marketed.

2.1.1 Color and Dyes

Dyes are essentially colored chemical substances used in homes and in industries to provide color to materials. They can be applied in solution to a substrate which may be a natural fiber such as cotton, wool, silk, and linen, or a synthetic fiber such as nylon, cellulose acetate or polyester. The substrate, to name just a few, may also be paper, wood, leather, hair, fur, plastic, wax, cosmetic base, or a foodstuff. Dyes are also used in photography.

In dyeing, colored matter from the dye solution or aqueous dispersion is transferred to the substrate by the process of absorption. The removal of the dye from the solution is called exhaustion. In most cases the substrate possesses a natural affinity for dyes and exhaustion readily takes place under suitable conditions of concentration and temperature. Exhaustion thus implies that there is a chemical or physical interaction between the substrate and the dye molecules, leading to the formation of bonds. The behavior of a dye is thus dependent both on its chemical structure and on the structure of the substrate. The presence of auxiliary substances may be necessary to control the rate of dyeing, and the pH must be suitably adjusted.

Colored materials owe their color to transitions between different electronic states of the molecules composing the matter. Such transitions manifest themselves as the absorption of the light. Every dye exhibits absorption arising from its chemical structure, and this may be represented by an absorption spectrum which is characteristic of the coloring matter and may be used for identification purposes. The absorption spectrum of a dye may be complex, and the purity of the color observed depends on the shape

of the curve. Bright colors are the result of narrow absorption bands with sharp peaks, and dullness is associated with broader bands lacking such peaks. High extinction transitions in the visible or infrared regions of the spectrum characterize the sensitizing dyes.

Absorption spectra are normally determined from samples in solution. Dyed materials absorb light in a characteristic pattern, and the unabsorbed light is mainly reflected rather than transmitted; in such cases, however, the physical form of the particles of coloring matter and substrate affect the nature of the reflected light.

2.2 DYES IN PHOTOGRAPHY

In photography, dyes have many uses. Their most important uses are (i) as spectral sensitizers, (ii) as desensitizers, (iii) as color images in color photography, and (iv) in antihalation and filter layers, and in color filters. Dyes which are used as photographic sensitizers and which have made color photography and high speed photography possible are the subject of this chapter. They belong almost exclusively to the cynanine or related dyes.

Sensitizing dyes have been well reviewed in the literature by L. G. S. Brooker et al. (89 - 94), F. M. Hamer (95), A. I. Kiprianov (96), G. E. Ficken (97), and D. M. Sturmer (98). Additional reviews of color/constitution, physical/chemical properties, and spectral sensitization can be found in special published proceedings of various international symposia on dyes (99-102).

The discovery of spectral sensitization of silver halides by Vogel in 1873 marked a very important stage in photographic industry. Vogel observed that certain dyed photographic plates showed unusual sensitivity in the green region of the spectrum and that the green sensitivity disappeared on

removal of the dye (103). While the sensitivity of the human eye extends over the spectrum from the violet at 400 nm to the red at 700 nm, with the greatest sensitivity in the yellow, the undyed silver halides, on the other hand, are sensitive only to the ultraviolet and the blue light. Vogel found that the green sensitivity was due to the presence of the yellow dye Coralline (the sodium salt of Aurine) which had been added to the emulsion to prevent halation (an undesired effect caused mainly by the scattering of light reflected from the rear surface of the plate).

After working with dilute solutions of various dyes, Vogel discovered that only certain dyes, including cyanine, possessed the power of making photographic emulsions sensitive to colors other than blue (104). Subsequently, the sensitizing action of other dyes which do not belong to cyanine or related types were discovered. Becquerel discovered the photosensitizing action of chlorophyll (105) in 1874 and Waterhouse discovered the sensitizing action of eosin to green and yellow light (105) in 1875. In 1883 work by J. M. Eder revealed that erythrosin was a better sensitizer than eosin for green light (106) leading to the making of the first "orthochromatic" plates.

Cyanine remained in use as a sensitizer for some years despite its tendency to cause fogging. In 1903 it was found that the isocyanines (produced in 1901) sensitized to green light without fogging (107,108). A year later, the discovery of Pinacyanol, the first sensitizer for red light, by Homolka (109) enabled satisfactory panchromatic plates to be produced (110), a way leading to the development of color photography. Since then many other effective dyes have been discovered and the range of sensitization has been greatly extended. The carbocyanines were found to absorb infrared light and sensitize to the infrared, and were the early infrared sensitizers

used for color photography (111); by these means the most distant photographs of the planets were taken (112).

By means of photographic sensitizers, it is possible to attain a true rendering of color in monochrome. Also by making film sensitive to color other than blue, its speed has been increased, i.e., exposure times have been reduced. It has been noted that in the motion picture industry, sensitizers made possible the replacement of arc lamps by silent filament lamps, which was necessary for sound recording (113).

The photographic sensitizing dyes are usually obtained by linking heterocyclic residues, such as quinoline, benzoxazole, benzothiazole, benzoselenazole, indoline imidazole or their substituted derivatives, by conjugated chains of varying length; the central carbon atom may carry an alkyl group. The primary type of chromophores for the dye molecules are the amidinium ion system (A), the carboxyl ion system (B), and the dipolar amidic system (C) (114), each type shown here using the two extreme resonance structures, where any of the formal changes are located at the ends of the chromophore (114).

(A) 

(B) 

(C) 

In general the sensitizing maximum of an adsorbed dye lies at a slightly higher wavelength than the dye's solution absorption maximum (115). It is also found that as the length of the conjugated chain is increased both the

absorption maxmium and the sensitizing range are displaced towards longer wavelengths (115,116).

2.3. THE CYANINE DYES

The first cyanine dye was discovered as early as 1856 by Greville Williams, who noted the tendency of quinolinium salts to give intense colors on heating with silver oxide (117). When he heated quinoline, containing lipidine, with isoamyl iodide and caustic soda and observed the crude blue dye, he decided to call it cyanine (117). Cyanine is a Greek term for dark blue, and the word was in the written vocabulary of several ancient Greek writers, including Homer. Williams' cyanine was later shown to have the structure (I) (118) and has become one of the numerous cyanine dyes prepared and classified in a larger group of methines and polymethine dyes.

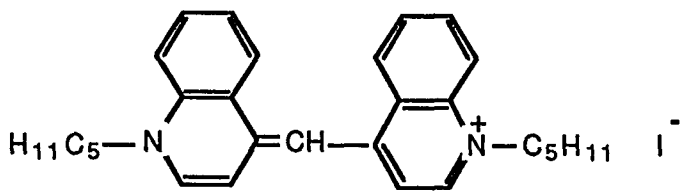

I

Methine and polymethine dyes are characterized,in general, by the presence of a chromophoric system containing an acyclic link or chain with a structure:

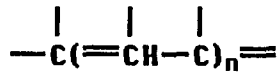

(where n=o or an integer) or 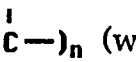 (where n is an integer). The typical cyanine molecules form an important class of methine dyes with links or chains of the first type containing an odd number of carbon atoms attached to two basic heterocyclic residues.

Some other cyanines, which were discovered later, and have already been mentioned, are isocyanines such as that of structure (II), discovered in 1901 (108) and Pinacyanol (I09) discovered in 1905, and first obtained by condensing quinaldine ethiode with formaldehyde or with ethyl orthoformate in acetic anhydride solution(119).

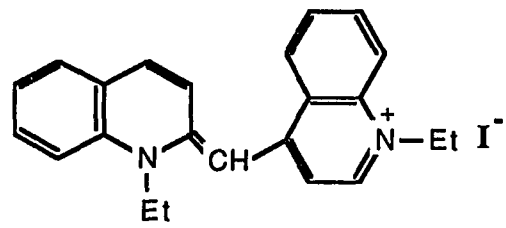

II

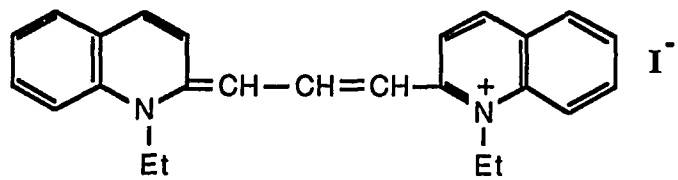

III

The few years that followed these discoveries saw various attempts by interested workers to prepare better spectral sensitizers and to establish the true chemical and structural identities for the dyes, (120-122). By 1925 structural identities for several useful spectral sensitizers were established, (95,123-125).

The period 1920-1960 saw major synthetic advances made in the field. W. Konig used orthoesters and vinylogs of these compounds

$EtO-(CH=CH-)_nCH(OEt)_2$, $n = 0, 1$

to prepare symmetrical dyes (126,127), while Piggott and Rodd developed reagents for unsymmetrical dyes (128). The merocyanines which were valuable sensitizers as well as intermediates for more complex dyes were

developed in the early 1930's (129,130). For the synthesis of infrared sensitizers, extended-chain quaternary salts were used (131).

The structures of many cyanines and related dyes have been studied using X-ray crystallography and nuclear magnetic resonance; studies related to their behaviour have been done using traditional electrochemical measurements and protonation equilibria. Data in these areas can be found along with the data on infrared vibrational frequencies and dipole moments of cyanines and merocyanine dyes and related compounds in Sturmer's review (98).

2.3.1 Classification and Nomenclature

Since the older cyanines are mainly derived from quinoline, it is convenient to group the quinoline compounds separately to illustrate classification and nomenclature of the cyanine dyes. Further classification of these dyes may be based on the mode of attachment of the ring systems. Historically, the terms simple cyanine, carbocyanine, dicarbocyanine, and so on, were used to designate both specific dyes derived from quinoline and also the generic dye structures from other heterocycles with one, three, five, and multi-odd methine carbon atoms. In naming, the ring position attached to the methine chain and the N-substituent are usually specified. For example, 1,1'-diethyl-2,2'-cyanine iodide is dye (IV) with R = Et , n = 0 and X = I. Thus three isomeric forms are possible for each methine length.

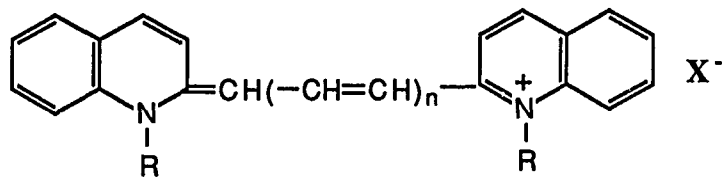

IV

n = 0, a simple cyanine
n = 1, a carbocyanine
n = 2, a dicarbocyanine
n = 3, a tricarbocyanine.

X in the formula represents an acid radical, R was at first, and is generally an alkylgroup, but it may also be an aryl. Dyes that differ only by the number of vinyl groups (CH = CH) in the conjugated chain are termed a vinylogous series. It is also possible that the ring systems are linked directly by means of nuclear carbon atoms. These cyanines are called apocyanines.

2.3.2 Synthetic Methods

The general synthetic methods developed after 1920 and extended to many new systems after 1950 have already been outlined in this chapter, section 2.1. The review by Ficken (97) provides supplemental references to more recent compounds.

Dye-forming reactions may be classed as oxidative or nonoxidative. The nonoxidative syntheses are the most versatile and employ varied combinations of suitable nucleophilic and electrophilic reagents. The oxidative syntheses are primarily of historical interest.

2.3.2.1 Oxidative Syntheses (114,117,125,132)

In the earliest methods used to prepare cyanines and many other sensitizers, a methylene base and the related quaternary salt combine to form the dye. Typical reaction sequences are shown in (Eq. 2.1) (114).

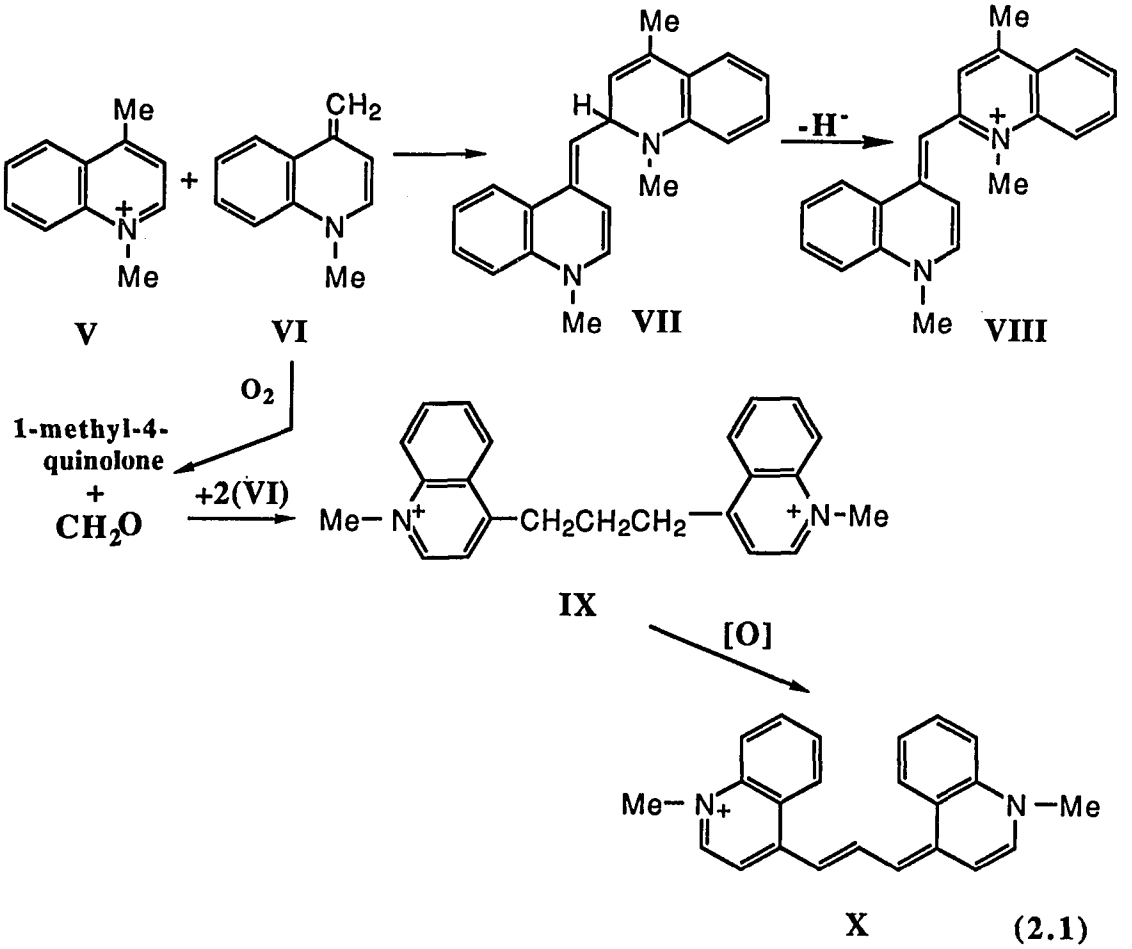

The quaternary salt (V) reacts with the methylene base (VI) to produce the dihydroquinoline (VII), which upon oxidation leads to simple cyanines such as (VIII) (114).

A slightly different path,under certain conditions, is necessary to form carbocyanine dyes . In the presence of oxygen the methylene base (VI) undergoes oxidative cleavage to give formaldehyde which then reacts with two additional equivalents of (VI) to produce the trimethylene compound

(IX), a precursor to the carbocyanine (X). Thiacarbocyanines and indocarbocyanines can also be similarly prepared.

2.3.2.2 Nonoxidative Syntheses (114,133-137)

Nonoxidative synthesis provides general synthetic methods for the preparations of the cyanines and related dyes, and unlike the oxidative methods they often combine reagents of quite different structures. The reactions involve combination of nucleophilic and electrophilic reagents, including those necessary for the synthesis of complex dyes (133). Symmetrical carbocyanine dyes, for example, can be prepared from two equivalents of an active methyl quaternary salt, which provides nucleophilic methylene bases and an orthoester as the electrophilic reagent. The resulting dye molecule derives most of its atoms from the heterocyclic quaternary salt; the orthoester provides only the central carbon of the trimethine chain.

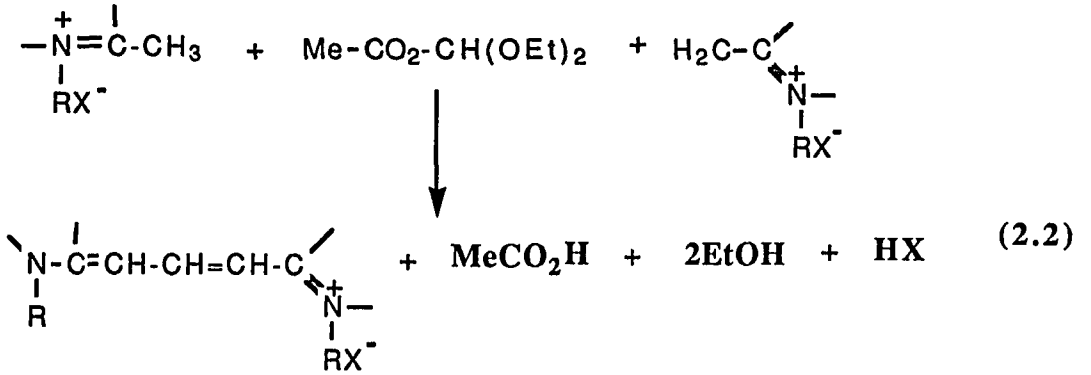

(2.2)

Methylene bases were recognized early as nucleophilic reagents with good reactivity. Reactive quaternary salts with additional vinyl groups led to improved preparations of long chain dyes (131). The enolate anions from many active methylene compounds also function as nucleophilic reagents

in merocyanine and oxonol syntheses. Other novel nucleophilic reagents can readily be found in the literature (98,114,138).

Three types of electrophilic reagents are useful for the synthesis of sensitizers: (a) heterocycles or aromatic rings with replaceable substituents, (b) functionally symmetric reagents like orthoesters, and (c) vinylogous amides and analogous reagents.

Aromatic substitution reactions occur readily on electrophilic reagents of type (a) of the general structure (XI). These reagents readily undergo aromatic substitution reactions with methylene bases and other nucleophiles to produce a variety of short chromophoric linkages such as simple cyanines (95,138-140).

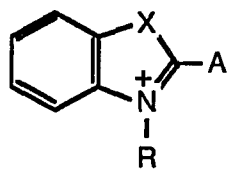

A = I, SR, SO_3^-, SO_2Me, OR, -CH=N-OR, CN.

XI

For carbocyanine and longer chain dyes, the electrophilic reagents of type (b) and (c) are employed (92, 95). The furfurals (structure (XII), n = 0 - 2) reacted as cyclic analogs of othoesters and were shown in 1935 to give tri-, tetra-, and pentacarbocyanines (114).

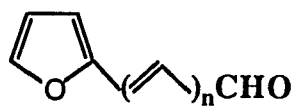

XII

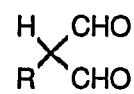

XIII

More recently, a large number of dyes were prepared from substituted malonaldehydes (XIII) (141,142), crotonic acid, (143). Acetylenic reagents like 3,3-diethoxypropyne or HC=C-CMe=CH-CHO for dye synthesis have also been known for some time (144,145).

2.3.2.3 Ring-Closure Reactions

The reactive quaternary salts which are often used in preparation of dyes,are usually prepared by simple ring closure reactions. An example is the preparation of an optically active dye (XIV), as shown in Eq.(2.3) (146).

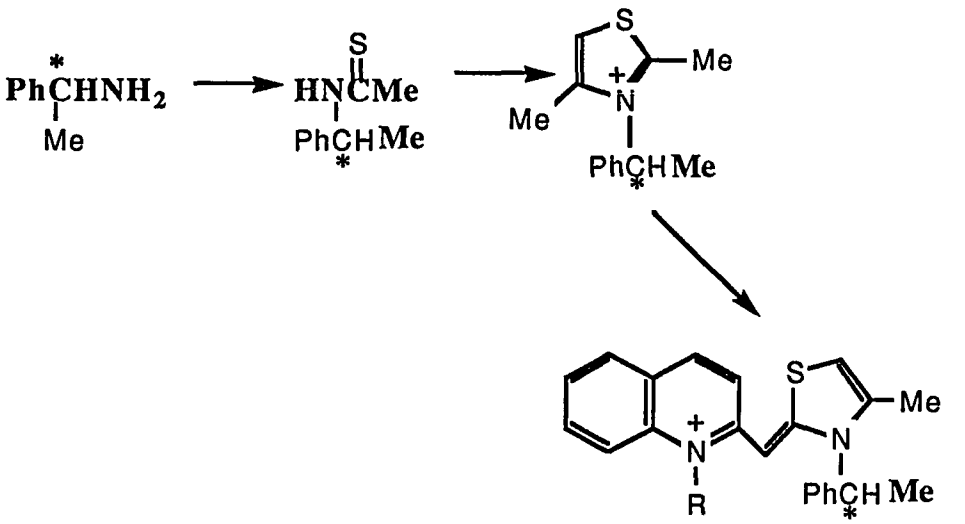

(2.3)

XIV

Many dyes are prepared in this way by ring-closure reactions at or near the dye forming step of a synthetic sequence (147,148).

2.3.3 Some Properties and Uses of Cyanine Dyes

2.3.3.1 Spectral Sensitization

Much has already been said about the importance of the cyanine and related dyes in photographic sensitization. Considerable progress has been made in recent years in undertanding the mechanism of optical sensitization.

Cyanines and related dyes like the large conjugated molecules are described by general quantum theory as shown in Fig. 2-1. The bonding and nonbonding orbitals of the ground states are filled with sigma (σ), pi (π), and

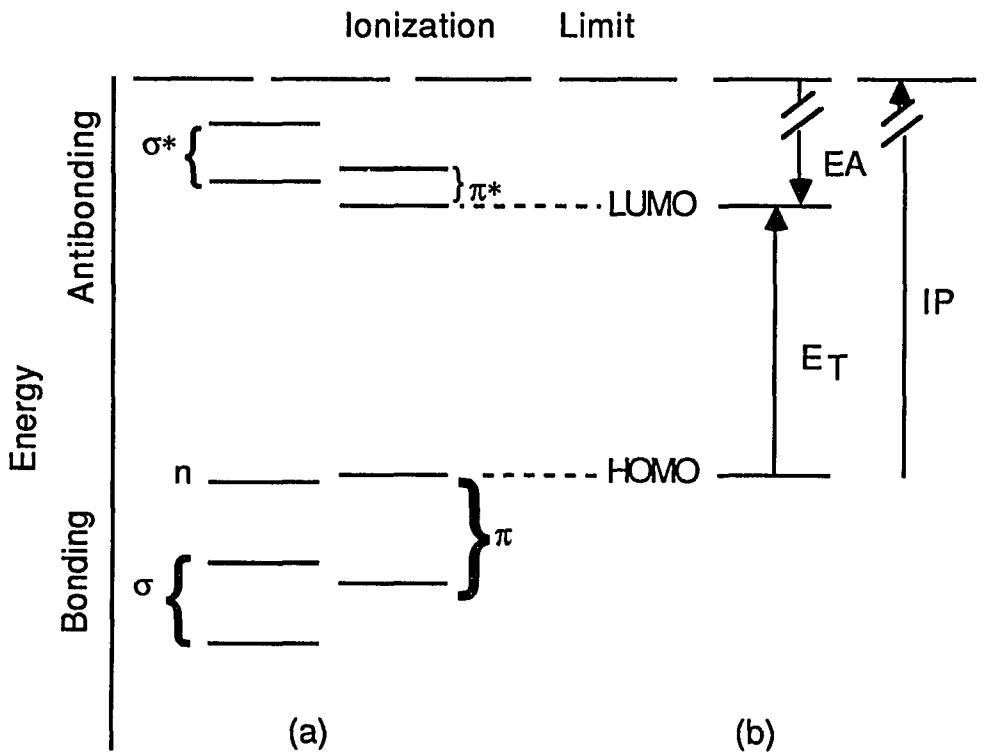

Fig. 2-1: Quantum mechanical orbital descriptions of cyanine and related dyes showing (a) Bonding and antibonding orbitals and (b) Energy transitions between the orbitals involved in spectral sensitization.

lone-pair (n) electrons, according to their relative energies which will depend on the specific molecular system. The antibonding orbitals are pi (π^*) and sigma (σ^*) as shown. $\pi \rightarrow \pi^*$ and $n \rightarrow \pi^*$ electronic transitions are possible in the visible and infrared spectral regions, but because of low extinction coefficients of the latter, the former predominates.

In Fig. 2.1(b) the Highest Occupied Molecular Orbital (HOMO) and Lowest Unoccupied Molecular Orbital (LUMO) are shown. Combinations of these orbital energies with appropriate correction terms lead to transition energies E_T (singlet-singlet, singlet-triplet). Electron affinity EA and ionization potential IP, result from other considerations. In general, E_T is not equal to $|IP-EA|$ or to the analogous polarographic quantities $|E_{ox}-E_r|$ (114).

Most cyanines show in their electronic spectra prominent vibrational shoulders associated with the long-axis polarized, long-wavelength electronic transition (149-151). The shoulders included one or two vibrational quanta (0->1', 0->2') relative to the absorption maximum (0--0').

A sensitizing dye must absorb the light, must be adsorbed to the silver halide, and must transfer the absorbed energy to the silver halide substrate. It probably affects the stability of the union between silver and the halogen. Also since only a few dyes actually sensitize, chemical structure plays some part in their action (152).

Under the conditions employed for sensitizing, the dyes are molecularly dispersed, the optimum quantity varies from 5 to 100 parts per million, but aggregation and resultant changes in absorption spectra have been observed at higher concentrations.

A cyanine dye may sensitize in different regions of the spectrum depending on the state of aggregation (154-156). Supersensitization by

mixtures of dyes, and by compounds which have no sensitizing activity by themselves, is also possible. Koslowsky and Mueller had first reported that the sensitivity of a cyanine dye could be doubled or tripled by adding an ammonium or alkali aurous thiocyanate to the emulsion (157).

2.3.3.2 Adsorption Onto Substrates

Of prime importance in photographic sensitization is the adsorption of the dye to the silver halide grains. It has been found that with certain dyes, there are some correlations between adsorption and strength of sensitization but in general these are not parallel properties (158,159). The amount of dye which produces the maximum sensitization was found in 1937 to be directly proportional to the silver halide surface, and it was concluded that at the optimum concentration the dye was adsorbed in a unimolecular layer (160). It was proposed then that the first layer of the dye was adsorbed through the polar nitrogen atoms, with the molecules projecting upwards; while the second layer might be oriented in the opposite direction. Later it was found that there were at least two states of aggregation with different absorption and sensitizing properties (161). It was suggested that the dyes were partly adsorbed as single molecules attached by the nitrogen atoms to the surface, possibly partly lying flat, and partly as molecules oriented as units packed parallel, adsorbed edge-on, and again attached by the nitrogen atoms (162).

Further studies of physicochemical and photographic properties of five thiacyanines revealed that the first adsorption was monomolecular followed by the aggregative state which was manifested by another band in the region of longer wavelength (163). The heat of adsorption of sensitizing dyes was subsequently determined and the area occupied per dye molecule

was calculated. A recent estimate is that at normal sensitizing concentrations half the grain is covered by dye and it was suggested that sensitizers of the cyanine classes are probably attached to the surface in islands of closely packed oriented molecules with relatively bare intervening spaces (164).

2.3.3.3 Bacteriostatic and Chemotherapeutic Activites of Cyanine Dyes

As early as 1922, certain commercial sensitizers were investigated for their possible physiological applications. Cyanine, styryl, and similar dyes appear to have interesting properties as bacteriostatic and chemotherapeutic agents (165). Sensitol Green (an isocyanine) was described as a good antiseptic for Bacillus Coli (166). The action of cyanine itself on tubercle bacilli was only temporary (167).

Brooker has found that many of the cyanine type dyes, prepared in soluble form, have pronounced antifilarial and anthelminthic action (168). Some were also found to show antimalarial activity, but not equal to the well-known antimalarials. Cyanine dyes such as pyrimido-2'-cyanines, were found to be useful therapeutics for worm infestations (169). The Japanese are said to have made progress with dyes of the neocyanine type as cures for leprosy (170) but two of the compounds included in their claim have been found to be inactive against leprosy and tuberculosis (153).

A symmetrical indotricarbocyanine, having 4,5-benzo-3,3-dimethylindolenine nuclei, absorbed infrared light and hence proved useful in diagnosing congenital heart defects (171).

2.3.3.4 Some Other Uses

Some cyanines that are not useful as photographic sensitizers have, on the other hand, proved valuable as filter dyes. Examples are symmetrical methine-trimethine-cyanines having two 3-linked pyrrole (including indole) or two pyrocoline nuclei (172,173) and di- and tetra-methinecyanines with one 3-linked pyrrole or indole nucleus (174).

Cyanines have begun to be especially useful in the organic dye laser field which itself has grown enormously in recent years, particularly with respect to continously tunable lasers that operate at wavelengths from 340 to 1150 nm. There are good reviews on the general subject of organic dye lasers (175-177), which give elaborate coverage of the subject. The extensive work of the authors shows that cyanine, oxonol, and merocyanine chromophores are all suitable for dye laser applications. They find that in the best dyes the chromophore was less branched which makes singlet-triplet intersystem crossing negligible.

2.3.4 Aggregate Formation

The unperturbed molecular absorption bands for cyanines and other sensitizing dyes are obtained only in very dilute aqueous or alcohol solutions. Deviations from Beer's law and other perturbations are observed and can be rationalized in terms of dye aggregation, i.e. the formation of dimers, trimers, and n-mers. Interaction among dye molecules produce large spectral shifts and distinct changes in band shape. These changes were first explained by Forster with a classical oscillator model (178). Later explanations were based on the theory of energetically delocalized states, i.e. excitons, which has been applied by Davydov to spectra of excited molecular crystals (179-184). According to the exciton model(185-187), the excitation

achieved in a single molecule of a periodic molecular assembly is transferred by coupled oscillation from molecule to molecule in a period which is shorter than the vibrational time of the component molecules in the assembly.

Solutions of a single dye or a mixture of dyes can show, with increased concentrations, either progressive shifts of absorption maxima to shorter wavelength as a result of H-aggregation or abrupt shifts to longer wavelength as a result of J aggregation, as first noted by Jelley and Scheibe (188-190). Many reviews have appeared which discussH and J aggregation (191-196).

The major absorption peaks for many H-aggregated dyes have larger band widths than monomers, but an extremely sharp H-band designated H* has been found for several dyes (197). Most J-aggregates exhibit sharp absorption bands. Monomer aggregate absorption shifts vary with the methine chain length within a vinylogous series. West and Pearce reported a variation between 1180 cm^{-1} (thiacyanine) and 2175 cm^{-1} (thiatricarbocyanine) in the thiacyanines (197). Formation of mixed aggregates has also been reported, and the mixed aggregate systems exhibit different absorption spectra than those of the aggregated components (197).

Aggregation in solution is a moderately exothermic process (197) and the decrease in free energy for many typical cyanine and related dyes is relatively small. Moderate changes in solvent properties like dielectric constant, ionic strength, and hydrogen bonding, that affect the solvent-solvent interaction, can markedly affect aggregate equilibria. It has been suggested that attraction between water molecules at the expense of water-dye interaction contributed to the energetics of dimerization (191). The experimental work relating the effects of inorganic salts and organic

materials on aggregation was reviewed by Herz (192). Added inorganic salts generally increase the dielectric constant of a solvent and facilitate aggregation, while simple organic additives diminish the effective dielectric constant of a solvent and enhance the repulsion between similarly charged dye ions (192).

With regards to relationships between aggregation and dye structure, Brooker suggested that "compact" dyes aggregate more readily than "loose" dyes and "crowded" dyes(198). The first two categories refer to planar dyes and the third to nonplanar dyes.

Luminescence from dye aggregates often exhibit distinctive spectral features similar to those found in the absorption spectra. The relative energies for allowed and forbidden electronic transitions in these aggregates are found to depend on the angle (α) of dipole-dipole interactions of the molecules in an aggregate (114). J-aggregates (angle $\alpha \rightarrow 0$) exhibit highly allowed transitions between the ground state and the first excited singlet state. Fluorescence from this state was found to be generally strong. H-dimers and higher H-aggregates (angle $\alpha \rightarrow 90^{o}$) were found to exhibit weak transitions between the ground state and first excited singlet state, with the more probable transitions of H-aggregates involving higher excited singlet states (114). Excitation into these latter absorption bands produces a weak fluorescence and a relatively efficient phosphorescence. These observations suggest that the excited H-aggregates are more rapidly deactivated by internal conversion and intersystem crossing than monomers or J aggregates (114).

There are many theoretical descriptions of aggregates (199-203), but for our purposes, and for brevity, it will be sufficient to consider the Davydov exciton model developed by McRae and Kasha (180), and to limit initial considerations to the dimeric molecules, with the assumption that the axis

of the composite molecule, the dimer in this case, parallels its transition polarization axis, i.e., the transition dipole is placed along the long axis of the molecule.

The model provides for splitting of the excited state E for the dimer because of electronic degeneracy. The energy of the excitonic state of the dimer relative to the monomer excited state energy depends on whether the dipole-dipole interaction will be attractive or repulsive. The selection rule for light absorption is deduced from vector sums of the transition dipoles for the given exciton state. Fig. 2.2 shows that upon excitation of the dimer from its ground state (G), the transition to the lower excited level will be allowed when the transition dipoles are in line with the molecular axis of the dimer, i.e. when the angle α between the transition dipoles and the molecular axis of the aggregate equals zero. Consequently the maximum absorption of the dimer will be red-shifted relative to the absorption of the monomer. In the other case when the transition dipoles are perpendicular to the molecular axis of the dimer, i.e. $\alpha = 90^{o}$, transition to the higher excited levels will be allowed so that singlet-singlet transitions of the dimer will be blue shifted relative to that of the monomer dye. In fact, this latter case is observed for $\alpha > 54^{o}$ (180).

Much of the early work on J aggregates in solution was done with 2,2'-cyanines, the selena and thia-2' derivatives, and their analogs (188,189). 1,1'-diethyl-2,2'-cyanine chloride has played a major role in these early studies and is still being used as the model compound. In aqueous solution and at room temperature, the spectra of this dye was found to obey Beer's law only below 10^{-5}M. At higher dye concentrations the monomer absorption band near 525 nm decreases with the formation of an H-band (principally due to dimer formation) at wavelengths somewhat shorter than

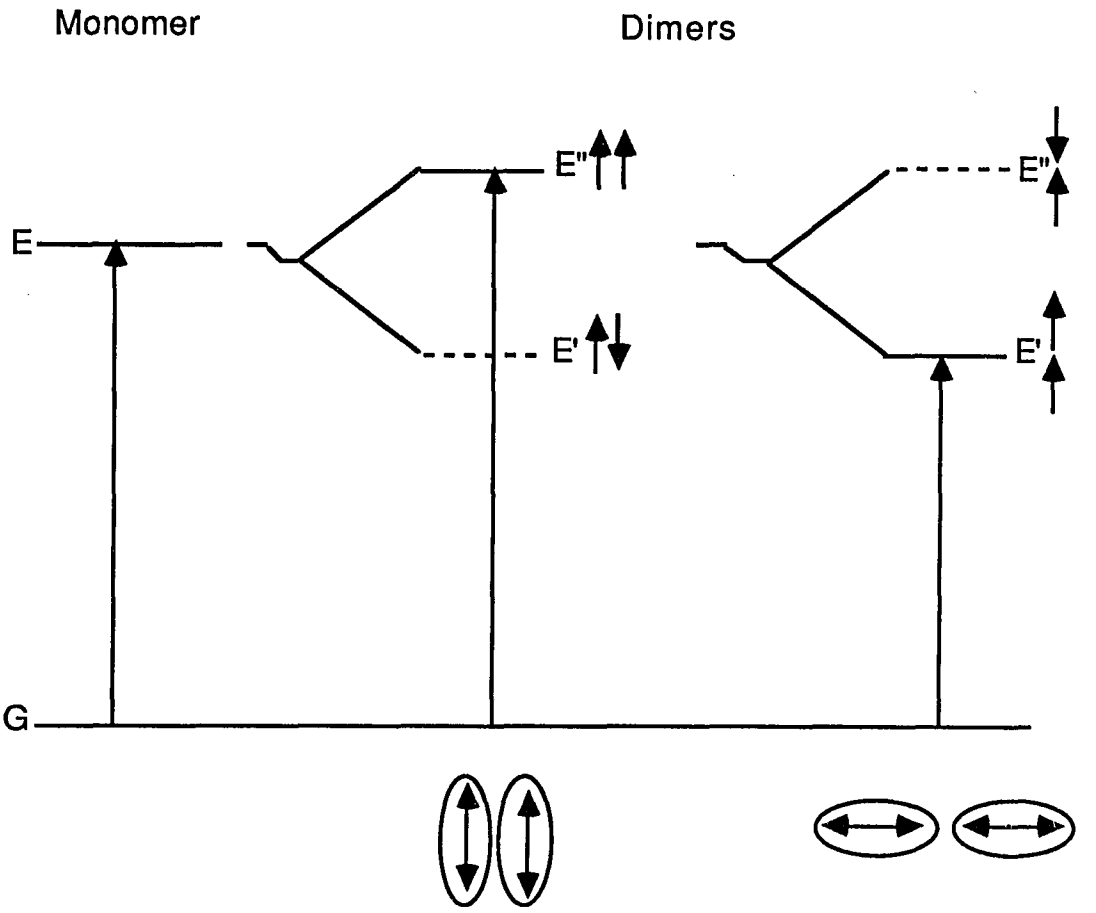

Fig. 2-2: Energy level diagram for a dye monomer and its dimeric exciton band showing two extreme geometrical arrangements of transition dipoles. The allowed transitions are from the ground state (G) to the excited states (E).

490nm. The J-band near 573 nm was found to appear suddenly at concentrations greater than about 3×10^{-3} M, with a half-width of ca. 160 cm^{-1} and molar extinction coefficient of approximately 2.6×10^5 $M^{-1}cm^{-1}$ (196). The sudden change from monomeric state to J-state was explained by Daltrozzo and coworkers (196). In agreement with their model, formation of the J-band is favored by low temperature and by increased concentration of dye or its counterion.

From recent work on the temperature dependence of aggregation of 1,1'-diethyl-2,2'-cyanine bromide in mixed solvents, Alfano and others (204) reported that when the temperature was lowered below 210 K the steady-state and time-resolved picosecond fluorescence spectra of the J-band aggregate state of the dye showed the appearance of two narrow bands centered at 572 and 577 nm in the fluorescence as well as the absorption spectra. They interpreted their observations as arising from the formation of the J-aggregate. Their measured relaxation time of the J-band is 20 ps as compared to 300 ps for the monomer band (204) . The splitting of the J-band into two components was earlier observed from luminescence studies by W. Cooper (205) who attributed it to two geometrical structures.

Semiconductor sensitization is an area where potentially-aggregate forming dyes can play a significant role. Much work, in fact, has been done to examine the energetics for dye-sensitzed photocurrent at semiconductor interfaces (206-212). Enhanced quantum efficiency of sensitized photocurrent of ZnO electrode by J-aggregate of cyanine dyes has been and reported (206). The adsorbed cyanine dyes serve the purpose to inject electrons into semiconductor substrates as a result of light not intrinsically absorbed by the semiconductor. The resultant mobile electrons can lead to

reactions at the surface of the semiconductor that have wide commercial implications.

CHAPTER 3

THEORIES OF THE RAMAN SCATTERING EFFECT

3.1 INTRODUCTION

Cabannes and Rocard showed immediately after the observation of the Raman effect that the essential features of the ordinary Raman effect can be interpreted classically (213). Van Vleck (214) in 1929 carried out an important expansion of the Kramers-Heisenberg dispersion equation and was able to demonstrate rigorously certain Raman selection rules. Though he was able to make some simplifications, when the sum over all virtual vibronic states that appeared in the dispersion theory was reduced to a sum over electronic states, the possibility of computing polarizabilities from basic electronic structure or, alternatively, interpreting scattering data in terms of electronic structure appeared remote. A review of the fundamental quantum-mechanical theory associated with the names of Heisenberg, Kramers, Dirac, and others can be found in the authoritative article by Placzek (215) published in 1934.

Placzek, in his polarizability theory (215), developed a comprehensive idea for vibrational Raman scattering, thus making classical considerations to be almost universally applicable in practical ordinary Raman spectroscopy. The application limits of his polarizability theory were recognized by Placzek himself who then gave much valuable advice for modifications of the theory which would extend its applicability to the

case of resonance Raman studies. Most of the developments since have occurred within the framework of this theory.

Shorygin and others (216,217) have reported semi-classical methods which combine the polarizability theory with the dispersion equation for treating the vibrational resonance Raman effect. Although these methods can give, at least qualitatively, satisfactory interpretations for certain important properties of the resonance Raman effect, the classical theory itself is unquestionably deficient in the treatment of atomic and molecular phenomena; a totally satisfactory description of the resonance effect can only be given by employing the methods of quantum mechanics.
In 1958 Behringer (218) elaborated upon the correct quantum-mechanical approach outlined by Van Vleck and Placzek and was able to employ Frank-Condon-principle arguments to provide some insight into Raman and resonance Raman intensities.

In the field of surface enhanced Raman scattering, extensive progress has been made in experimental and theoretical investigations of the phenomenon. Much of the work done so far has centered around two models, one electromagnetic and the other chemical involving charge transfer between the adsorbed molecules and the substrate. It has therefore become necessary to modify the general Raman scattering theory to account for these developments.

The development of the theory is now outlined, first for the general Raman case, followed by the developments made to include resonances. A theory we found necessary to give proper accounts of enhanced Raman and resonance Raman effects involving adsorbed aggregated dyes will be presented later in this chapter.

3.2 THE DEVELOPMENT OF THE GENERAL THEORY

Detailed derivations of the general theory are given in a number of standard texts. The classical model considers matter as containing separable charges held together by forces in addition to pure coulomb attractions. An oscillating separation of these charges results in the creation of an oscillating electric dipole. A molecule in an electromagnetic field will have its charge distribution periodically disturbed by the field which will lead to an oscillating separation of charges, creating an oscillating electric dipole. The resultant induced alternating dipole moment acts as a source of radiation and gives rise to light scattering.

The dipole moment is generally expressed as the dipole moment per unit volume (the polarization $\hat{p}$) and is proportional to the inducing field $\hat{E}$, to which it is mathematically connected, by the polarizability, α, of the particle,

$$\hat{p} = \alpha \hat{E} \tag{3.1}$$

Both $\hat{p}$ and $\hat{E}$ are vectors, while α is in general a tensor. It becomes a scalar quantity only in isotropic situations when the direction of $\hat{p}$ and $\hat{E}$ are the same. It also, in general, varies with the frequency of the field.

The inducing electromagnetic field is given by

$$\hat{E} = \hat{E}_0 \cos 2\pi\nu t \tag{3.2}$$

where ν is its frequency. The polarization then becomes

$$\hat{p} = \alpha \hat{E}_0 \cos 2\pi\nu t \tag{3.3}$$

The dipole radiates at the frequency of oscillation leading to Rayleigh scattering.

If the irradiated particle is itself undergoing some sort of periodic fluctuation (perhaps thermally excited) which is quite distinct from the

forced oscillatory charge separation, the polarizability will be different and it consists of two parts and may be written as

$$\alpha = \alpha_0 + \sum \alpha_n \cos 2\pi\nu_n t \qquad (3.4)$$

The first, α_0 is a constant which represents the static polarizability and the second is a sum of terms having the periodic time dependence of the normal frequencies of the system under consideration. The normal frequencies ν_n may be rotational or vibrational frequencies of a molecule, lattice frequencies of a crystal, or even, in Brilliouin scattering, acoustic frequencies of a solid.

With (3.2) and (3.4), Eq. (3.1) becomes

$$\hat{p} = \hat{E}_0 \alpha_0 \cos 2\pi\nu t + \hat{E}_0 \sum \alpha_n \cos 2\pi\nu t \cos 2\pi\nu_n t \qquad (3.5)$$

The second term on the r.h.s. may be expressed in terms of the "beat" frequencies $(\nu \pm \nu_n)$ by

$$\tfrac{1}{2}\hat{E}_0 \sum \alpha_n \{\cos 2\pi(\nu + \nu_n)t + \cos 2\pi(\nu - \nu_n)t\} \qquad (3.6)$$

These "beat" frequencies will appear weakly in the scattered radiation, and represent the Raman scattering phenomenon. Substituting Eq. (3.6) into (3.5) the general expression for the scattering becomes (8)

$$\hat{P} = \hat{E}_0 \alpha_0 \cos 2\pi\nu t + \tfrac{1}{2}\hat{E}_0 \sum \alpha_n \{\cos 2\pi(\nu + \nu_n)t + \cos 2\pi(\nu - \nu_n)t\} \qquad (3.7)$$

Equation (3.7) correctly predicts the major qualitative features of the Raman effect. The first term represents the component of the polarization having the frequency of the exciting field, and it accounts for Rayleigh scattering. The second term in which each variable component of the

polarizability, α_n, gives rise to components of the polarization having frequencies $(\nu - \nu_n)$ and $(\nu + \nu_n)$ accounts for the Stokes and anti-Stokes bands.

For the general anisotropic case the angular dependence of Rayleigh and Raman scattering as well as the polarization of the scattered light, are consequences of the tensor properties of α. The relationship between $\hat{p}$ and $\hat{E}$ in Eq. (3.1) becomes

$$\begin{aligned} p_x &= \alpha_{xx}E_x + \alpha_{xy}E_y + \alpha_{xz}E_z \\ P_y &= \alpha_{yx}E_x + \alpha_{yy}E_y + \alpha_{yz}E_z \\ P_z &= \alpha_{zx}E_x + \alpha_{zy}E_y + \alpha_{zz}E_z \end{aligned} \qquad (3.8)$$

From classical electromagnetic theory, the total energy scattered by the dipole moment per unit of time is given by (219)

$$I = \frac{2\overline{\ddot{p}^2}}{3c^2} \qquad (3.9)$$

where c is the velocity of light and the bar indicates the time average.

The classical description predicts the existence of the Raman effect and describes its dependence on the frequency of the exciting radiation, but does not predict the fact that some normal frequencies do not give rise to Raman scattering. This and other fine details must be deduced from quantum mechanics.

The quantum mechanical treatment considers the perturbation of the wave functions of the scattering molecule by the electric field of the incident light (frequency ν_0), and develops an expression for the induced electric moment matrix element P_{ab} (otherwise known as the induced transition moment) associated with the transition between two states, a and b, and defined by the following relation (210):

$$P_{ab} = \int \Psi_b^* P \Psi_a d\tau \qquad (3.10)$$

P_{ab} is the induced dipole moment, Ψ_a and Ψ_b are the time-independent wave functions of the states, and the integral is extended over the whole range of the coordinates.

The quantum mechanical result is of the form (10)

$$P_{ab} = \frac{1}{h} \sum_r \left(\frac{M_{ar} M_{rb}}{\nu_{ra} - \nu_0} + \frac{M_{ar} M_{rb}}{\nu_{rb} + \nu_0} \right) E \qquad (3.11)$$

Here h is Planck's constant, r denotes any level of the complete set belonging to the unperturbed molecules, ν_{ra} and ν_{rb} are the frequencies corresponding to the differences between the states denoted by the subscripts, M_{ar} and M_{rb} are corresponding transition moments, and E is the electric vector of the incident light. The states r which are sometimes referred to as "intermediate levels" or "third common levels" of the scattering, have "virtual" roles to play; no actual transition to any state r takes place in the normal Raman effect. P_{ab}^2 gives the intensity of the scattering between the states a and b (i.e. $a \rightarrow b$) according to the equation

$$I_{ab} = C(\nu_0 + \nu_{ab})^4 P_{ab}^2 \qquad (3.12)$$

in which C is a constant equal to $64\pi^2/(3c^2)$, with c the velocity of light and I_{ab} the intensity per molecule. The frequency $\nu_0 + \nu_{ab}$ is that of the scattered radiation. When a = b, the state of the scattering molecule remains unchanged and $\nu_{ab} = 0$ (the scattering is coherent Rayleigh scattering); when $a \neq b$, we have the incoherent Raman effect. Depending

upon whether the transition is to a lower or higher energy state, ν_{ab} can be negative or positive giving Stokes and anti-Stokes scattering, respectively.

It is clear from equations (3.11) and (3.12) that the dependence of the intensity of a Raman line upon the frequency ν_0 of the exciting light is defined not only by the factor $(\nu_0 + \nu_{ab})^4$, but also by the denominators in the summation over the states r which appear in the expression for P_{ab}^2. A choice of ν_0 in the visible region for colorless samples, makes ν_0 small compared with both ν_{ra} and ν_{rb}, the frequencies of electronic absorptions in the ultraviolet. Under such circumstances ($\nu_0 << \nu_{ra}$ or ν_{rb}) the Raman intensity simply becomes proportional to the fourth power of the frequency of the Raman line. On the other hand, if ν_0 is chosen to lie near a particular absorption frequency ν_{ra}, then the term containing the factor $1/(\nu_{ra} - \nu_0)$ will tend to become important in determining the intensity. I_{ab} should rise markedly as ν_0 approaches the absorption frequency. This is the resonance Raman effect. The actual calculation of intensities requires knowledge of electronic levels and the associated transition moments. The theory as presented so far cannot meet this quantitative aspect of the effect.

3.3 THE POLARIZABILITY THEORY (220)

It was pointed out by Placzek (215) that owing to the relatively large masses of the atomic nuclei, Raman scattering is normally due almost entirely to the electrons. The transference of energy between the incident light and the rotational or vibrational motions of the nuclei is thus brought about by the influence of these motions upon the polarizability of the "electron cloud" (10).

Provided that the frequency of the exciting radiation is far from any absorption band of the sample and greater than the frequency of the Raman transitions, the value of the polarizability for any instantaneous positions of the moving nuclei is practically identical with the value for stationary nuclei in the same positions. Within these limits, it is only the electronic polarizability which is responsible for the scattering of visible light by atoms and molecules, and from a classical point of view the Raman effect originates from the parametrical dependence of this polarizability on the instantaneous nuclear positions. Another condition is that the electronic state of the scattering molecule (in practice the ground state) shall be nondegenerate.

In quantum mechanical terms it is necessary to consider in place of the classical induced moment $\hat{p} = \alpha\hat{E}$ of Eq. (3.1), the matrix elements P_{ab} and α_{ab} for the transition a -> b in question. We can write

$$P_{ab} = (\int \psi_b(q) * \alpha\psi_a(q)d\tau)E = \alpha_{ab} \cdot E \qquad (3.13)$$

where α is the polarizability operator. The symbol q denotes the 3N normal coordinates of the system. The wave function Ψ is presumed to be expressed in terms of these coordinates.

The quantum mechanical expectation value of one of the matrix elements $\left[\alpha_{ij}\right]^{ab}$ associated with the transition $a \rightarrow b$ is

$$\left[\alpha_{ij}\right]^{ab} = \int \psi^*_b(q)\alpha_{ij}\psi_a(q)dq \qquad (3.14)$$

The wave functions Ψ which appear in (3.13) and (3.14), in the Born-Oppenheimer approximation, are the products of wave functions ϕ, each of which depends on only one normal coordinate. That is

$$\psi_a = \prod_{n=1}^{3N} \phi_n(q_n, v_n) \qquad (3.15)$$

with a similar expression for Ψ_b. The quantity v_n is a quantum number associated with the wave function ϕ_n. The operator α_{ij} is now assumed to be a function of the normal coordinates and is expanded into a Taylor series in these coordinates. We get

$$\alpha_{ij}(q) = (\alpha_{ij})_0 + \sum_{n=1}^{3N} \left(\frac{\partial \alpha_{ij}}{\partial q_n}\right)_0 q_n + \cdots \qquad (3.16)$$

Substituting Eq. (3.16) and the expressions for Ψ_a and Ψ_b into Eq. (3.14) with simplification of notation by dropping the subscript ij and writing $\phi_n(q_n, v_n)$ simply as $\phi(v_n)$, we get

$$[\alpha_{ij}]^{ab} = (\alpha_0) \prod_{n=1}^{3N} \int \phi(v'_n)\phi(v_n) dq_n$$
$$+ \sum_{n=1}^{3N} \left(\frac{\partial \alpha}{\partial q_n}\right)_0 \prod_{m \neq n} \int \phi(v'_m)\phi(v_m) dq_m \cdot \int \phi(v'_n) q_n \phi(v_n) dq_n \qquad (3.17)$$

In this expression, the operator α_0 corresponds to the static polarizability and is a constant. The integrals which multiply it equal zero if $v'_n \neq v_n$ and equal one if $v'_n = v_n$. In the latter case we are left with a constant α_0 which corresponds to Rayleigh scattering as in the classical treatment. In the same way the integrals $\int \phi(v'_m)\phi(v_m) dq_m$ equal zero if $v'_m \neq v_m$ and equal one if $v'_m = v_m$, reducing Eq. (3.17) to

$$[\alpha_{ij}]^{ab} = \alpha_0 + \sum_{n=1}^{3N} \left(\frac{\partial \alpha}{\partial q_n}\right) \int \phi(v'_n) q_n \phi(v_n) dq_n \qquad (3.18)$$

With the harmonic oscillator approximation, the integral in Eq. (13.18) can be evaluated, and with the Boltzmann expression for the population density of the energy levels, an expression for the scattering intensity in terms of $(\partial \alpha / \partial q)_0$ may be derived. After a lengthy calculation

the power scattered per molecule into a given Stokes Raman band, when the molecule is illuminated with I_0 watts cm^{-2} is (221)

$$I = \frac{K}{M} \frac{I_0(\nu_0 - \nu)^4 g(45\alpha^2 + 7\gamma^2)}{\nu[1 - \exp(-h\nu / kT]} \qquad (3.19)$$

In this expression g is the degeneracy of the molecular level giving rise to the Raman scattering, ν_0 the exciting frequency, ν the Raman frequency, M the molecular mass, and K is a known constant. The incident light may have arbitrary polarization and γ is the anisotropy invariant of the polarizability tensor α. The quantities α and γ are given by (10).

$$\bar{\alpha} = \frac{1}{3}\left[\left(\frac{\partial\alpha_x}{(\partial q)}\right)_0 + \left(\frac{\partial\alpha_y}{(\partial q)}\right)_0 + \left(\frac{\partial\alpha_z}{(\partial q)}\right)_0\right] \qquad (3.20)$$

$$\gamma^2 = \frac{1}{2}\left[\left(\frac{\partial\alpha_x}{\partial q} - \frac{\partial\alpha_y}{\partial q}\right)^2 + \left(\frac{\partial\alpha_y}{\partial q} - \frac{\partial\alpha_z}{\partial q}\right)^2 + \left(\frac{\partial\alpha_z}{\partial q} - \frac{\partial\alpha_x}{\partial q}\right)^2\right] \qquad (3.21)$$

In the derivation of Eq. (3.19) complete randomness of orientation was assumed hence it is valid only for gases and to a limited degree, for non-polar liquids.

By making some rather drastic assumptions, it is possible to use equations (3.19), (3.20) and (3.21) to derive bond parameters. A thorough discussion is given by Hester (10) and also by Behringer (12) who discussed the polarizability theory and its limitations.

3.4 THE VIBRONIC THEORY AND RAMAN INTENSITIES

In addition to its restrictive nature, the polarizability theory failed to account for resonance or near-resonance scattering, in particular the resonance Raman effect. With a rise in interest in the resonance Raman effect, a return to the dispersion theory, which in modified forms is valid under resonance conditions, was inevitable.

Studies done in the field of vibronic spectroscopy have found that, in the first approximation, it is the "forbidden" (vibrationally induced) intensities in allowed electronic transitions that are responsible for Raman intensities (222). It has been found that in the resonance Raman effect in particular, it is the "forbidden" character in the allowed electronic band near resonance that determines the resonance Raman intensities. When the results of the vibronic theory are introduced directly into the dispersion theory expression for the components of the polarizability an equation is recovered which gives the selection rules directly and in addition provides a framework for studying a variety of other properties (223). Since the theory is well discussed elsewhere (223), it is not reproduced here.

3.5 VIBRO-EXCITON THEORY FOR AGGREGATED DYES

3.5.1 Introduction

To account for the observed Raman scattering of molecules on surfaces several theoretical treatments of the proposed enhancement mechanisms have been put forth (60-66). Many of these treatments are mainly centered on two models, as mentioned in the general introduction Chapter 1, one electromagnetic and the other chemical. In the electromagnetic model, small protrusions on surfaces which support optical frequency surface plasmon resonances with consequent strong local

enhancement of both the electric field of the Raman exciting radiation and the radiation induced dipole moment of the adsorbed molecules, are the sources for many of the gross characteristics of SERS (60). The electromagnetic model accounts for SERS active substrates, the need for surface roughness (224), SERS in colloidal active metal solution (51), the existence of the effect beyond the first monolayer (225,226) and a correlation between excitation frequency and very low frequency vibrations of the metal particles (227).

A number of investigation (29,228-231) have indicated SERS contributions from other mechanisms which the electrodynamic model cannot fully rationalize, which is suggestive of some mechanism other than electrodynamic enhancement. The chemical mechanisms, which introduce a chemical interaction character into the theory, are used to explain the adsorbed molecule specificity exhibited in SERS. Important in this regard have been charge transfer theories involving the substrate and either the ground or excited state of the adsorbed molecule (63,228).

Two distinct charge-transfer mechanisms have been suggested, both involving some kind of charge transfer between the molecule and the substrate. One mechanism, for ground-state models, proposed that the transferred charge affects the surface plasmon modes, and modulation of the charge transfer by molecular vibrations leads to a corresponding charge in the surface plasmon contribution to light scattering by the metal surface (63,230,232). Strongly enhanced Raman sidebands are proposed as a result of the amplitude modulation of the scattered ratiation. The other mechanisms, for the excited state models, proposed that there exists a charge-transfer transition, where an electron is excited from a filled state located at one of the charge-transfer partners to an empty state located at the

other one. The virtual excitations to the charge transfer state can be in partial resonance with the exciting radiation when the energy of the exciting photon matches the charge-transfer transition energy. This yields large contributions to the Raman scattering polarizability tensor of the combined metal-molecule system (61,233,234). In this sense the surface enhancement is viewed as a kind of resonance Raman scattering.

Detailed SERS and/or surface resonance Raman scattering (SRRS) theoretical formulations have not been able to sufficiently explain enhanced Raman scattering by dye molecules on surfaces. Interpretation of excitation spectra of surface Raman bands of dyes have incorporated SERS and SRRS mechanisms, (66,235-238) as well as a charge transfer mechanisms (239). A characteristic of surface Raman scattering by dyes has been shifts of excitation maxima associated with enhanced resonance Raman scattering relative to the excitation maxima for the dyes in solution. Generally, the shifts have been observed to be to the red. The explanations for such shifts have been substrate induced shifts in molecular states (235) and/or dense packing on the substrate (236). Yamada *et al.* (239) have suggested the excitation maximum shift as due to a charge transfer resonance evidenced by an overlap of the absorption peak of adsorbed dye and the substrate absorption maximum. Siiman *et al.* (237), in addition, have reported that the excitation profile peaks for SRRS at high dye concentration shift further to the red and explains such shifts as due to the emergence of dipole-dipole interactions as the concentration increase.

In our laboratory, enhanced Raman scattering of cyanine dyes on silver surfaces has been investigated (36,54,55,71). Molecular exciton theory has been extensively applied in the study of changes in the absorption spectrum upon aggregation for such dyes (186). We have interpreted our

observations of increased Raman scattering by cyanines when the incident exciting radiation is in resonance with the shifted aggregated absorption band as due to a RRS with the molecular exciton states of the aggregate which acts (possibly) in concert with the electromagnetic mechanism.

We have advanced a Raman enhancement theory for aggregated molecules fundamentally based on the formation of molecular vibro-exciton levels which function as excited states in the vibrational Raman problem (72). Vibrational selection rules were determined and an intrinsic enhancement, of magnitude N, for an aggregated structure containing N molecules, was associated with the increased polarizability of the aggregate. In addition, a further enhancement associated with a resonance between exciting radiation and the aggregate absorption band was briefly discussed. A Herzberg-Teller treatment was an integral aspect of the treatment of the vibronic problem.

In one of the aforementioned articles (Ref. 72), only states of the molecular species were used, and substrate states were ignored. In other words, the affect of aggregation on the Raman scattering process, whether occurring in homogeneous solution or on the surface of a substrate, was viewed to be identical.

What follows uses the findings of Ref. 72 and expansions of the theory (to include a metallic substrate with an energy state of its own that may participate in the enhancement process). The expansion of the theory will first be discussed to provide the basis for some of the experiments performed in the investigations to be presented in Chapter 4.

3.5.2 Molecular Vibro-Exciton Theory Applied to Raman Scattering.

A. Vibro-Exciton Wavefunctions.

For this expansion of the theory, it is recognized that the primary coupling that leads to a difference between the Raman scattering problems for aggregated molecules in the absence and in the presence of a substrate, is the mixing of zeroth-order state functions caused by adsorbate-substrate interaction. For the latter situation, the "corrected" wavefunctions are linear combinations of adsorbed aggregate and substrate zeroth-order stationary states (37,63,240).

Although in the present treatment of the scattering problem the mixing of aggregate and substrate states is acknowledged, it is assumed to be sufficiently small as only to be a higher order perturbation on the wavefunctions, but principally responsible for "resonances" in the transfer of charge or energy between the adsorbed aggregate and the substrate. Thus, in the following, the stationary-state wavefunctions for the aggregate are used in the Raman scattering problem and allowed to "resonate" with the substrate state-functions.

The molecular vibro-exciton approach was thoroughly developed in Ref. 72. Briefly, the theory applies to a finite aggregate structure consisting of N molecules. The excitonic state is developed from the premise that only one molecule of the aggregate is excited and that a superposition of spatially separate molecular wavefunctions must be taken since quantum mechanically we are unable to specify which molecule is excited. The Hamiltonian for the aggregated adsorbate is

$$H = \sum_{n=1}^{N} \left(H_n + \sum_{m>n} V_{mn} \right) \qquad (3.22)$$

where H_n represents the hamiltonian operator for molecule n and V_{mn} is the interaction potential between molecules m and n where m is any of the other molecules in the aggregate besides molecule n, i.e., m can have the values 1 to N with the exception of n.

After a somewhat lengthy development, it was shown in Ref. 72 that the normalized vibro-exciton wavefunction is expressed as:

$$\Psi_{ki} = \left[\frac{2}{N+1}\right]^{1/2} \sum_{n} \theta_{ni} \sin \frac{\pi nk}{N+1} \tag{3.23}$$

where k is the electronic quantum number label which can have integer values 1 to N, the sum over n (the molecule label) also goes from 1 to N, and i is the vibrational quantum number label which implicitly specifies the number of quanta i in a particular vibrational mode. θ_{ni} in Eq. (3.23) is the antisymmetrized function

$$\theta_{ni} = \{(SN)!\}^{-1/2} \sum_{\nu} (-1)^{\nu} P_{\nu} \phi_{ni} \tag{3.24}$$

in which S is the number of π-electrons, P_ν is the antisymmetrization operator, and ν is the number of pair permutations required to recover an arbitrary fiducial arrangement of electrons among the molecules. In addition, ϕ_{ni} is a particular excitation arrangement identified as

$$\phi_{ni} = \varphi^*_{ni} \left\{ \prod_{\substack{l=1 \\ l \neq n}}^{N} \varphi_{li} \right\} \tag{3.25}$$

where φ^*_{ni} is an excited vibronic state of molecule n, and i is the composite vibrational quantum number identified above. Ψ_{ki} is is now used in Raman scattering theory as the excited state wavefunction.

B. Aggregate/Surface Raman Scattering Theory

1. General

The general expression for the Raman scattering intensity is given by second-order perturbation theory (219,241) as

$$I(\kappa') = \frac{\tilde{N} I \kappa'^4}{16\pi^2 \varepsilon_0^2} \left| \sum_r \left\{ \frac{(\vec{\mu}^{mr} \cdot \vec{e}')(\vec{\mu}^{ro} \cdot \vec{e})}{E_{ro} - \hbar c \kappa} + \frac{(\vec{\mu}^{mr} \cdot \vec{e})(\vec{\mu}^{ro} \cdot \vec{e}')}{E_{ro} + \hbar c \kappa'} \right\} \right|^2 \qquad (3.26)$$

where the scattered radiation's wave vector is κ'; $\tilde{N}$ is the number of scattering species; m represents the upper state in the scattering process; the sum is over excited states r; the μ's are transition dipole moment vectors; the e's are microscopic electric field strength vectors, and E_{ro} is equal to the energy difference, $E_r - E_o$, between the upper state r and the ground state o.

In terms of the polarizability, the Raman intensity becomes

$$I(\vec{\kappa}') = \frac{\tilde{N} I \kappa'^4}{16\pi^2 \varepsilon_0^2} e'_i e_j e'_\kappa \bar{e}_\ell \alpha_{ij}^{mo}(\omega, \omega') \bar{\alpha}_{\kappa\ell}^{mo}(\omega, -\omega') \qquad (3.27)$$

where i, j, κ, and ℓ are laboratory coordinates, and ω and ω' are the initial and scattered radiation's frequencies, respectively.

The aggregate-substrate interaction is evidenced by a mixing of their quantum states. In addition, the single molecule states are perturbed from those of the "crude" adiabatic approximation (242) by nonadiabatic terms in the hamiltonian for the isolated molecule. The former reality, as discussed earlier, is treated as a higher-order perturbation phenomenon which evidences itself in nonzero energy and/or charge-transfer transition

probabilities between aggregate and substrate states. The latter phenomenon has been treated by the Herzberg-Teller approximation (37,63,72,221), in which the single molecule's vibronic states are defined by first-order perturbation theory.

In this discussion, as in those references mentioned immediately above, mixing of the ground and excited single molecule states with nearby states, due to nonadiabatic terms in the hamiltonian, is taken into account by the respective terms

$$|\varphi_g\rangle = |\varphi_g^0\rangle + \sum_\alpha \sum_{t \neq g} \frac{h_{gt}^\alpha Q_\alpha}{E_g^0 - E_t^0} |\varphi_t^0\rangle \tag{3.28}$$

and

$$|\varphi_r\rangle = |\varphi_r^0\rangle + \sum_\alpha \sum_{s \neq r} \frac{h_{rs}^\alpha Q_\alpha}{E_r^0 - E_s^0} |\varphi_s^0\rangle \tag{3.29}$$

where, in Eq. (3.28), g represents the ground state quantum number (instead of the subscript o used in Eq. (3.26)), t represents states that can mix with the ground state of the molecule and are thus taken to be metal substrate states which can lie close in energy to the ground state (37), h_{gt}^α is the coupling term between the states g and t (for the molecule with equilibrium ground state configuration (as indicated by the superscript o)), and Q_α is the displacement of mode α. In Eq. (3.29), r represents an excited vibronic state of the molecule, while s is taken to represent excited vibronic states of the molecule as well as metal states that can be near resonant with a particular single molecule excited state r. The other terms in Eq. (3.29) are analogous to those in Eq. (3.28).

Upon substituting the last two equations into the expression for the polarizability, the relationship originally derived by Tang and Albrecht (221) is found:

$$\alpha_{ij}^{gv',\,gv''} = A + B + C \tag{3.30}$$

where

$$A = \sum_{r,v} \left[\frac{[M_i]^0_{g,r}[M_j]^0_{g,r}}{E_{rg} + \varepsilon_{rv,\,gv''} - \hbar c\kappa} + \frac{[M_i]^0_{g,r}[M_j]^0_{g,r}}{E_{rg} + \varepsilon_{rv,\,gv'} + \hbar c\kappa} \right] \times$$

$$\langle \chi_{gv'} | \chi_{rv} \rangle \langle \chi_{rv} | \chi_{gv''} \rangle \tag{3.31}$$

$$B = \sum_{r,v} \sum_{\alpha} \sum_{s \neq r,\,g} \left\{ \left[\frac{[M_j]^0_{g,s}[M_i]^0_{g,r} h^{\alpha}_{rs}}{E_{rg} + \varepsilon_{rv,gv''} - \hbar c\kappa} + \frac{[M_i]^0_{g,s}[M_j]^0_{g,r} h^{\alpha}_{rs}}{E_{rg} + \varepsilon_{rv,gv'} + \hbar c\kappa} \right] \times \right.$$

$$\frac{\langle \chi_{gv'} | \chi_{rv} \rangle \langle \chi_{rv} | Q_{\alpha} | \chi_{gv''} \rangle}{E^0_r - E^0_s} + \left[\frac{[M_i]^0_{g,s}[M_j]^0_{g,r} h^{\alpha}_{rs}}{E_{rg} + \varepsilon_{rv,\,gv''} - \hbar c\kappa} + \right.$$

$$\left. \left. \frac{[M_j]^0_{g,s}[M_i]^0_{g,r} h^{\alpha}_{rs}}{E_{rg} + \varepsilon_{rv,gv'} + \hbar c\kappa} \right] \frac{\langle \chi_{gv'} | Q_{\alpha} | \chi_{rv} \rangle \langle \chi_{rv} | \chi_{gv''} \rangle}{E^0_r - E^0_s} \right\} \tag{3.32}$$

and

$$C = \sum_{r,v} \sum_{\alpha} \sum_{t \neq r,g} \left\{ \left[\frac{[M_j]^0_{t,r}[M_i]^0_{g,r} h^0_{gt}}{E_{rg} + \varepsilon_{rv,\,gv''} - \hbar c\kappa} + \frac{[M_i]^0_{t,r}[M_j]^0_{g,r} h^{\alpha}_{gt}}{E_{rg} + \varepsilon_{rv,\,gv'} + \hbar c\kappa} \right] \times \right.$$

$$\frac{\langle \chi_{gv'} | \chi_{rv} \rangle \langle \chi_{rv} | Q_{\alpha} | \chi_{gv''} \rangle}{E^0_g - E^0_t} + \left[\frac{[M_i]^0_{t,r}[M_j]^0_{g,r} h^{\alpha}_{gt}}{E_{rg} + \varepsilon_{rv,\,gv''} - \hbar c\kappa} + \right.$$

$$\frac{[M_j]^0_{t,r}\,[M_i]^0_{g,r}\,h^{\alpha}_{gt}}{E_{rg}+\varepsilon_{rv,gv'}+\hbar c\kappa}\left]\frac{\langle \chi_{gv'}|Q_\alpha|\chi_{rv}\rangle\langle\chi_{rv}|\chi_{gv''}\rangle}{E^0_g-E^0_t}\right\} \qquad (3.33)$$

where the [M]'s are the electric dipole moment vectors integrated over electronic coordinates for the ground state equilibrium configuration, v is the excited molecular state vibrational quantum number, v' and v" refer to the upper and lower vibrational states in the scattering problem, the χ's are the vibrational wavefunctions, and ε, with its respective subscripts, is the vibrational energy difference referenced to the ground state g.

The contributions to the polarizability (Eq. (3.30)) will first be dealt with in terms of their general significance before they are specialized to the case of aggregated molecules on surfaces. Starting with the A contribution, one can expect that when the exciting frequency is close to a "resonance," the v dependence in the denominator of the two contributing factors cannot be ignored, and as a result, closure over the vibrational states (see Ref. 72) cannot be applied, leading to contribution of vibrational overlap integrals between excited states and the vibrational levels of the molecular ground state. The excited states are not limited to single molecule states as the summation over r also includes substrate states, complex vibronic states of the aggregate, as well as vibronic states associated with "chemical" interaction between the adsorbate and the substrate. For the present treatment of the scattering problem, the substrate is considered to be a metal, and, in line with the treatment of Lombardi *et al.* (37), and Lippitsch (63), the "chemical" interaction is attributed to a "charge-transfer" type interaction involving metal states close to the Fermi level; these states presumably have small overlap with ground state molecular, vibrational levels.

When only a few interacting excited states are present, the A term should make itself evident by the resonance enhancement of only a few vibrational bands in the Raman spectrum. The A term, because of its dependence on overlap integrals, has been termed the Franck-Condon term (62).

The B term, defined as it is in terms of a summation over states s close to the excited molecule state r (as evidenced by the term $E^{o}_{r} - E^{o}_{s}$ appearing in the denominator), is expected to depend strongly on metal states in the vicinity of the Fermi level. This term, however, is most significant in the nonresonant Raman case were vibrational closure relegates the A term to make a contribution only to Rayleigh scattering. Intensity borrowing through the h^{α}_{rs} factor allows B to contribute to Raman scattering. In addition, because of the explicit dependence of the intensity borrowing factor on the vibrational mode (α), enhancements from this term applies to the single molecule Raman modes. One notes that because state s can be a metal state, whose position (in the conduct of acquiring a Raman spectrum on an electrode, for example) is typically varied to maximize the Raman signal, normally one acquires a spectrum on an electrode which is more intense than, for example, a colloidal silver system because of the tuning into resonance through the $E^{o}_{r} - E^{o}_{s}$ term. Experiments in our laboratory, in fact, have shown effectively a factor of $1x10^{2}$ greater enhancement in electrode systems as compared to colloidal silver systems (55). It also follows that the enhancement on most substrates (whether colloidal particles or electrodes) is expected to be greater than that due to the "intrinsic" enhancement, attendant with forming an aggregate containing N

molecules, that would be the sole avenue for enhancement for homogeneous solution aggregates.

The C term, like the B term, has significance only in the nonresonant Raman case. However, the experiments that have given birth to the present theoretical issue have involved surface Raman scattering of the cyanine dyes. These dyes function as spectral sensitizers where they absorb from their ground states and inject electrons into substrates from their first excited electronic states. As a result, in this treatment, we assume that the transition moments between the metal states and excited molecular states are zero (i.e., $[M]^0_{t,r}=0$). Thus, the C term is not important in this treatment of surface Raman scattering.

2. Specialization to Aggregated Molecules

Numerous experiments have shown significant changes in the absorption spectrum of many molecules upon aggregation. For the cyanine dyes, though, both "blue" and "red" absorption bands can form, the "red" band, however, is often most prominent on surfaces (114). The theory of this phenomenon has been skillfully addressed by Davydov (186), Kasha and others (180-182,243,244).

Aggregate formation as presented here is the enabler of the Raman enhancement for both resonance and nonresonance (normal) Raman scattering. In Ref. 72 the J-aggregate absorption feature, which typically is very sharp, was assigned its central frequency ν_J for the nonresonance case. For the resonance case, however, the A term of the polarizability becomes dominant as a result of the energy difference $E_{rg} - \hbar c\kappa$ in Eq. (3.30), approaching zero.

The A term, specialized to the aggregated molecule model is given by Eq. (3.34):

$$A = \frac{i}{h}\left[\frac{2}{(N+1)}\right]\sum_{k,v}\cot^2[\pi k/2(N+1)]\left\{\frac{1}{\nu_{kv,ov''}-\nu_0+i\Gamma_0}+\right.$$

$$\left.\frac{1}{\nu_{kv,ov'}+\nu_0+i\Gamma_v}\right\}[M_i]^0_{0,1}[M_j]^0_{0,1}\langle\chi_{ov''}|\chi_{1v}\rangle\langle\chi_{1v}|\chi_{ov'}\rangle \qquad (3.34)$$

in which the quantum number k is odd valued in the range 1 to N and labels the exciton states, and $i\Gamma_v$ is the phenomenological, imaginary phase factor related to the line width of the Raman transition.

When the actual vibro-excitonic energies, $h\nu_{kv,ov''}$, which include the dipole-dipole interaction energy (72), is used in the denorminator of the A term (properly accompanied by the phenomenological, imaginary phase factor $i\Gamma_v$ related to the line width of the Raman transition), one can sum over vibro-exciton states (under appropriate conditions) and determine, through resonance tuning, the dipole-dipole interaction energy for a particular cyanine dye.

The B term, important in the nonresonant case, where closure over excited states is allowed, takes the following form upon using the vibro-excitonic wavefunction:

$$B'' = \frac{2(N+1)}{h}\left[\frac{\nu_j}{\nu_j^2-\nu_0^2}\right]\left\{\sum_{s,\alpha}{}' h^{\alpha}_{1s}\left[[M_j]^0_{0,s}[M_i]^0_{0,1}+\right.\right.$$

$$\left.\left.[M_i]^0_{0,s}[M_j]^0_{0,1}\right]\frac{\langle\chi_{ov'}|Q_\alpha|\chi_{ov''}\rangle}{E^0_1-E^0_s}\right\} \qquad (3.35)$$

where the "prime" on the summation over s excludes state r=1, and the "double-prime," following the notation of Ref. 72, acknowledges that a

sequence of two definitions have led to this final result. The "1" labels the single molecule's first excited state, while the s is a metal state in the vicinity of the molecular state.

CHAPTER 4

EXPERIMENTAL

4.1 INTRODUCTION

Substrate surface potential experimental studies, to be reported, aim at exploiting the theory to determine the "intrinsic" enhancement due to the number of aggregated cyanine dye molecules, N, adsorbed on substrates, and also to test the theory by studying the dependency of the Raman intensities on the separation between the first excited singlet level of the single molecule and the substrate state, s (i.e. $E_1^0 - E_s^0$) which appears in Eq. (3.35).

For aggregated cyanine dyes, it is found that when the incident radiation overlaps the J-aggregate absorption, certain bands can be identified as gaining their intensity from the A term of the polarizability alone. Since the A term (Eq. (3.34)) does not depend on the factor $E_r^0 - E_s^0$ in its denominator while B" (Eq. (3.35)) does, and, in addition, all intensities are proportional to the concentration of scattering species (N) and the frequency of the particular Raman band raised to the fourth power, bands that depend only on A can be used as internal standards to isolate the $E_r^0 - E_s^0$ dependence of other Raman bands (71). This possibility allows us to extract from surface potential dependent resonance found for Raman band intensities, the shifting of exciton states into energy coincidence with the exciting radiation as a result of changes in the static electric field at the electrode surface (71). Experimental testing of these conclusions is provided

through investigation of the potential dependence of Raman bands of aggregated cyanines.

Most of the experiments were performed for two or more of the cyanine dyes and although various substrates were tried for various reasons the experiments reported here will center mainly around silver as the substrate. Some absorption studies were also done mainly to select preferred media and circumstances for inducing the J-aggregate formation.

4.2 EXPERIMENTAL SYSTEMS

4.2.1 Chemicals

Six cyanine dyes were used in several of our studies. Their structures are shown in Fig. 4-1. The dyes used were of the highest quality commercially available. The 1,1'-diethyl-2,2'-cyanine chloride and its corresponding iodide were from Eastman Kodak; while the iodide was used as supplied, the chloride was purified further by recrystallization. The other cyanine samples were supplied by the Accurate Chemical and Scientific Corp., Westbury, N.Y.

The silver nitrate and sodium borohydride used to prepare the silver sol were purchased from Aldrich Chemical Company and J. T. Baker Chemical Co., respectively. Both were of the highest purity commercially available and were used without further purification. The zinc oxide used to prepare the semiconductor electrode was a product of Johnson Matthey Chemical Limited, England, distributed by Alfa Products. The gold and silver wire,which were also used for electrodes, were of Gold Label quality from Aldrich Chemical Company, while the porous plug type calomel reference miniature electrodes was purchased from Fisher Scientific Company. The main source of the certified A.C.S. labelled potassium

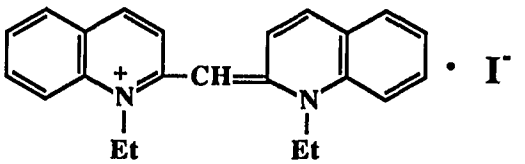

DYE 4-1: 1,1'-DIETHYL-2,2'-CYANINE (2,2'-CYANINE)

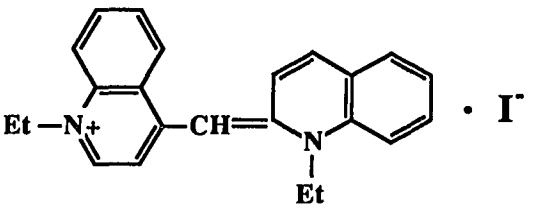

DYE 4-II: 1,1'-DIETHYL-2,4'-CYANINE IODIDE (2,4'-CYANINE)

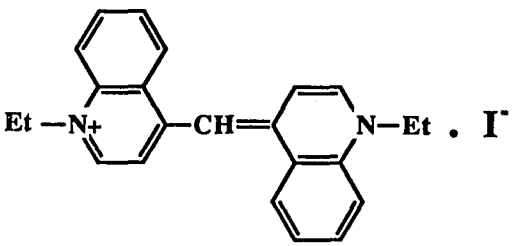

DYE 4-III: 1,1'-DIETHYL-4,4'-CYANINE IODIDE (4,4'-CYANINE)

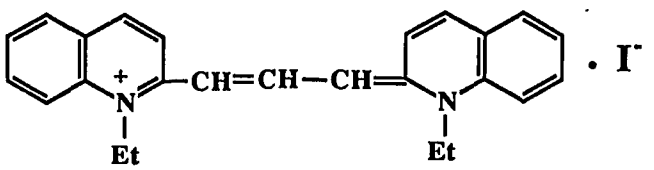

DYE 4-IV: 1,1'-DIETHYL-2,2'-CARBOCYANINE IODIDE (2,2'-CARBOCYANINE)

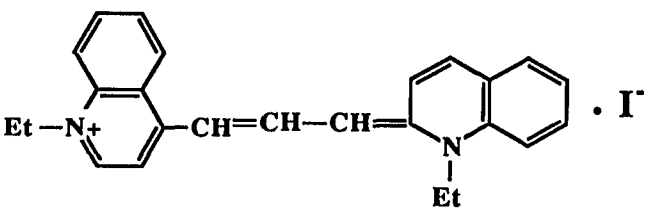

DYE 4-V: 1,1'-DIETHYL-2,4'-CARBOCYANINE IODIDE (2,4'-CARBOCYANINE)

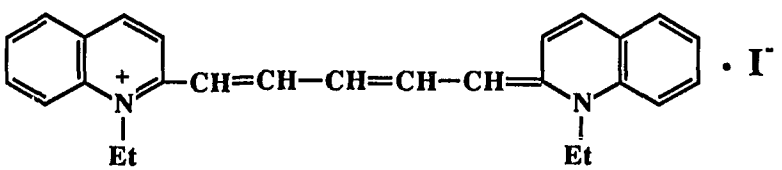

DYE 4-VI: 1,1'-DIETHYL-2,2'-DICARBOCYANINE IODIDE

Fig. 4-1: The Quino-Cyanine Dyes.

halides used in preparing the electrolytes was Amend Drug and Chemical Co. The other chemical systems used will be mentioned in the text.

4.2.2. Apparatus

Fig. 4-2 is a schematic of the equipment used to acquire Raman scattering spectra. Three laser systems were used and the diagram shows one of them, a Coherent Model 599 tunable dye laser being pumped by a Spectra Physics Model 2000 argon-ion laser. Specifically, Rhodamine 6G, supplied by the Exciton Chemical Co. was the dye used. The other laser systems used, but not shown in the diagram, are a Coherent Model 52 argon-ion laser to supply the blue (488 nm) and green (514.5 nm) radiation, and the Spectra Physics Model 166 krypton laser which supplied the red (647.1 nm) radiation. Ealing interference filters were used for the blue and green lines.

The electrochemical cell for the surface Raman studies was designed and built from pyrex glass in the department. The basic character of the cell is that reported in Ref. (3). The quartz cuvettes used for the sol and solution Raman spectra were supplied by Markson Corp., Phoeniz, AZ.

Bioanalytical systems (BAS) Model CV27 voltammograph and a Princeton Applied Research Corporation (PARC) Model 175 wave form programmer were used for potentiostatic control.

A Spex 1404 double monochromator, in conjunction with a RCA 31034 photomultiplier, a Uni-Photon System single photon amplifier discriminator, all interfaced to a Digital 11/23 minicomputer was used to acquire the spectra.

The uv/vis absorption and reflectance studies were acquired with a Perkin-Elmer Lambda 3A uv/vis spectrophotometer.

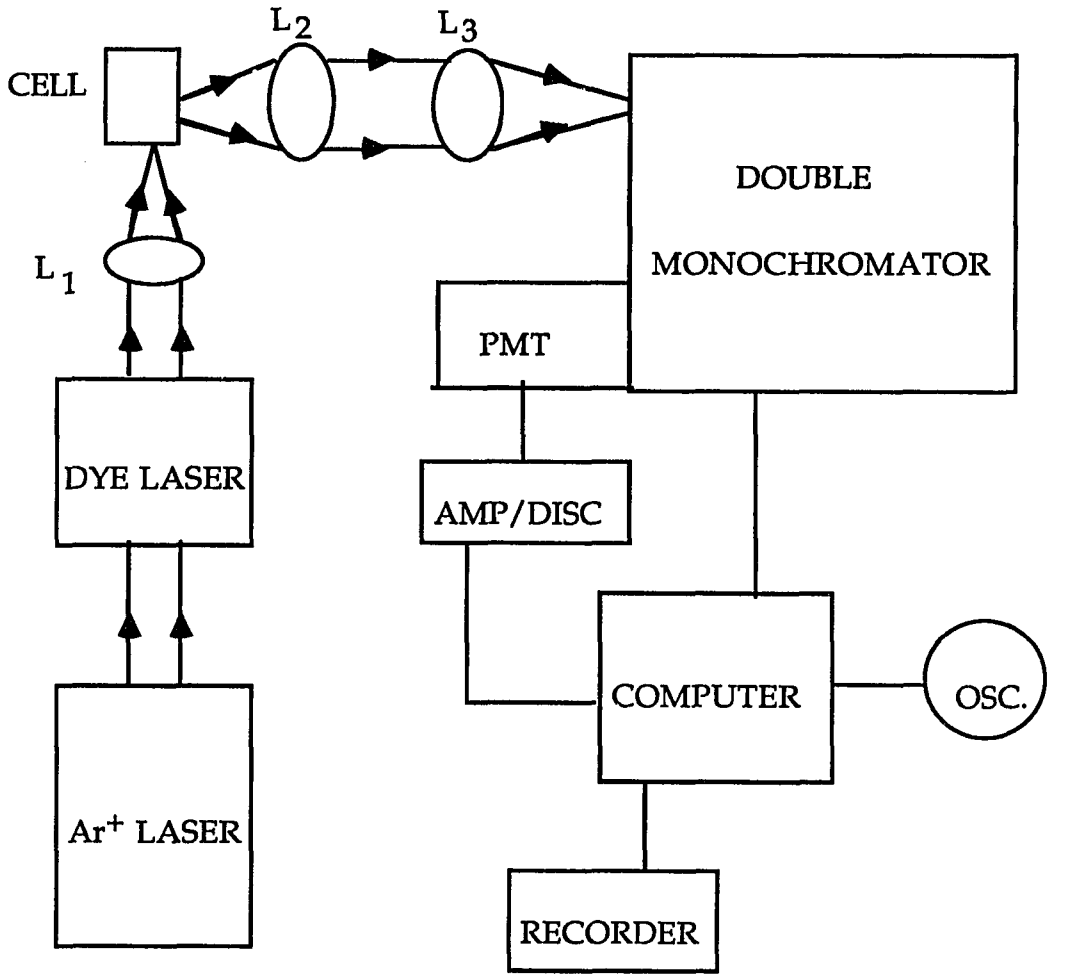

Fig. 4-2: Experimental set-up used for the Raman experiments. The L's are focusing lenses.

4.3 SAMPLE PREPARATIONS AND EXPERIMENTAL TECHNIQUES

Absorption spectra were taken of the aqueous dye solutions and mixtures of dye and colloid solutions at different concentrations. Experiments were also done using the dye solutions in the presence of various concentrations of potassium halides (KCl, KBr and KI).

Reflectance spectra were taken of the dyes, adsorbed onto ZnO polycrystalline pellets. Two drops of the 10^{-4} M aqueous solution of the dye were put on a pellet and allowed to dry before a spectrum was taken. In all cases the spectra were taken against suitable references which were also prepared in a similar manner but excluding the substance of interest.

The Raman scattering of the cyanines in aqueous solution in silver sol were acquired with the samples kept in 4 cc cuvettes. Some of the cyanine dyes were found to be thermally unstable in aqueous solution. Raman spectra could not be taken until the techniques were modified. For these samples - 2,4'-cyanine and 2,2'-carbocyanine - a flow cell was constructed as shown in Fig. 4.3. In this case a special cuvette with two leads was used. Both leads were joined to a reservoir containing the bulk sample solution. The one which filled the cell was joined to one piece of teflon tubing which led from the reservoir via a peristatic pump. In this way the solution was constantly circulated through the system and this helped to prevent local heating thus enabling Raman spectra to be taken.

In the case of electrochemical systems, Raman scattering was excited in an electrochemical cell consisting of a forty-five degree angle working electrode surface, Pt counter electrode, and saturated calomel electrode (SCE). A diagram of such a cell is shown in Fig. 4-4. Silver metal working electrodes were mainly used in the investigations. ZnO semiconductor

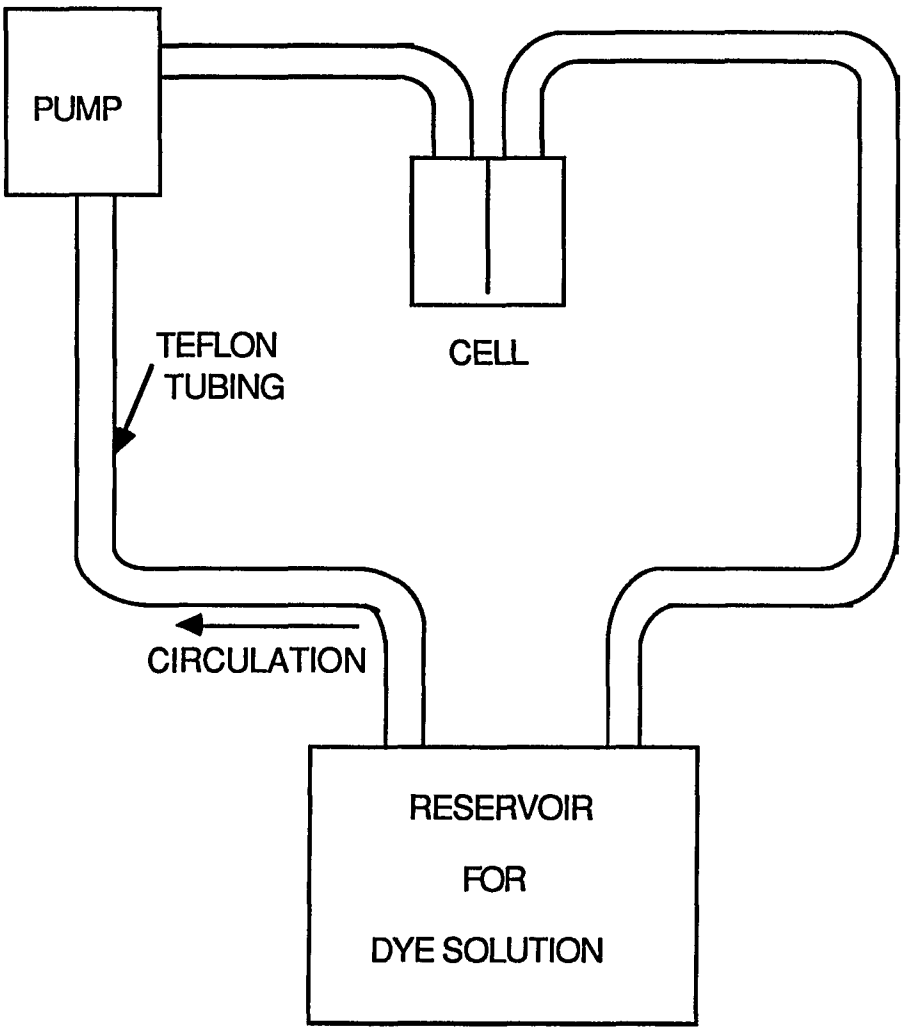

Fig. 4-3: Flow through system, employing a pump to circulate the dye solution through the cell.

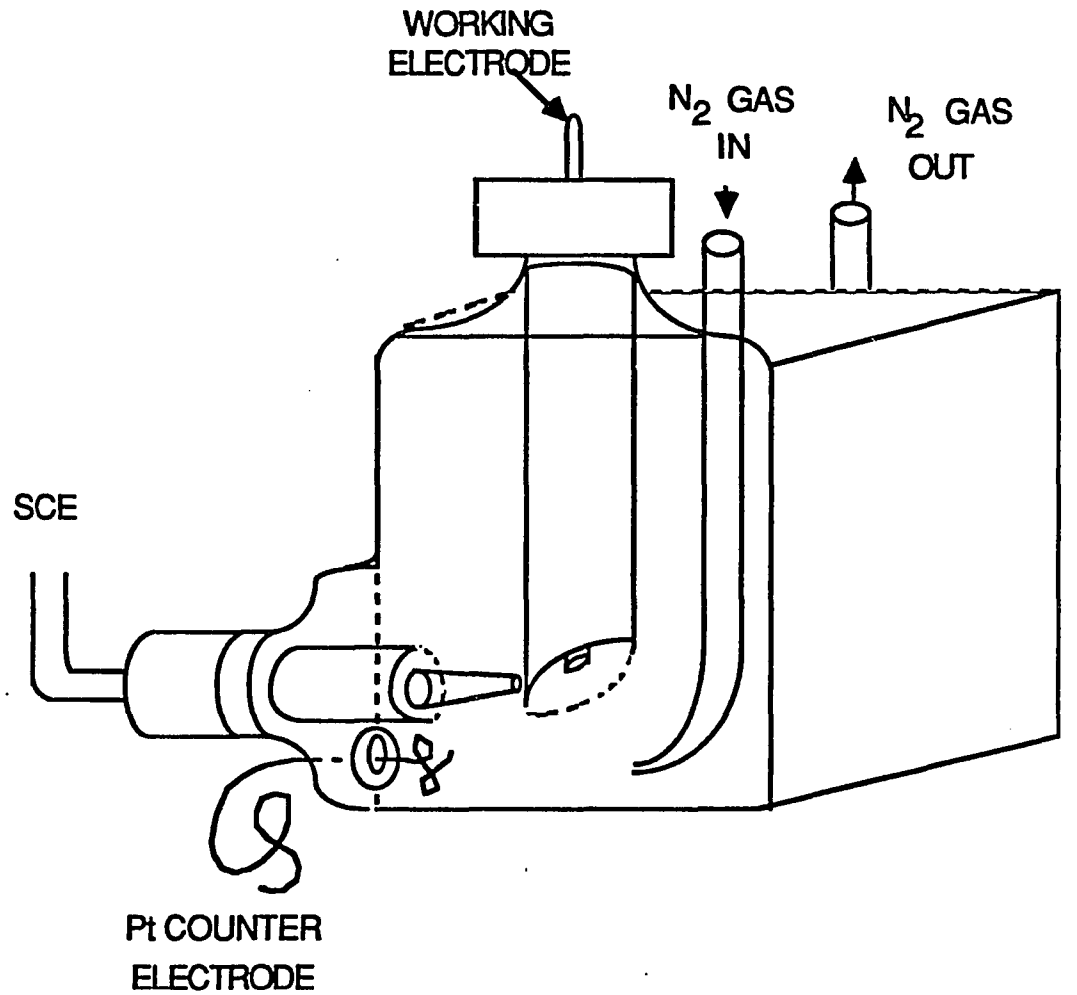

Fig. 4-4: The electrochemical cell for the Raman experiments.

electrodes as well as gold and glass electrodes were also used in some instances.

The metallic working electrodes were well polished using fine alumina and cleaned by use of an ultrasonicator. In some studies involving roughened Ag electrodes, a chemical pretreatment involving hydrogen peroxide and ammonia, was used in addition to the electrochemical pretreatment. The chemical pretreatment consisted of dipping the polished electrode into an equivolume mixture of 30% hydrogen peroxide and concentrated ammonia for about 10 seconds. In the case of electrochemical pretreatment, a redox cycle was used which involved stepping the electrode potential to a value which induced oxidation of the metal then returning to a value corresponding to reducing the metal. With KI as the supporting electrolyte, the redox cycling was from -0.4 V to 0.0 V and back to -0.4 V vs SCE (with a 5 second dwell). For KBr electrolyte, the cycle was -0.4 V to +0.2 V and back to -0.4 V (with 5 second dwell); the cycle was -0.1 V to +0.3 V to -0.1 V (with 5 second dwell) for KCl electrolyte. All voltages were vs SCE. In those cases in which the chemical method was followed by the redox cycling, there was no additional enhancement apparent in the Raman signal. For most experiments, the concentration of the supporting electrolyte was 0.1 M KCl or 0.08 M KI.

Incident radiation impinged from below to excite the sample and the scattered radiation was collected by an optical system with an axis perpendicular to the propagation direction and polarization of the incident laser excitation. The actual angle of collection of scattered radiation (as measured with respect to the incident direction) was selected by orienting the electrode to obtain maximum Raman signal while siting on a particular

band: typically, the resultant angle was significantly less than ninety degrees, as is to be expected from reflection calculations (226).

Electrode potentials were controlled using the CV 27 voltammograph and the PARC 175 waveform programmer. To acquire the surface scattering spectrum at a given voltage the desired potential is applied to the cell and at least 10 minutes is allowed before scanning; the potential is kept on the cell during the entire scan. In all the electrochemical experiments the solutions were deoxygenized by bubbling pure N_2 gas and maintaining the N_2 gas over the solution.

All measurements were made at room temperature (about 23^0C). In Raman experiments, no beam scrambler was placed before the entrance slit of the monochromator.

4.3.1 Preparations

All aqueous solutions were prepared using deionized distilled water. Dye solutions were prepared at about 10^{-4} M and diluted accordingly for various experiments. Typical concentrations used for surface Raman scattering were of 10^{-6} M or 5×10^{-7} M. For the absorption spectra, the dilution of choice was usually 10^{-5} M. The stock potassium halide solutions were prepared in either 0.1 M or 1 M concentrations depending on the kind of experiment.

The silver sols (i.e. the colloidal silver metal particles) were prepared by sodium borohydride, reduction of silver ions,following the procedure used by Creighton et al. (51). Equal volumes of 10^{-3} M $AgNO_3$ and 2×10^{-3} M $NaBH_4$ aqueous solutions were cooled to ice temperature and the $AgNO_3$ solution was added slowly to the $NaBH_4$ solution with constant stirring in

the ice bath. The resulting sols were yellow and showed visible absorption spectra similar to that shown in Fig. 5-3.

Mixtures of dye solution and sol were made by adding the calculated amount of the dye solution to the required amount of sol and bringing it up with water to the desired volume of 5 cc or 50 cc depending upon whether the cell was a simple cell or a flow cell, respectively. In pH experiments, the pH of the solutions was adjusted using HCl and KOH, and the pH measured with a Coleman Metrion IV pH meter.

The ZnO semiconductor pellets and electrodes were prepared using modified methods used by Yamada et al. (227). The ZnO pellets were prepared by sintering. The commercial polycrystalline powder was immersed in dilute hydrochloric acid for 10 min with occasional stirring, washed with deionized water, and dried. The powder was then molded by compression to 10 torr into pellets of about 1 mm thickness and heated at 1100°C for 1 1/2 hr. The electrode was made of a glass tube with a 4 mm bore diameter and an edge cut at a 45° angle as shown in Fig. 4-5. A sintered pellet was well cut and fixed at the 45° angle end using epoxy resin at the edges of the tube. Some gallium-indium, 75.5:24.5 (eutectic) purchased from Alfa Products was put in the tube first to provide the ohmic contact on which a copper wire was connected with silver print (a product of GC Electronics). More silver print was added to fill the tube and the end of the tube was cemented with epoxy resin. To use the electrode, it was first dipped in a concentrated 10^{-3} M aqueous solution of the cyanine dye for 30 min to allow the ZnO to adsorb the dye. The electrode was then washed with deionized water and the color of the dye was visible on the electrode. It was then ready to use like the other working electrodes.

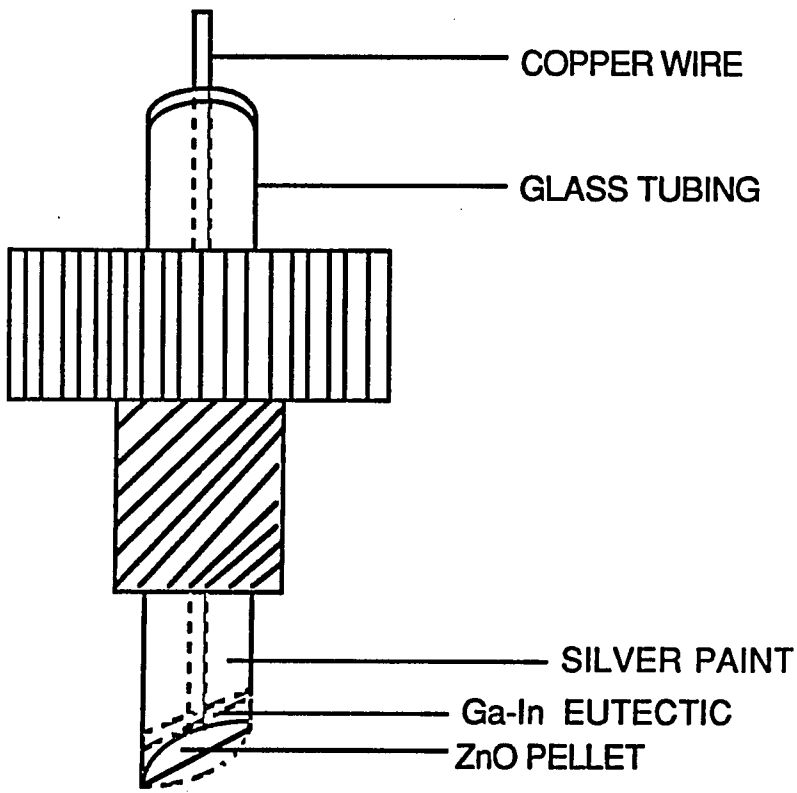

Fig. 4-5: ZnO semiconductor electrode for the Raman experiments.

4.3.2 Obtaining Raman Spectra

The laser was turned on only after the cooling water system to the laser had been turned on, and the cooling water was turned off 15 minutes after the laser was turned off. The Coherent argon ion laser, Model 52, was cooled by a closed-loop cooling system (Neslab Coolflow liquid/liquid recirculator system 1). Since the cooling water was in contact with the plasma tube anode and could be considered to be at that potential, sufficiently deionized water was used. The other lasers were cooled directly by filtered tap water which made regular changing of the water filter essential to prevent buildup of water deposits which might result in inefficient cooling of the laser, thus significantly shortening its lifetime.

Once the laser had run for about half an hour or so, the output power was maximized by adjusting the vertical and horizontal controls on the rear of the laser using a power meter as a guide while the laser power was moderate. The vertical and horizontal controls adjust the position of the prism and thus allow the operator to select lines of different energy for lasing action and maximize power output. In the case of the dye laser system, both the dye and the pumping laser controls were adjusted to maximize the output power. Once the laser settings were optimized for a particular wavelength, the laser line was isolated from other plasma lines by use of an appropriate discriminator grating (premonochromator) or interference filter of Fabry-Perot type.

The isolated laser line was then used to calibrate or set the monochromator position. This procedure was done with extreme care to prevent damage to the photomultiplier tube. The laser power was turned down and the slits set to the lowest possible setting. The sample was held in the sample holder and with all optics in position, a preliminary alignment

was done to make sure that the scattered beam of light was well centered on the entrance slit, which must be closed. The monochromator was scanned over a narrow range across the exciting line. This was usually repeated several times to pin down the position which gave the maximum signal. The exciting line position was then set to the position that gave the maximum signal.

The Spex 1404 double monochromator was used to disperse the Raman scattered light, usually with a bandpass of about 2 cm^{-1}. There were four slits which were set manually and are therefore constant throughout the scan. There were no slit programs to regulate energy, and the resolution of the instrument varied almost continuously.

The laser line was blocked and the monochromator set at the strongest Raman signal of the sample. The slits were then opened to values which would give the desired resolution and symmetrical peaks. The lower the slit width the better the resolution according to the following standard equation

$$BP = \frac{SW}{D_L} \tag{4.1}$$

where the maximum theoretical resolution (band pass, BP) is related to the mechanical slit width. D_L is the linear dispersion obtained from dispersion data for the gratings. At the same time Raman scattering is a weak phenomenon and the signal is related to the slit width by the following expression

$$\text{signal} \propto (P_0) x (SW)^2 \tag{4.2}$$

where P_0 is the incident power. Thus a compromise is usually necessary to get good resolution and good signal to noise ratio.

Considerable time was always invested to align the instruments properly in order to obtain quality Raman data. The signal corresponding to the most intense Raman line of the sample was now used to properly align the system. With the monochromator "sitting" on the most intense Raman band and the slits opened as desired, the laser line was unblocked and the signal output maximized using a counter to find the best positions of the focusing lens, sample holder, the auxiliary mirrors (if any), and the collection lenses. Once the finer adjustments of the collection optics were made by maximizing the signal from the sample the way was now clear for taking a spectrum.

Apart from opening and closing the slits, which were done manually, any other control now was done by the computer. The scan limits were set usually over a 2000 wave numbers range starting from about 100 wave numbers from the laser line (at the red end). The scan speed and integration time were chosen and finally the spectrum is taken with the appropriate laser power.

Mechanical backlash of the wavenumber reading was another problem. This was due to the fact that there must be clearance between the nut, the lead screw, and the rider attached to the cosecant arm. The computer would automatically ride the monochromator back past the start to take up the backlash before starting to scan. The entrance slit was temporarily closed and opened when the monochromator is approaching the starting wavenumber. Spectral scanning and data collection were computer controlled. The computer also allowed storage and manipulation of the spectral data.

The detector employed for all spectra reported was the RCA 31034 photomultiplier. A good reference detailing the fundamentals and choice of

photomultiplier tubes is "Photomultiplier Handbook: Theory, Design, Application", RCA Electronics, Lancaster, PA, 1980. To reduce the so-called "dark current" primarily caused by thermal emission of electrons from the photocathode and dynodes and by dielectric leakage across the PM tube base pins and resistor chain, the tube was thermoelectrically cooled via the Peltier effect so that the weak Raman signal might be easily measured. Extreme caution was exercised when scanning close to the Rayleigh line or other strong lines.

The photon-counting system used was to detect the electron pulses caused by individual photons reaching the photocathode. The advantage was that a substancial fraction of the dark signal could be electronically discriminated from photon pulses so that the ultimate sensitivity of the detector could be increased. Its disadvantage is that the maximum signal was limited to a photon count rate of which photon events did not overlap.

CHAPTER FIVE

EXPERIMENTAL RESULTS

5.1 UV/VISIBLE SPECTROSCOPIC DATA

Interest in the photodynamics of spectral sensitizing dyes in solution and at solid-liquid interfaces, motivated our uv/visible absorption studies. These studies helped to reveal conditions and environments which favor J aggregation. Theory and experiments from our laboratory suggest that the same conditions and environments which promote the formation of J aggregation by these sensitizing dyes, yielding prominent J-aggregate absorption bands, promote enhanced Raman scattering by these dyes.

The absorption spectra of 10^{-5} M aqueous solutions of 2,2'-cyanine, 2,4'-cyanine and 4,4'-cyanine are shown in Fig. 5-1. The principal monomer bands are broad with maximum at 522, 555 and 584 nm, respectively. The shift of monomer absorption maximum from 2,2'-cyanine to 4,4'-cyanine results from the increase in the distance between the ring nitrogen atoms. Spectra as presented are not of the same scale but normalized individually. There was no conspicuous J-aggregate absorption band under the conditions which the spectra were taken.

Fig. 5-2 shows the spectra for the three carbocyanines shown as Dye 4-IV, 4-V and 4-VI in Fig. 4-1. As expected the maximum monomer absorption peak positions appear at longer wavelengths as compared to the simple cyanines of Fig. 5-1. The result for 2,2'-cyanine was shown together with those of the carbocyanines for comparison. In all these absorption spectra and those to be introduced later, each spectrum was normalized individually and the concentrations of the dyes in aqueous solutions were

10^{-5} M unless otherwise stated. 2,2'-carbocyanine has its 0 - 0 vibronic monomer absorption maximum at 598 nm, 2,4'-carbocyanine has its at 647 nm and that of 2,2'-dicarbocyanine appears at 697 nm.

The photodynamics of these dyes are affected to varying extents by their absorption spectra. This effect is illustrated by the absorption spectra of 2,2'-cyanine taken in some of the environments employed for Raman work as shown in Fig. 5-3. In the figure, the spectrum of the ordinary 2,2'-cyanine solution is shown together with those for the dye in 0.8 M KI, and in silver sol. The absorption spectrum of the silver sol alone is also shown. As shown, when the medium was changed by adding 0.8 M KI or the silver sol, the J aggregate band came out prominently as seen in Fig. 5-3B and C.

Of the simple cyanines which can give J aggregate absorption bands in the visible region of the electromagnetic spectrum, the 2,2'-cyanine was found to give the most prominent band followed by the 4,4'-cyanine. These observations are presented in Fig. 5-4 which shows the absorption spectra of the three simple cyanines in silver sol. The J-band regions of 4,4'-cyanine and 2,4'-cyanine are shown on expanded scale to make the bands conspicuous, and spectrum A was offset to avoid congestion at the top.

The effect of KI on J aggregation was interesting because the other halides did not give such prominent J bands. The KI effect was further explored using different KI concentrations and also using different dye concentrations in a given KI concentration. Results for the former are shown in Fig. 5-5 where the 2,2'-cyanine dye concentration was held constant at 10^{-5} M while the KI concentration was varied. When the concentration of the KI was increased from 0.05 M, the J aggregate band in the KI solution began to appear as shown. At high concentrations of KI greater than 1 M, the solution began to loose its color and precipitation

occurred. Similar results were obtained when the KI concentration was held constant at 0.6 M while the 2,2'-cyanine dye concentration was varied as shown in Fig. 5-6. The J band began to appear and became increasingly intense with an increase in the dye concentration.

In strongly acidic media with pH less than 3, the solutions of these dyes loose their color due to protonation of the dye, while at high basic pH values the unprotonated dye solution exhibits intense color. The absorption spectra of solutions less than pH 2 hardly showed any peaks in the visible (see spectrum F in Fig. 5-7(b)). The effect of pH on the absorption spectrum of 2,2'-carbocyanine is shown in Fig. 5-7. Fig. 5-7(a) shows the effect in the basic pH range. A quick observation shows that there appear to be differences in the relative intensities of the two peaks in the visible part of the spectra. At pH 10 the longer wavelength peak is more intense than the shorter wavelength peak; at pH 8.5 the shorter wavelength band becomes higher in intensity than the longer wavelength one; at pH 7 the longer wavelength peak again becomes the higher intensity one. Similar observations can be made from Fig. 5-7(b) for the acidic range as one moves from pH 7 through pH 5.5 to pH 3.2. We explain this as due to different positions of preferential protonation and deprotonation.

Fig. 5-8 shows absorption spectra of ordinary aqueous 2,4'-carbocyanine together with those taken for the same dye and concentration in 0.1 M KCl and 0.05 M KBr. There has been changes in the spectra but a point of interest here is the peak at 710 nm, which is larger in 0.1 M KCl and becomes more conspicuous in 0.05 M KBr. Definitely this is not the position of the sharp J aggregate band which would be in the infrared region for the carbocyanines, but it is presumed here that the emergence of such bands, which were observed for other carbocyanines too, may have some

coordinated effect in the enhancement of Raman scattering when these dyes are excited with sources in the visible.

The J aggregate absorption band was also observed for mixtures of cyanine dyes and vatious semiconductor substrates. Fig. 5-9 shows the absorption spectra fr mixtures of 2,2'-cyanine with a few semiconductor substrates. Here the most prominent J-band was observed for the dye adsorbed on ZnO pellets as shown by spectrum A, taken as a reflectance spectrum of 2,2'-cyanine adsorbed on the pellet. The 10^{-5} M dye in a TiO_2 sol shows a very weak band which could not be observed for purely aqueous solutions of the dye with the same concentration. The TiO_2 sol was prepared following the methods of Duonghong et al. (247). No J-band was observed for the dye in SiO_2 suspensions at pH 9 under the experimental conditions used.

Table 5.1 summarizes the monomer main absorption bands and the J-aggregate absorption bands that appear in the visible region of the spectrum of the cyanines. The precision reported were deduced from numerous determinations in different environments.

Table 5.1 The main monomer absorption band and the J-aggregate absorption band that appear in the visible region of the spectrum for the cyanines.

Cyanine	Maximum Monomer Absorption Peak (nm)	J-Aggregate Absorption (nm)
1,1'-Diethyl-2,2-cyanine iodide	522 ± 2	575 ± 6
1,1-Diethyl-2,4'-cyanine iodide	555 ± 2	655 ± 10
1,1'-Diethyl-4,4'-cyanine iodide	584 ± 2	712 ± 10
1,1'-Diethyl-2,2'-carbocyanine iodide	598 ± 2	
1,1'-Diethyl-2,4'-carbocyanine iodide	647± 2	
1,1'-Diethyl-2,2'-dicarbocyanine iodide	697± 2	

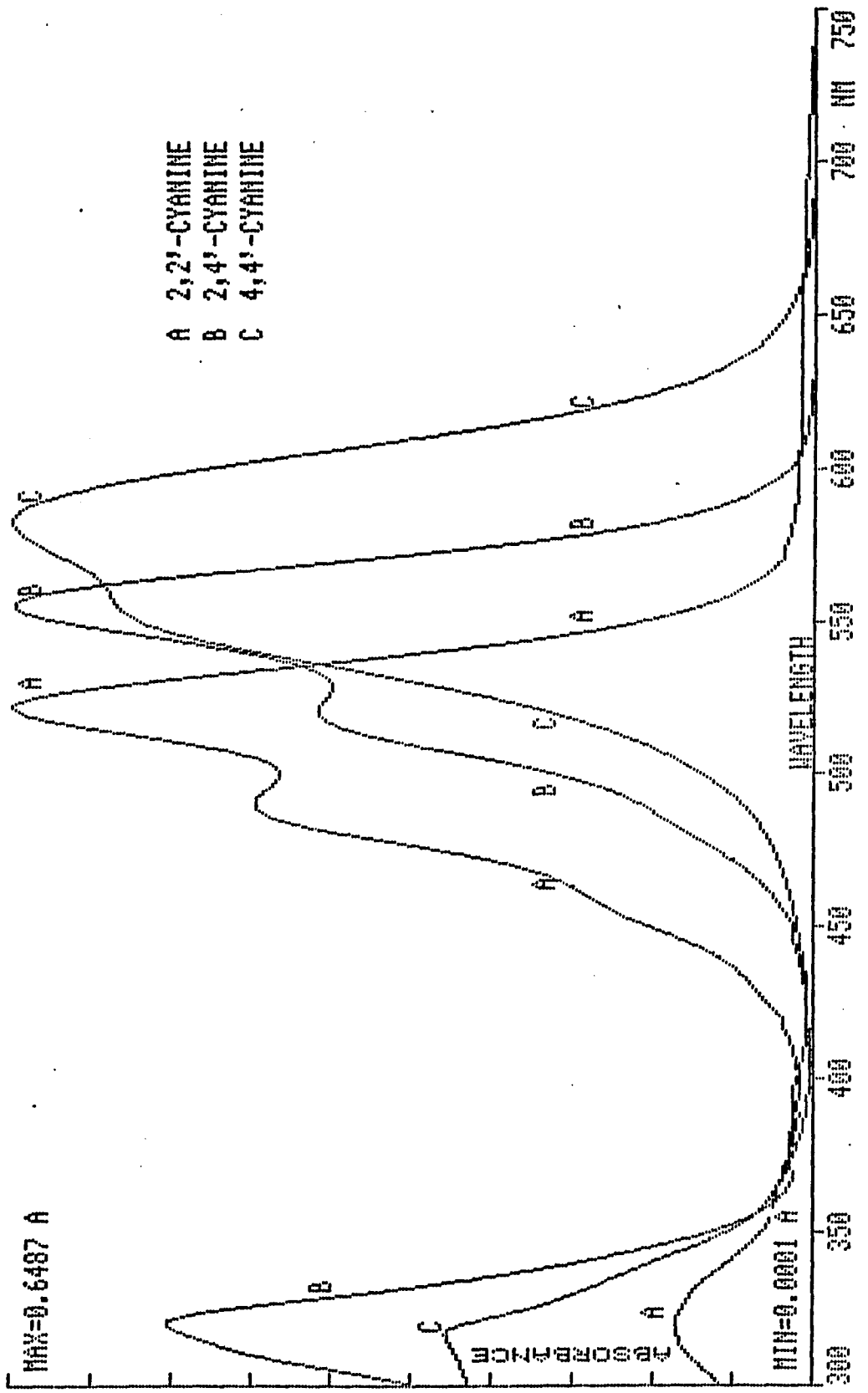

Fig. 5-1: Absorption spectra of the simple cyanines in aqueous solution

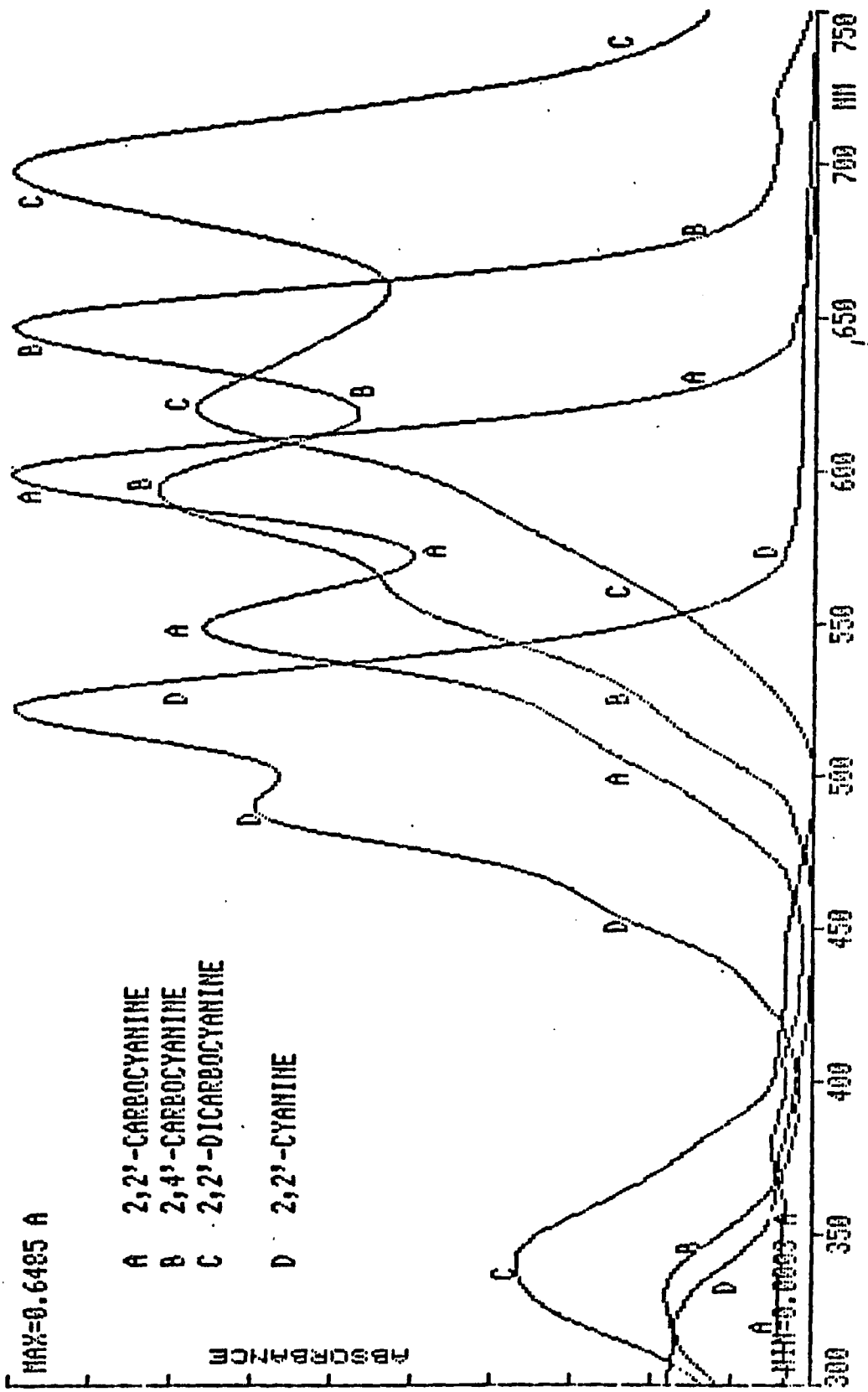

Fig. 5-2: Absorption spectra of the carbocyanines in aqueous solution

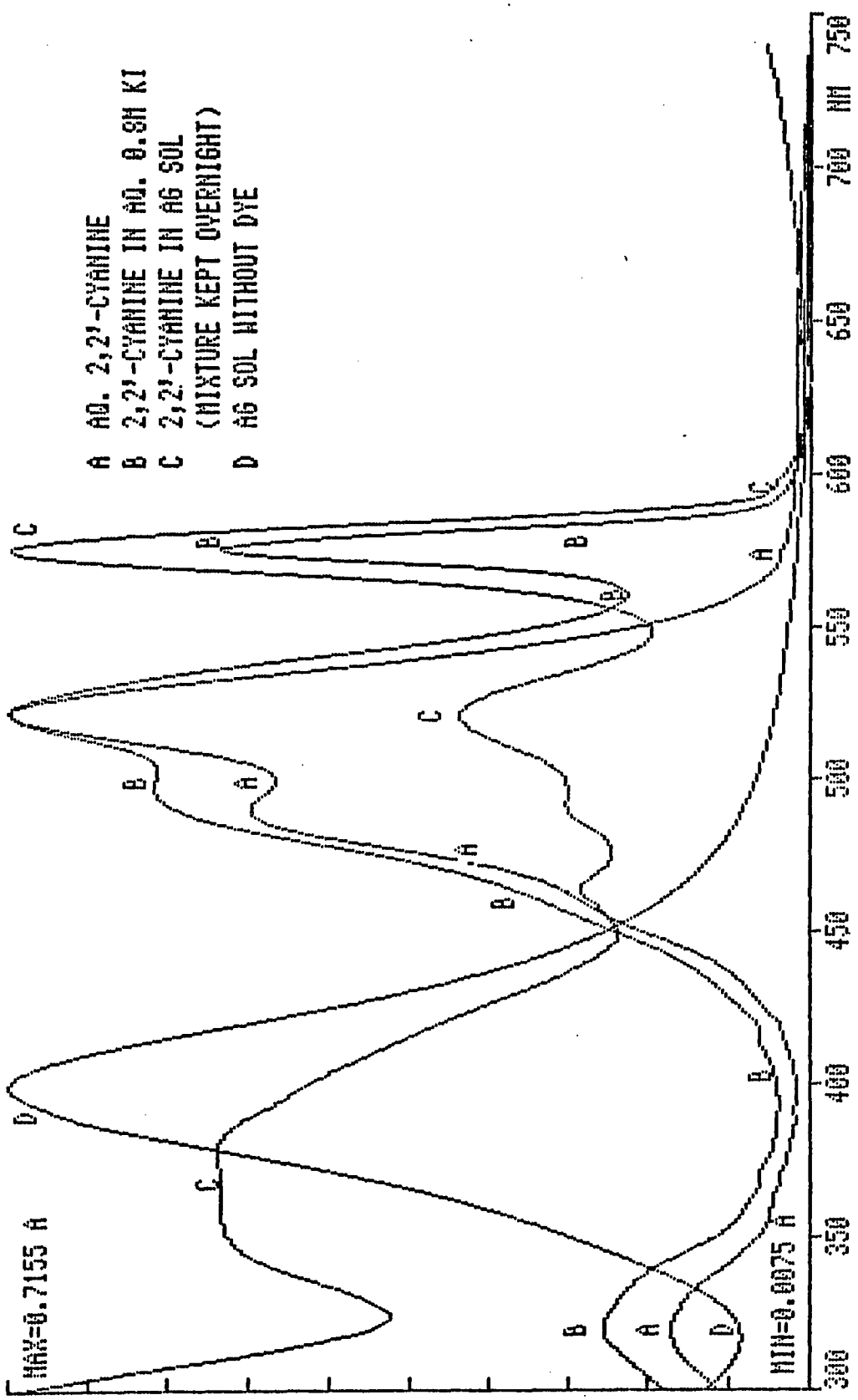

Fig. 5-3: Absorption spectra of 2,2'-cyanine taken in some of the supporting media for the Raman scattering, showing the J-band in some cases

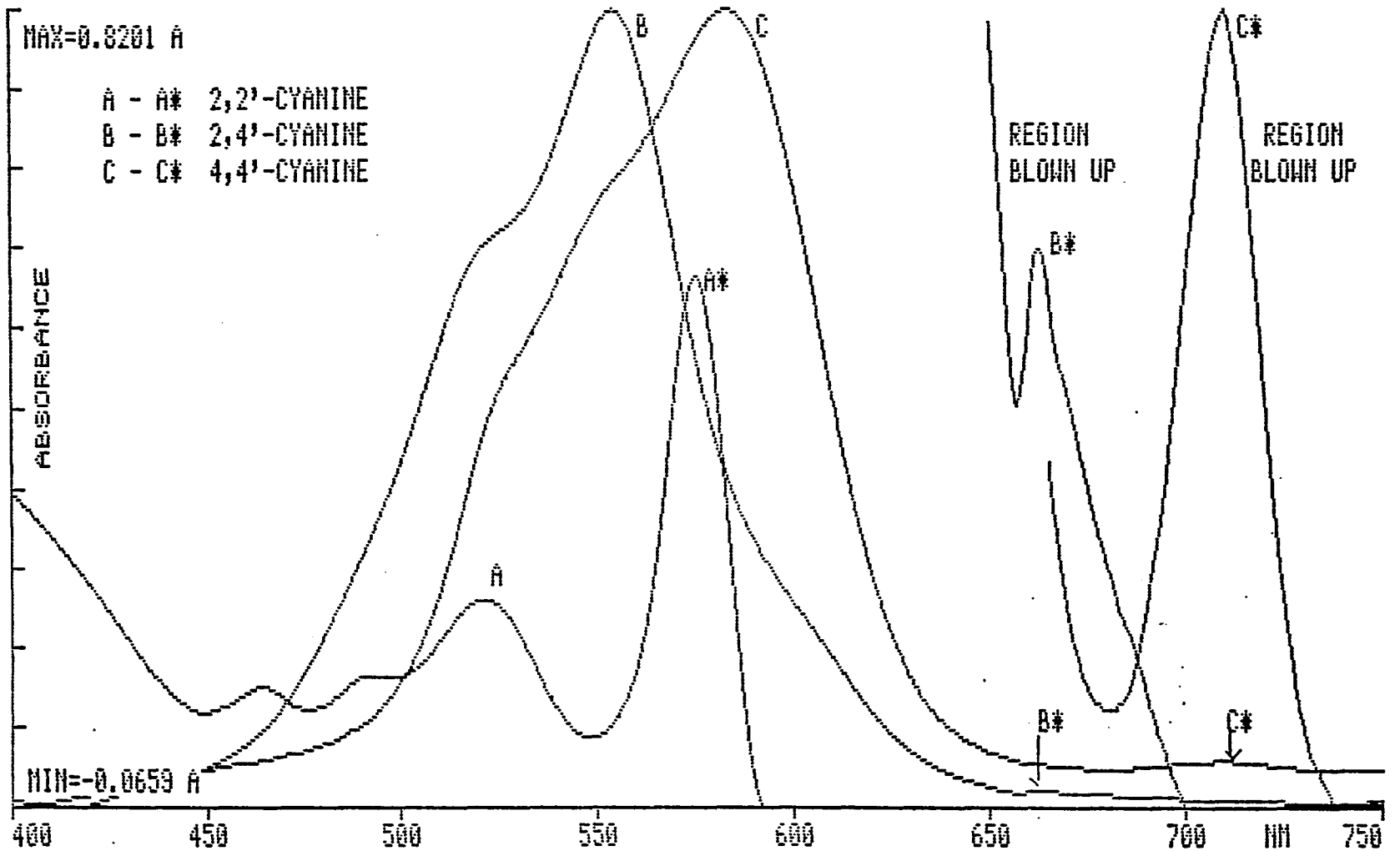

Fig. 5-4: Absorption spectra of the simple cyanines taken in silver sol, showing the J-aggregate band. A is offset to minimize congestion at the top

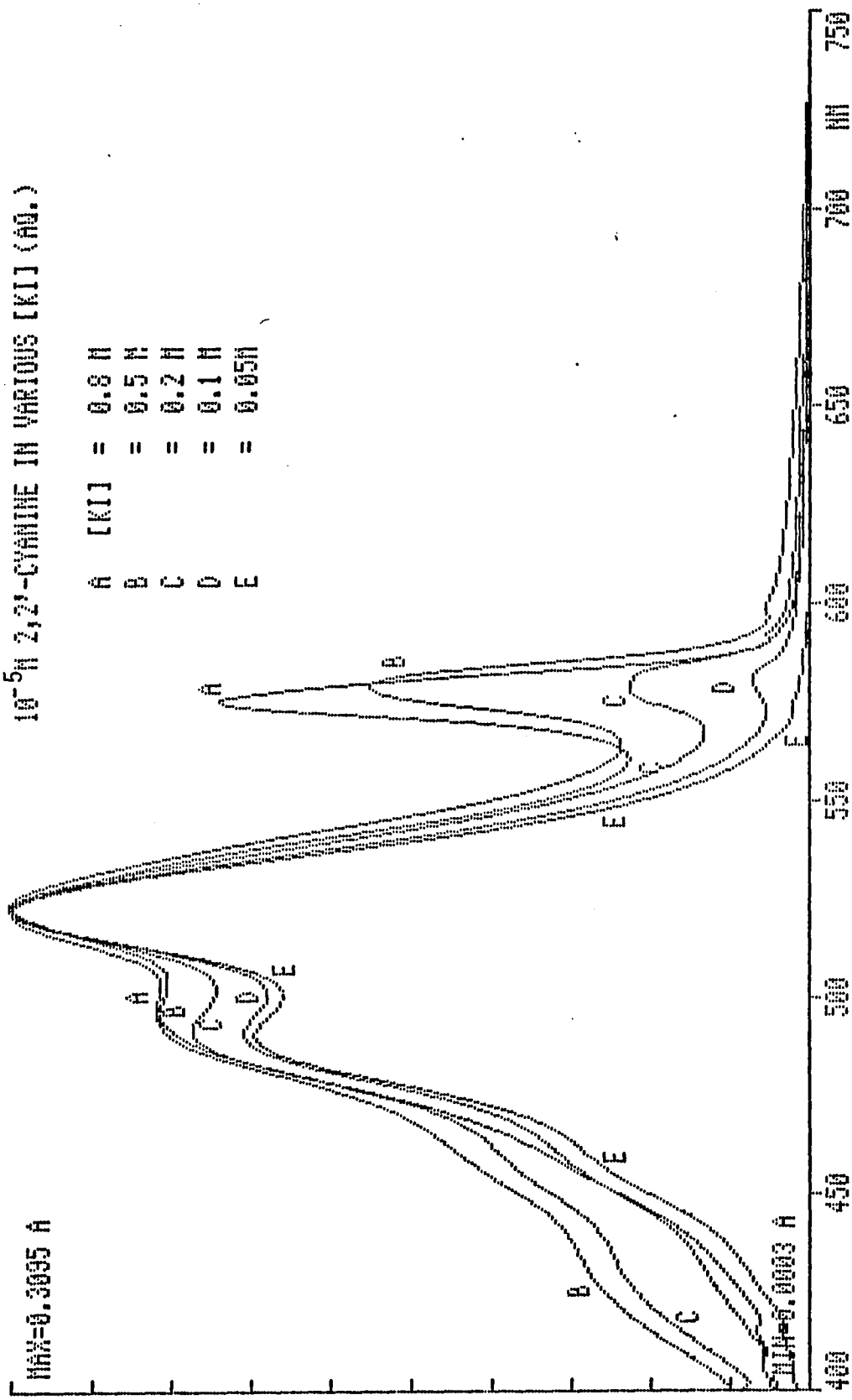

Fig. 5-5: Absorption spectra of 10^{-5} M 2,2'-cyanine in aqueous solutions containing different KI concentrations

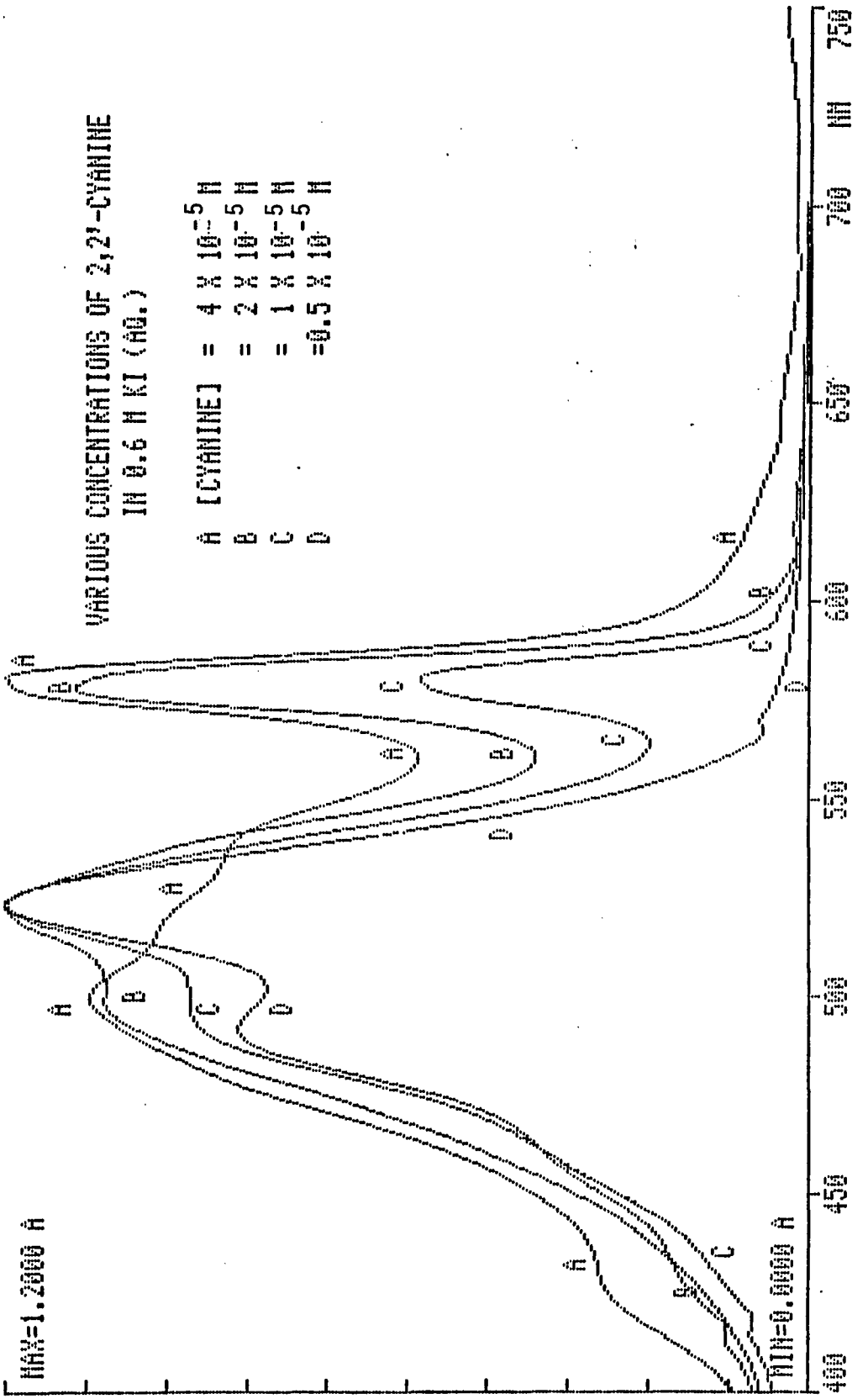

Fig. 5-6: Absorption spectra of 2,2'-cyanine at various concentrations in 0.6 M aqueous KI solution

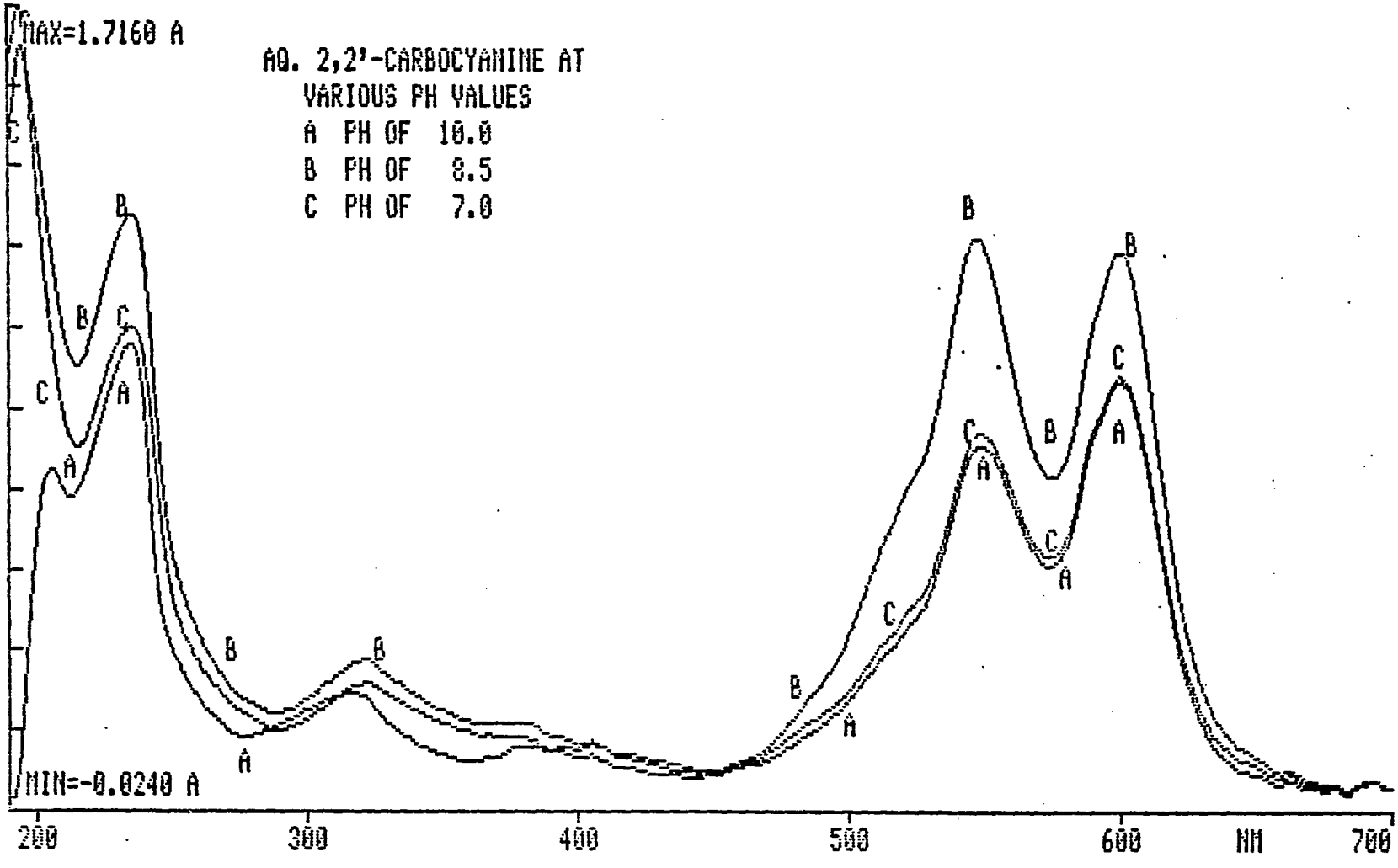

Fig. 5-7(a): Dependence of absorption spectra of 2,2'-carbocyanine on the pH of the aqueous medium. Spectra shown for basic media

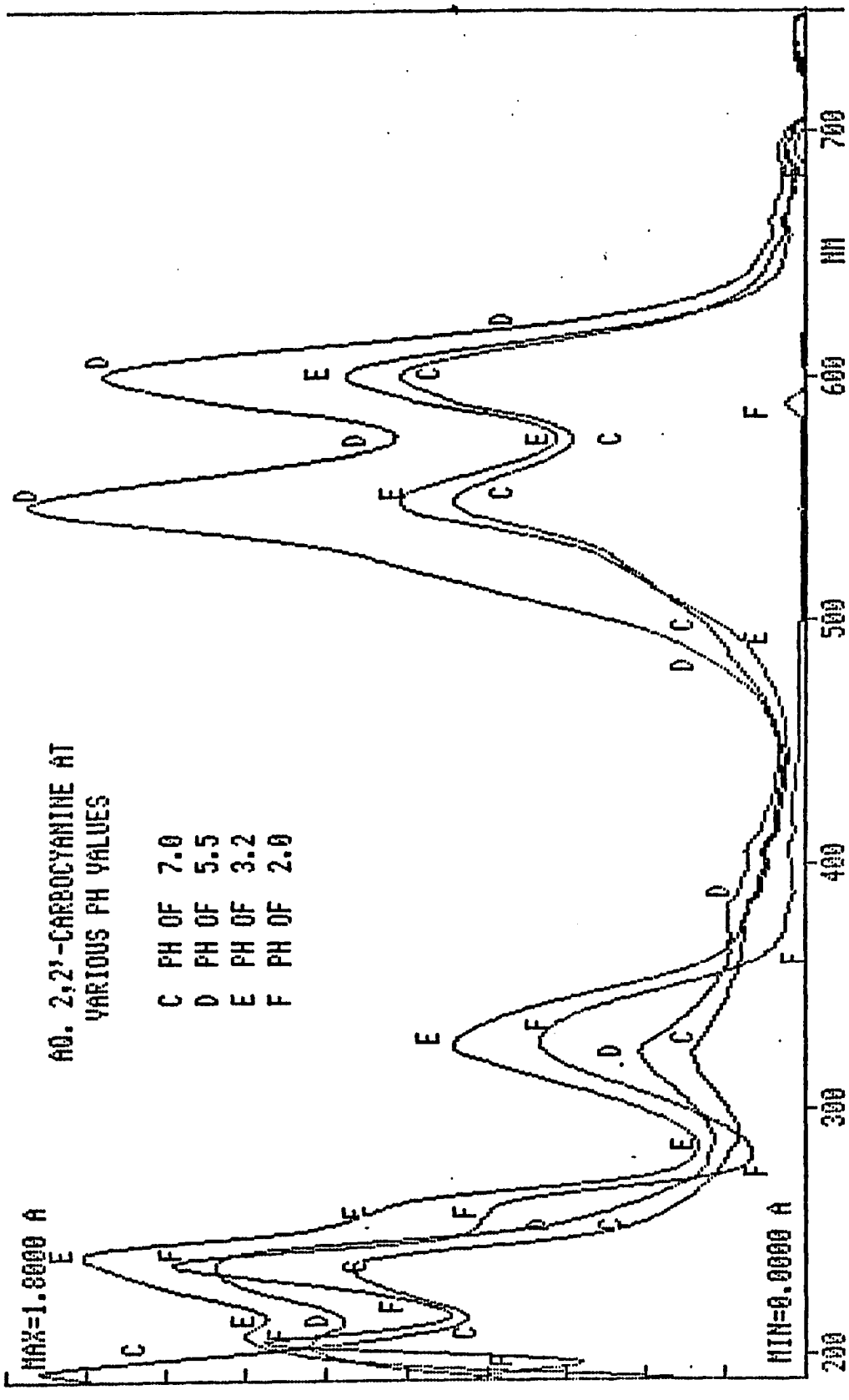

Fig. 5-7(b): Dependence of absorption spectra of 2,2'-carbocyanine on the pH of the aqueous medium. Spectra shown for acidic media

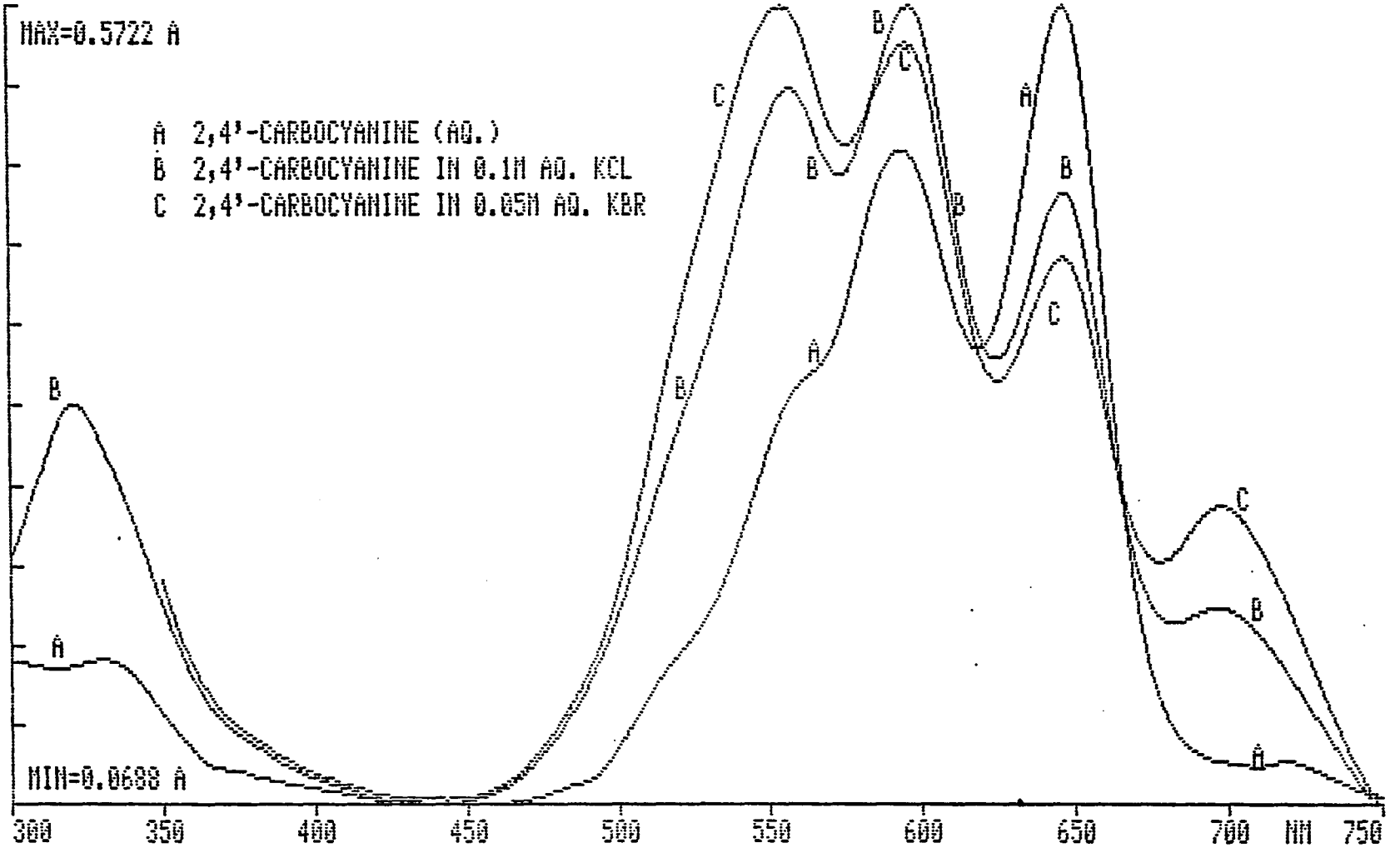

Fig. 5-8: Absorption spectra of 2,4'-carbocyanine in aq. 0.1 M KCl and 0.05 M KBr solutions compared to a spectrum of its aq. solution

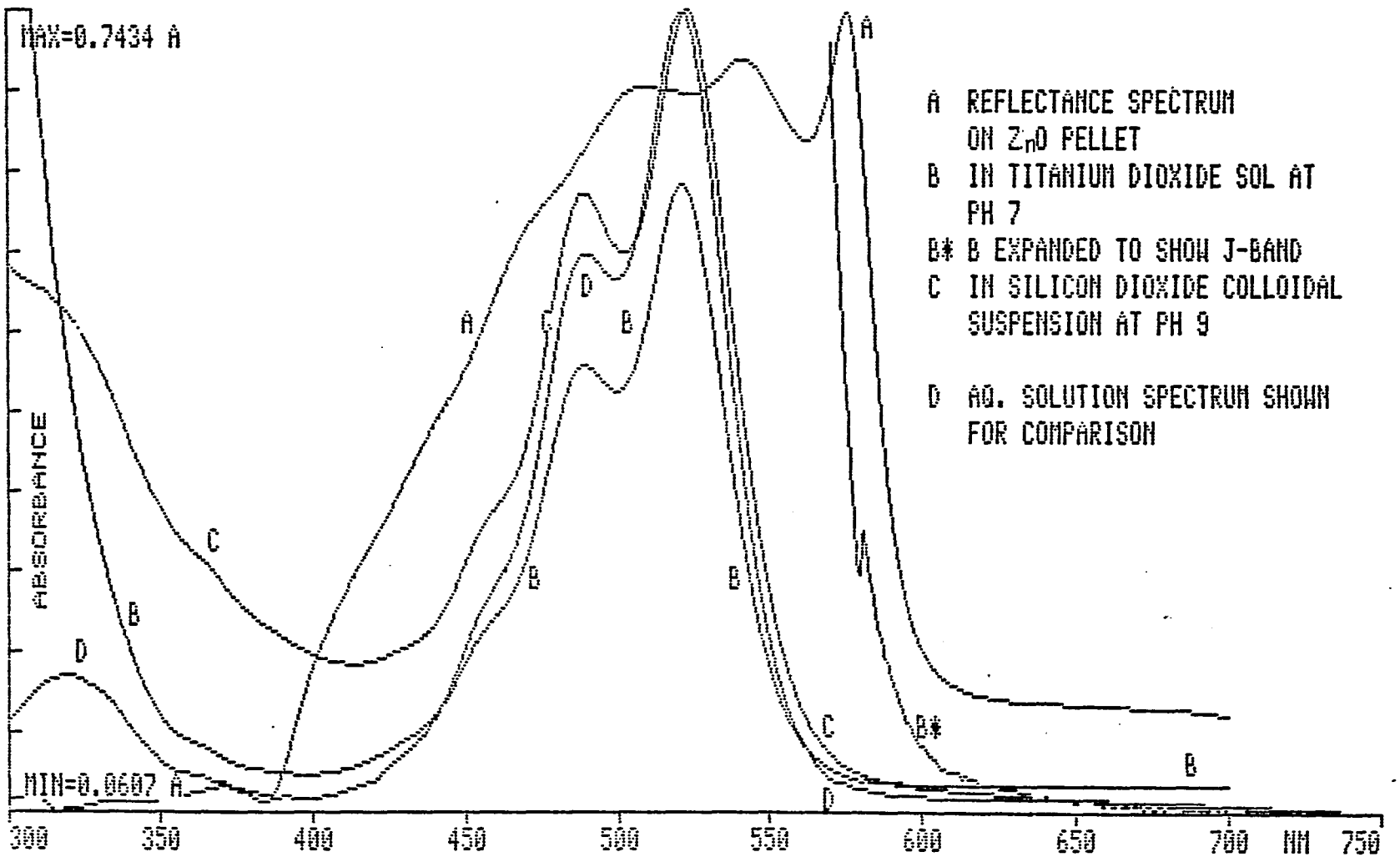

Fig. 5-9: Absorption spectra of 2,2'-cyanine taken in some semiconductor systems. Spectra are scaled individually.

5.2 RAMAN SPECTROSCOPIC DATA

Raman spectra for the cyanines were acquired with the apparatus and procedure indicated in Chapter 4. The room temperature solution spectrum of aqueous 2,2'-cyanine (10^{-5} M) excited with 514.5 nm wavelength excitation from a Model 52 Coherent argon laser is shown in Fig. 5-10 . The laser line power was about 45 mW at the sample, and the resolution was 2 cm^{-1}. The full scale setting was $5 \times 10^{+3}$ counts/sec. The aqueous spectrum, as other solution Raman spectra for cyanines, shows a strong fluorescence background.

Fig. 5-11 shows Raman spectra of 2,2'-cyanine excited by 488 nm light on some substrates. In all cases the concentration of the cyanine solution was 10^{-6} M and the power before the sample was 30 mW. The spectra are compared on the same intensity scale setting of 10^{+4} counts/sec. Spectra (A) and (B) were taken on polished silver and gold electrodes respectively at open circuit potential. Spectrum (C) was on a polished glass electrode. Although the platinum counter electrode and the saturated calomel reference electrodes were included in the set up of the cell, the spectrum was taken with an open circuit as in the case of (A) and (B). In the three cases, the dye solutions were made in a 0.1 M aqueous solution of KCl. Spectrum (D) was taken of a dye solution/SiO_2 suspension mixture with pH of 9. Upon closer observation and using an expanded scale, the high frequency bands in the spectrum on the glass electrode are revealed; the spectrum of the dye in the SiO_2 suspension reveals very little for identification purposes.

The Raman spectra of the carbocyanines adsorbed on a silver electrode in 0.06 M KI and excited by 647.1 nm radiation are shown in Fig. 5-12. The electrode was chemically roughened in each case. Each spectrum is

shown on different scale setting, but the dye concentration was 10^{-6} M in all cases. Spectrum (A) is 2,2'-carbocyanine with a scale setting of $4 \times 10^{+5}$, (B) is 2,4'-carbocyanine with a scale setting of $7 \times 10^{+4}$, and (C) is 2,2'-dicarbocyanine with a scale setting of $3 \times 10^{+4}$.

5.2.1 Raman Scattering by the Cyanines Adsorbed on Colloidal Silver Particles

All the dyes were found to give Raman scattering when they were adsorbed on silver metal sol particle surfaces and formed aggregates. Our studies show that enhanced Raman scattering enhancement occurs when the dyes aggregate on the substrate particles. Examples of Raman scattering spectra for aqueous solutions of 2,4'-cyanine and 2,2'-carbocyanine are shown in Fig. 5-13 and Fig. 5-14 respectively. 2,4'-cyanine is found to be less stable in aqueous solutions than 2,2'-carbocyanine. Fig. 5-13 shows the spectra for 5×10^{-6} M, 2,4'-cyanine excited by 488 nm and 514.5 nm excitations, respectively. It was found necessary to use a flow system shown in Fig. 4-3 to avoid photodecomposition in aqueous solution. Fig. 5-14, shows similar spectra for 5×10^{-6} M, 2,2'-carbocyanine/silver sol mixture. An important observation made for the surface adsorbed scattering on sols is the diminution of fluorescence and an increase in the Raman scattering signal on addition of the sol particles which is concomitant with the J-aggregate formation. This was the case for all the dyes studied.

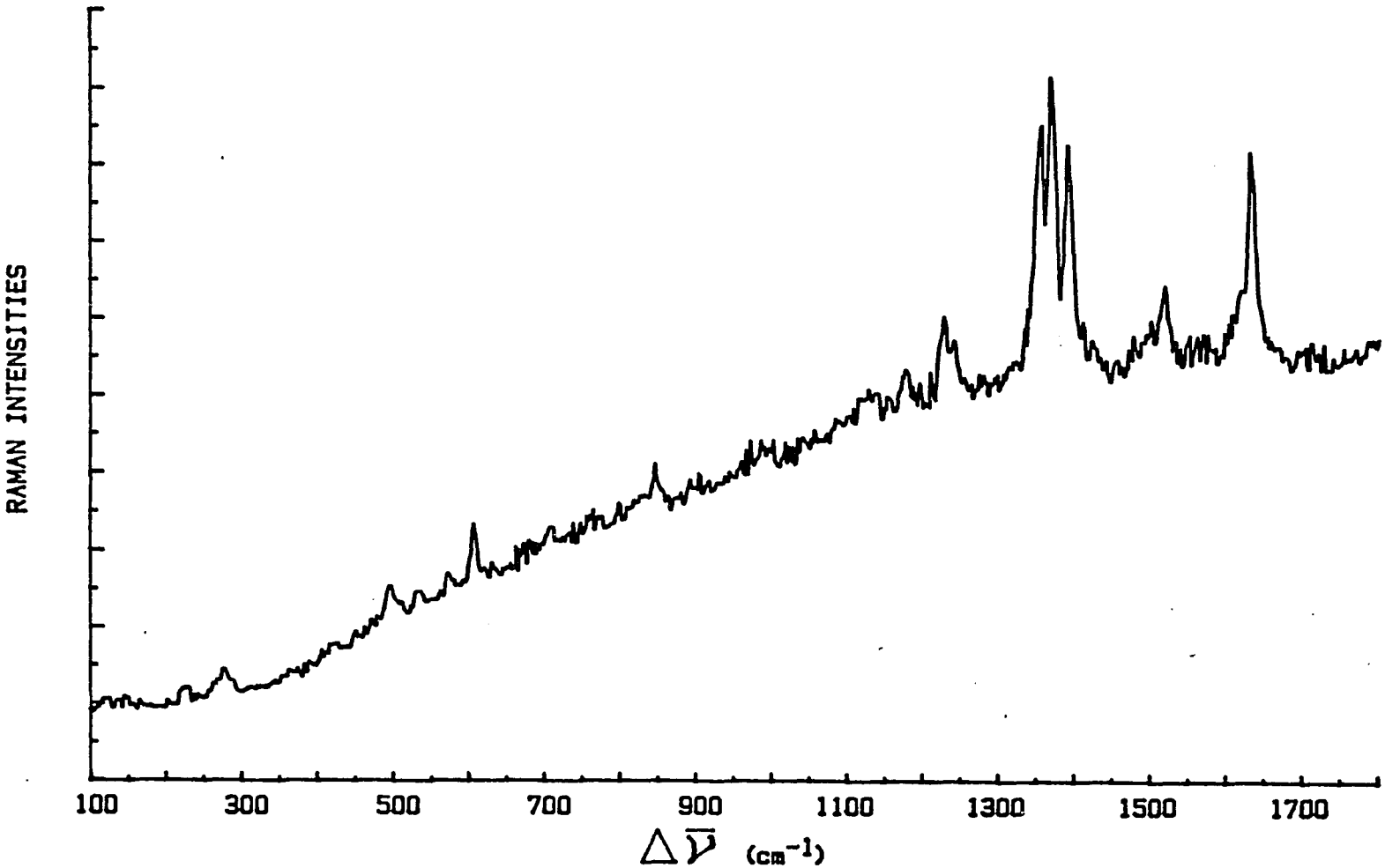

Fig. 5-10: Solution Raman spectrum of 10^{-5} M aq. 2,2'-cyanine excited by 514.5 nm radiation of 45 mW power at sample. Scale setting was 5 x 10^{+3} counts/sec.

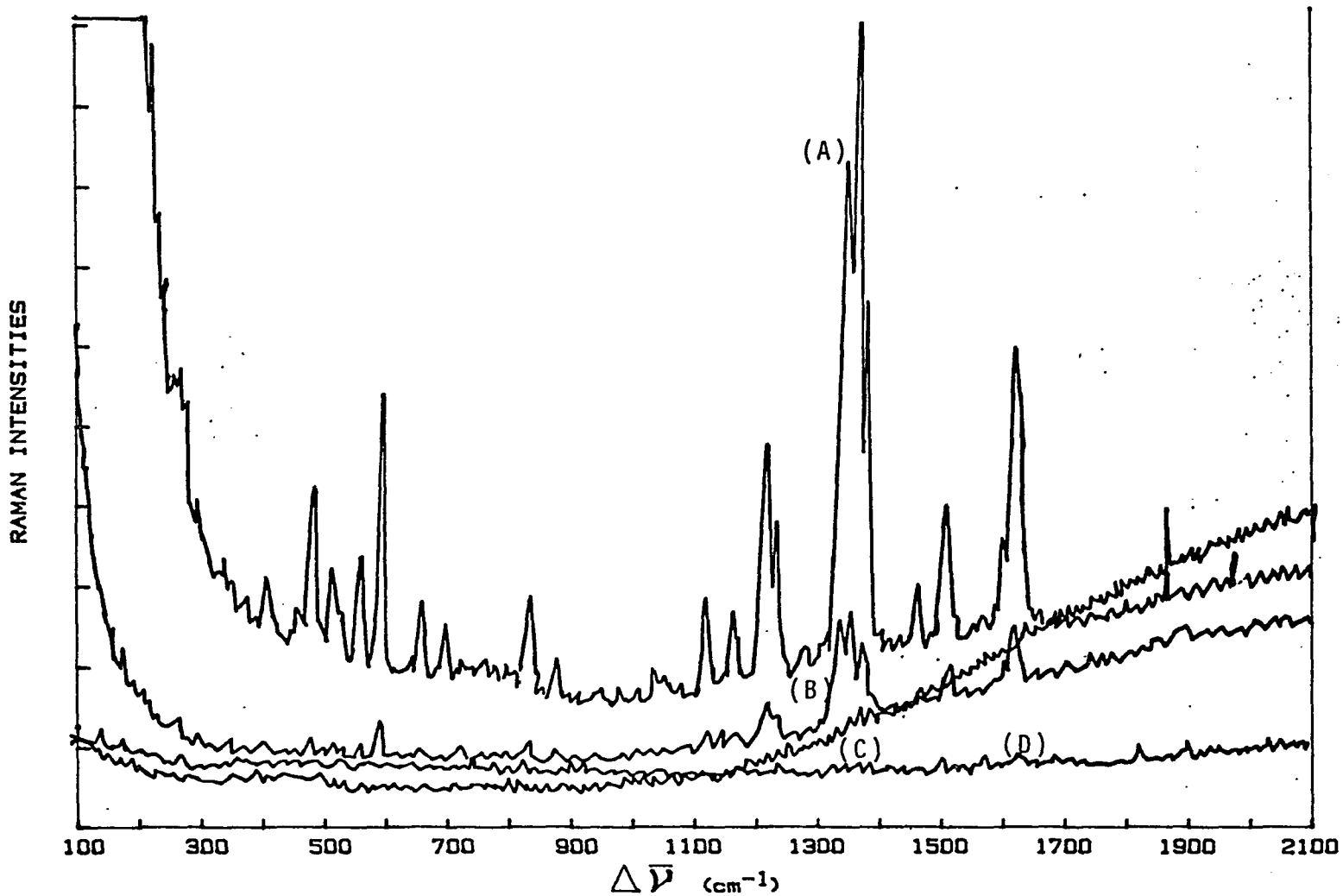

Fig. 5-11: Raman spectra of 2,2'-cyanine adsorbed on (A) smooth Ag electrode, (B) smooth Au electrode, (C) polished glass, (D) SiO_2 suspension, excited by 30 mW of 488 nm radiation. Dye solution was 10^{-6} M and scale setting was 1 x 10^{+4} counts/sec. in all cases.

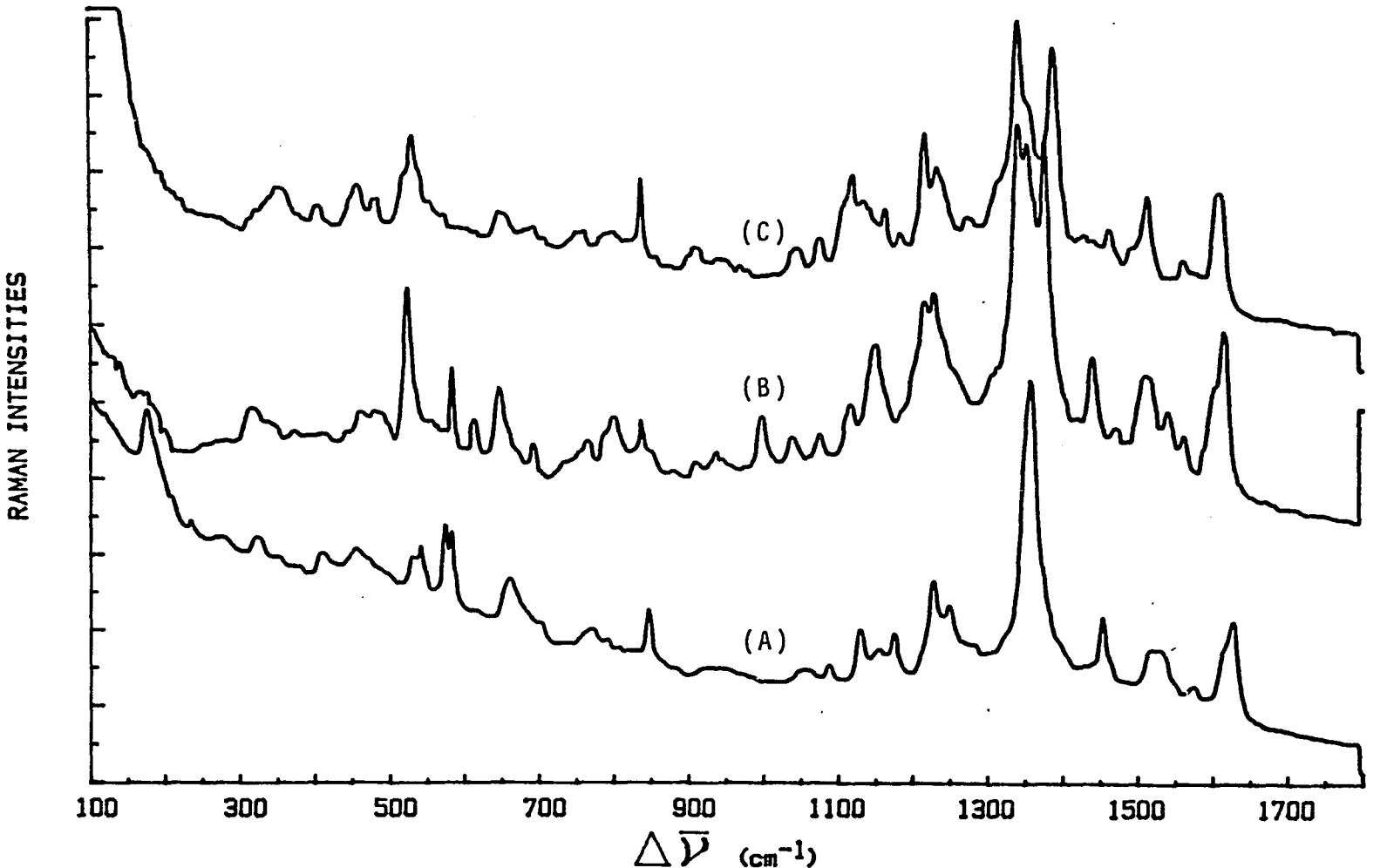

Fig. 5-12: Raman spectra of the carbocyanines on silver electrodes in 0.06 M KI and excited by 647.1 nm radiation: (A) 2,2'-carbocyanine with scale setting of 4 x 10^{+5}, (B) 2,4'-carbocyanine with scale setting of 7 x 10^{+4} (C) 2,2'-dicarbocyanine with scale factor of 3 x 10^{+4} counts/sec. Dye solution was 10^{-6} M.

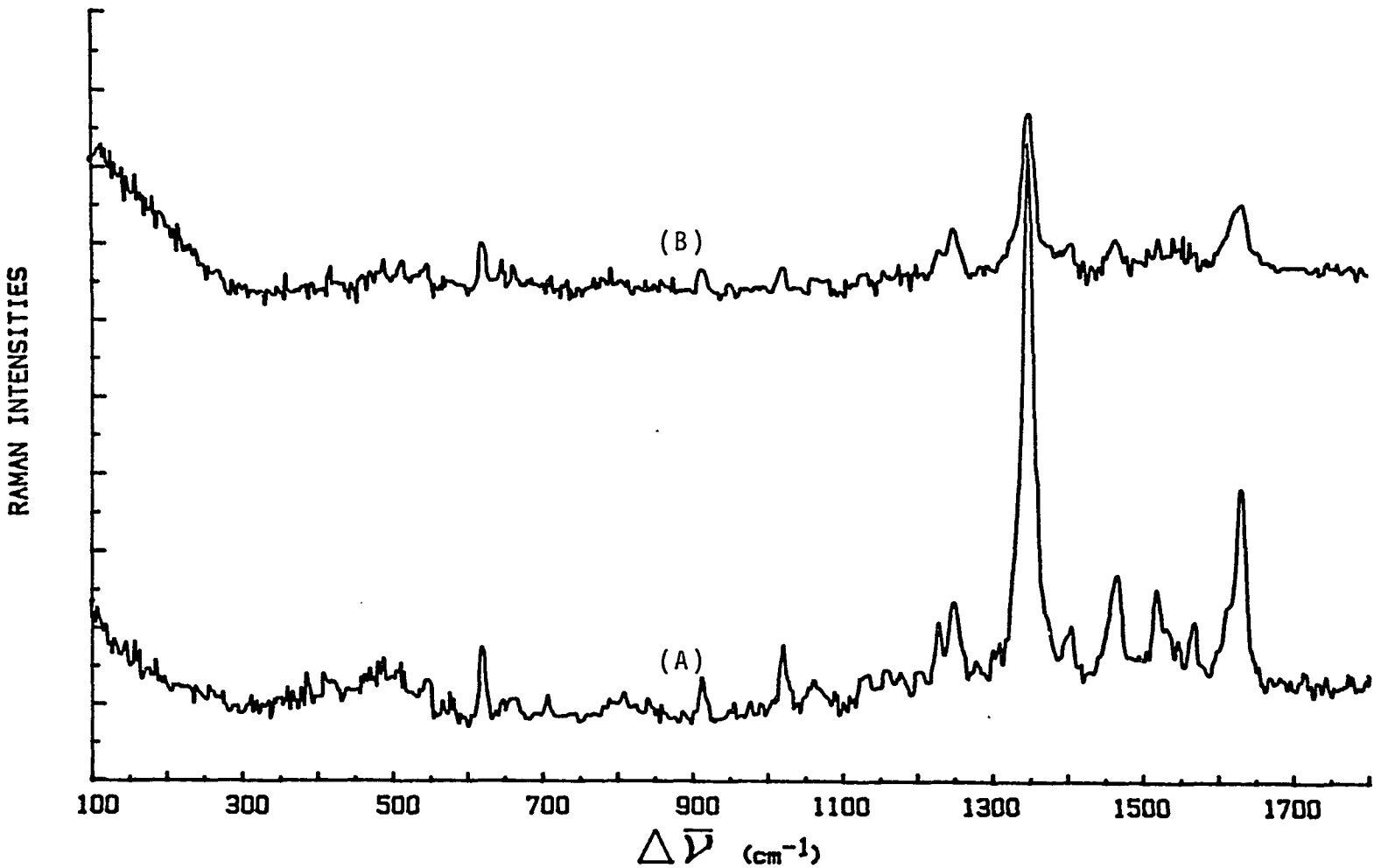

Fig. 5-13: Raman spectra of 2,4'-cyanine on silver sols excited by (A) 488 nm and (B) 514.5 nm lines respectively. Dye solution was 5 x 10^{-6} M and scale setting was 5 x 10^{+3} counts/sec.

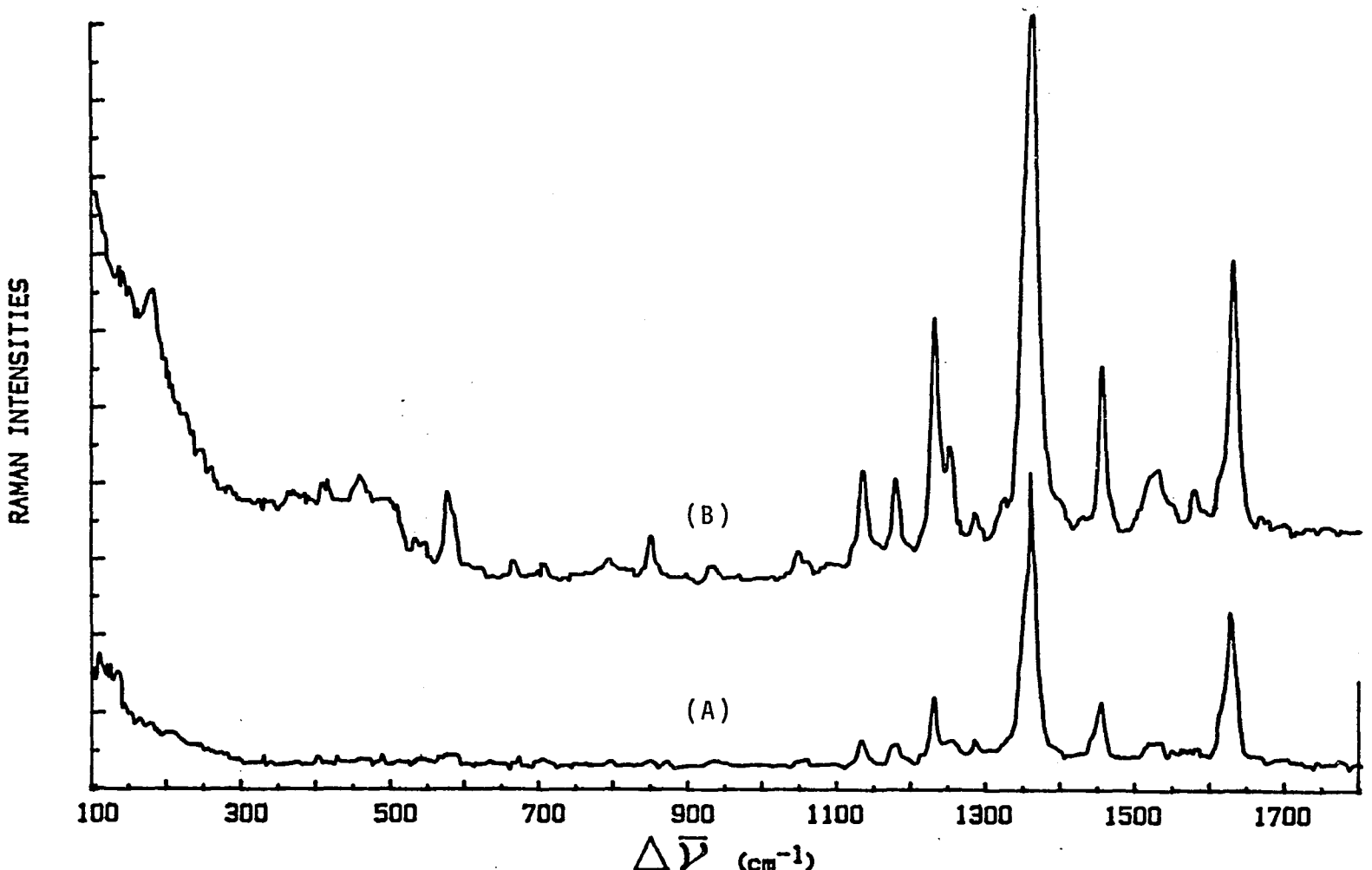

Fig. 5-14: Raman spectra of 2,2'-carbocyanine on silver sols, excited by (A) 488 nm and (B) 514.5 nm lines, respectively. Dye solution was 5×10^{-6} M and scale setting was $8 \times 10^{+3}$ counts/sec.

5.2.2 Enhanced Raman Scattering by Molecular Excitonic Systems in Electrochemical Cells

5.2.2.1 Excitation Profiles

Results from studies using various excitation sources to excite the cyanines reveal useful information with regards to the excitation wavelength dependence of the enhanced Raman bands of aggregated sensitizing dyes. The excitation profiles of Raman spectra of the cyanines adsorbed at silver/aqueous interfaces were measured with four excitation frequencies in the range of 488 to 647 nm. Spectra for three dyes are shown in Fig. 5-15 through Fig. 5-17. Fig. 5-15 shows the excitation profile for 2,2'-cyanine adsorbed on a silver electrode and excited by (A) the 488 nm blue line, (B) the 514.5 nm green line, (C) the 583 nm line and (D) 647.1 nm red line. The dye solution concentration in each case was 5×10^{-7}M in a supporting electrolyte of 0.08 M KI. The spectra (A), (B) and (C) have the same scale setting of $2 \times 10^{+4}$, while (D) has a scale setting of $3 \times 10^{+4}$. The electrodes were electrochemically pretreated and the laser power reading at the laser was 200 mW in each case.

Fig. 5-16 and Fig. 5-17 show similar results for 4,4'-cyanine and 2,2'-carbocyanine, respectively, using three of the four excitation wavelengths. In the case of 4,4'-cyanine, (A) 488 nm, (B) 514.5 nm and (C) 647.1 nm excitation wavelengths were used, and in Fig. 5-17 for 2,2'-carbocyanine, (A) 488 nm, (B) 583 nm and (C) 647.1 nm lines were used for the excitation. Scale settings for spectra (A) and (C) of Fig. 5-16 were $2 \times 10^{+4}$ and that of (B) was $8 \times 10^{+4}$. Scale settings for spectra of Fig. 5-17 were $4 \times 10^{+4}$, $5 \times 10^{+3}$, and $4 \times 10^{+5}$, respectively. The other conditions are as described for Fig. 5-15.

The excitation wavelengths are from off-resonant to near-resonant with the J aggregate band in the case of 2,2'-cyanine and 4,4'-cyanine. These

two dyes have their J-bands around 575 and 710 nm, respectively. Each of the adsorbates shows a pronounced excitation profile maximum for the lower bands for excitation wavelengths which are close to its J aggregate band.

5.2.2.2 Effect of the Supporting Electrolyte

The dependence of supporting electrolyte in the enhancement of Raman scattering by the aggregated dyes was investigated and some of these results are shown in Fig. 5-18 and Fig. 5-19 for 2,4'- and 4,4'-cyanines, respectively using 0.1 M KCl and 0.1 M KI. Fig. 5-18 shows the results for the 2,4'-cyanine on a silver electrode in an electrochemical cell. The electrode was chemically roughened as described in the text. The excitation wavelength was 488 nm and the laser power was 30 mW at the sample. Similar conditions were used to obtain spectra for the 4,4'-cyanine shown in Fig. 5-19. The dye concentration in these cases was 10^{-6} M.

5.2.2.3 Effect of Electrode Pretreatment

Results obtained from different methods of electrode pretreatment are shown in Fig. 5-20 through Fig. 5-22. Four methods were used for the pretreatment. In (A) the electrode was polished with fine alumina, sonicated but no roughening was done; in (B) the electrode was treated as in (A) but was chemically roughened by dipping it in a 1:1 mixture of hydrogen peroxide and ammonia for a few seconds; in (C) the polishing and cleaning was followed by electrochemical roughening which was done through a redox cycle from -0.4 V to 0 V, with pulse width of 5 sec, and back to -0.4 V while the electrode was in the degased 0.08 M KI electrolyte 5×10^{-7} M dye mixture. In case (D) the treatment was almost the same as in (C) but the

redox cycle was given in the absence of the dye. Results for all these treatments are shown for 2,2'-cyanine in Fig. 5-20. The aggregated dye was excited by 488 nm radiation and the same scale setting of $2 \times 10^{+4}$ was used for all the spectra shown. The dye solutions were 5×10^{-7} M in 0.08 M KI.

In the cases of 2,4'-cyanine and 4,4'-cyanine, only the chemical and the first type electrochemical pretreatments are reported in Fig. 5-21 for 2,4'-cyanine and Fig. 5-22 for 4,4'-cyanine. Dye concentration in these cases was 10^{-6} M; the laser power was 200 mW, and the scale setting for the spectra in the two figures was $3 \times 10^{+4}$. The other conditions were the same as described for Fig. 5-20.

5.2.2.4 Potential Dependence

Raman spectra for 2,2'-cyanine and 4,4'-cyanine were studied with potential variation. The potential dependence of the Raman bands was measured for potentials ranging from -0.4 V to -1.3 V vs. SCE. Spectra for selected potentials are shown in Fig. 5-23 for 2,2'-cyanine, excited by 583 nm radiation, and in Fig. 5-24 for 4,4'-cyanine excited by 647.1 nm excitation radiation, all at a solution pH of about 7 as prepared with the deionized distilled water. The dyes were adsorbed on a silver electrode which was pretreated electrochemically.

Fig. 5-23 provides the voltage dependent spectra of 5×10^{-7} M 2,2'-cyanine chloride in 0.08 M Kl for potentials -0.8, -0.95, -1.1, and -1.2 V all vs. SCE, shown from bottom to top respectively. The scale setting in all cases was $3 \times 10^{+4}$ counts/sec, and the laser power at the sample was about 30 mW. Fig. 5-24 shows the voltage dependent results for 10^{-6} M 4,4'-cyanine in 0.08 M KI for potentials -0.85, -0.95, -1.1 and -1.3 V all vs. SCE, also from bottom to top respectively. The scale setting in all spectra shown in Fig. 5-24 was 4 x

10^{+4} counts/sec, and the laser power was also 30 mW at the sample. The general trend for the spectral bands (with background substraction applied) was a gradual rise in intensity to some maximum intensity near -1.1V vs. SCE, followed by a diminution of intensity at some negative potentials.

5.2.2.5 pH Dependence

The surface Raman scattering by 4,4'-cyanine adsorbed from dye solutions of different pH's was determined, and some of the results are shown in Fig. 5-24 through Fig. 5-26. Fig. 5-25 and Fig. 5-26 show spectra acquired at a solution pH of 2 and 12 respectively. As in Fig. 5-24, they show some of the spectra obtained with potential variation. In Fig. 5-25 where the pH is 2, the spectra shown are for potentials -0.75, -0.85, -0.95 and -1.0 V all vs SCE, and shown from bottom to top respectively. The spectra shown for pH 12 in Fig. 5-26 are for potentials -0.4, -0.70, -0.90 and -1.2 V all vs. SCE and are from bottom to top respectively. All other conditions for these two figures are the same as for Fig. 5-24 which was already described under the previous subsection.

While the results of pH 12 almost resemble those of pH 7 in Fig. 5-24, those of pH 2 show significant variations in the relative band intensities at lower negative potentials. The results for the lower negative potentials for pH 2 differ from those of pH 7 and pH 12, but beyond a potential of -0.90 V the behavior in the case of pH 2 was found to resemble those of the high pH values.

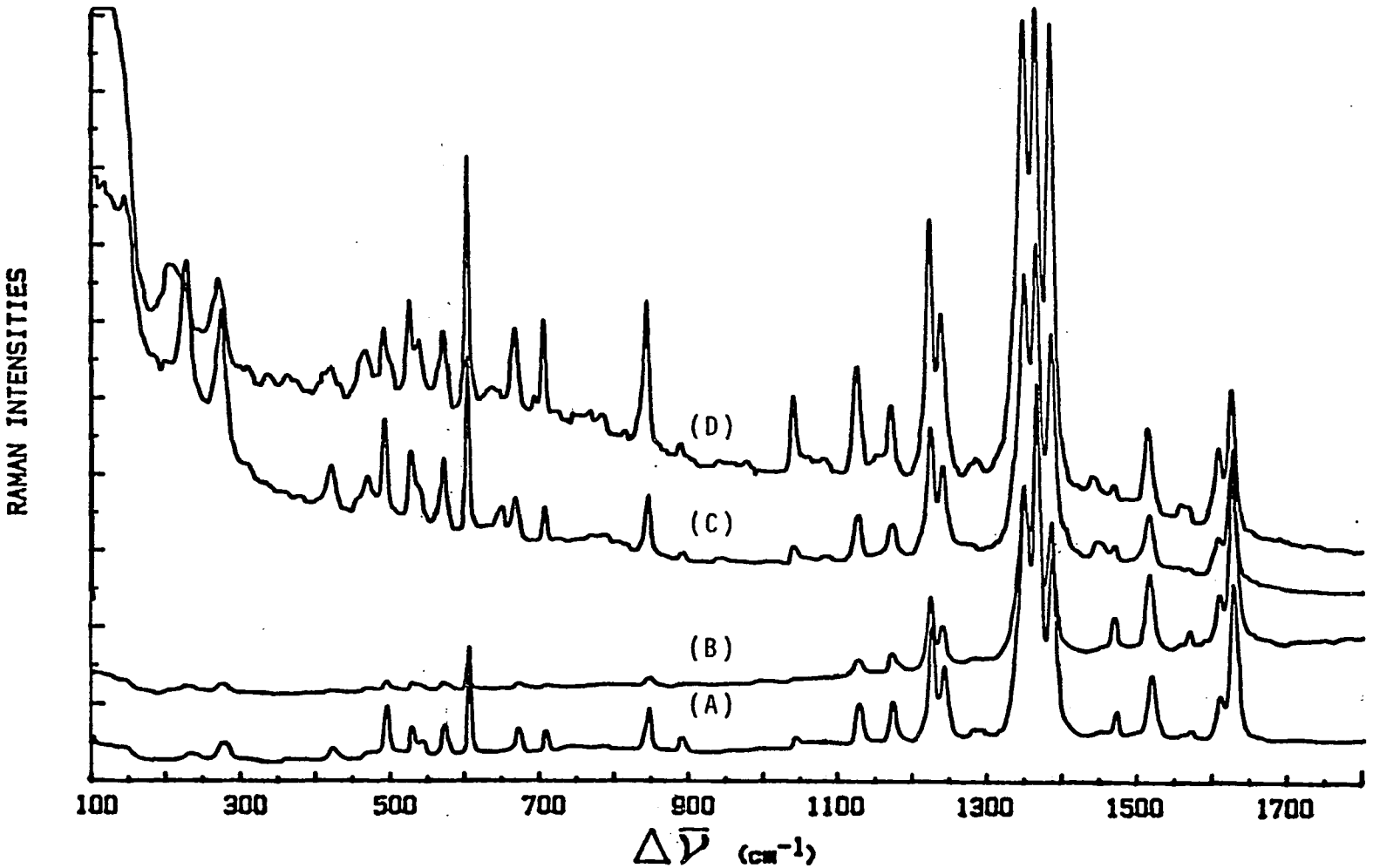

Fig. 5-15: Raman spectra of 2,2'-cyanine on a silver electrode excited by different sources: (A) 488 nm, (B) 514.5 nm, (C) 583 nm, and (D) 647.1 nm, radiations, respectively. Dye solution was 5×10^{-7} M in 0.08 M KI. Scale setting for spectra (A), (B) and (C) was $2 \times 10^{+4}$, and was $3 \times 10^{+4}$ counts/sec for (D).

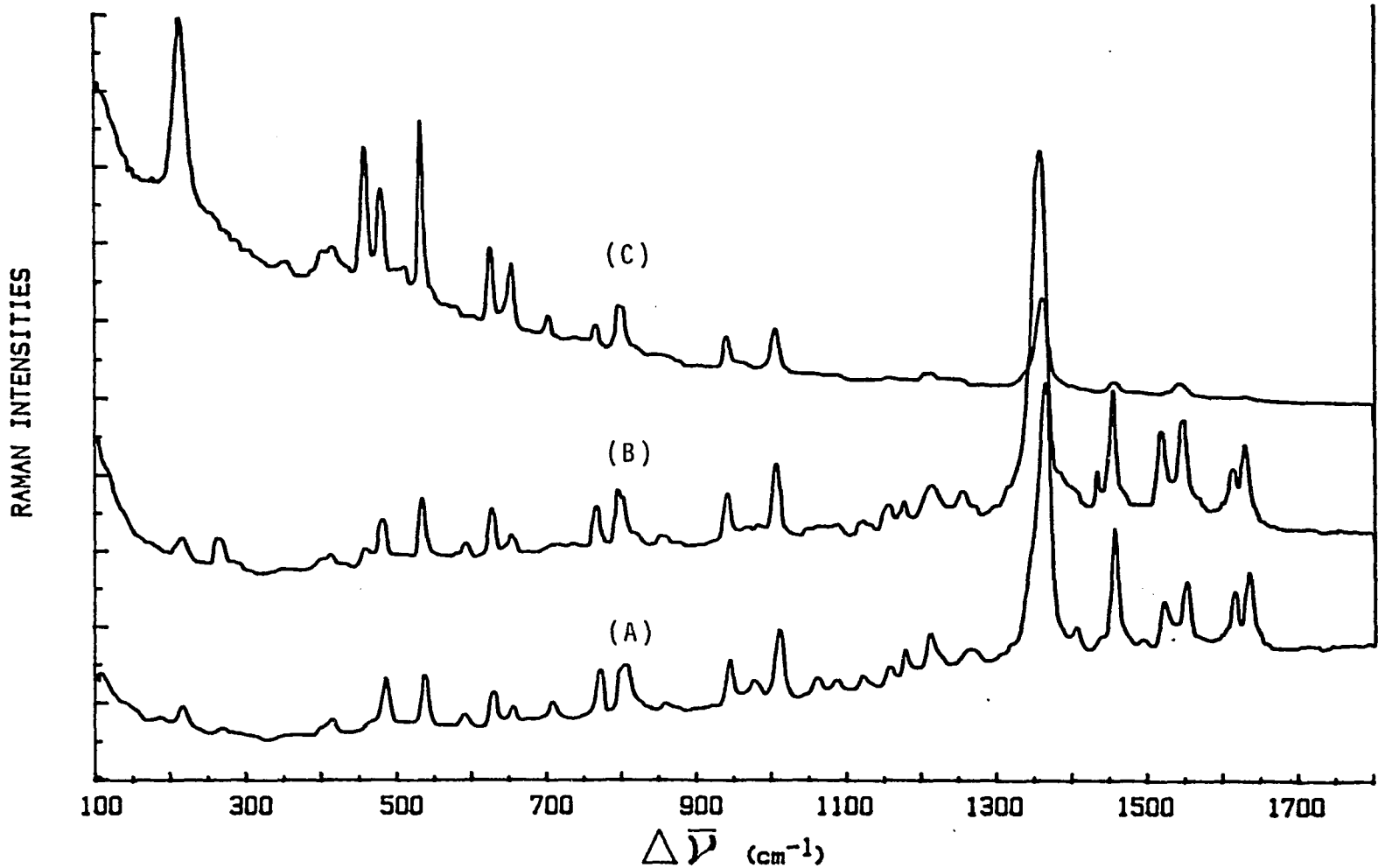

Fig. 5-16: Raman spectra of 4,4'-cyanine adsorbed on a silver electrode excited by different sources: (A) 488 nm, (B) 514.5 nm, and (C) 647.1 nm radiations, respectively. Dye solution was 10^{-6} M in 0.08 M KI. Scale setting for (A) and (C) was $2 \times 10^{+4}$, and was $8 \times 10^{+4}$ counts/sec for (B).

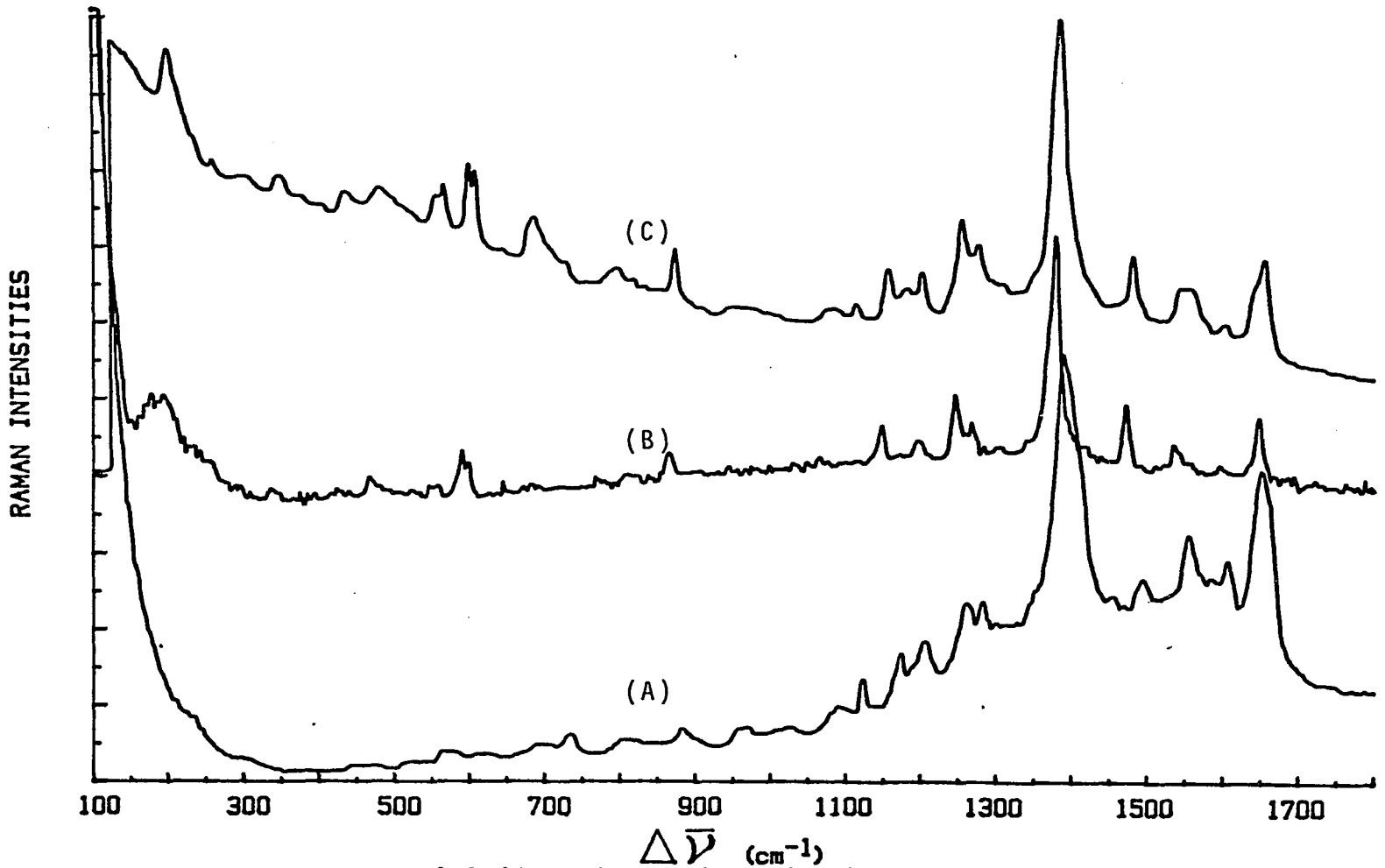

Fig. 5-17: Raman spectra of 2,2'-carbocyanine adsorbed on a silver electrode excited by different sources: (A) 488 nm, (B) 583 nm and (C) 647.1 nm radiations, respectively. Dye solution was 10^{-6} M in 0.08 M KI. Scale settings were 4 x 10^{+4}, 5 x 10^{+3} and 4 x 10^{+5} counts/sec, respectively.

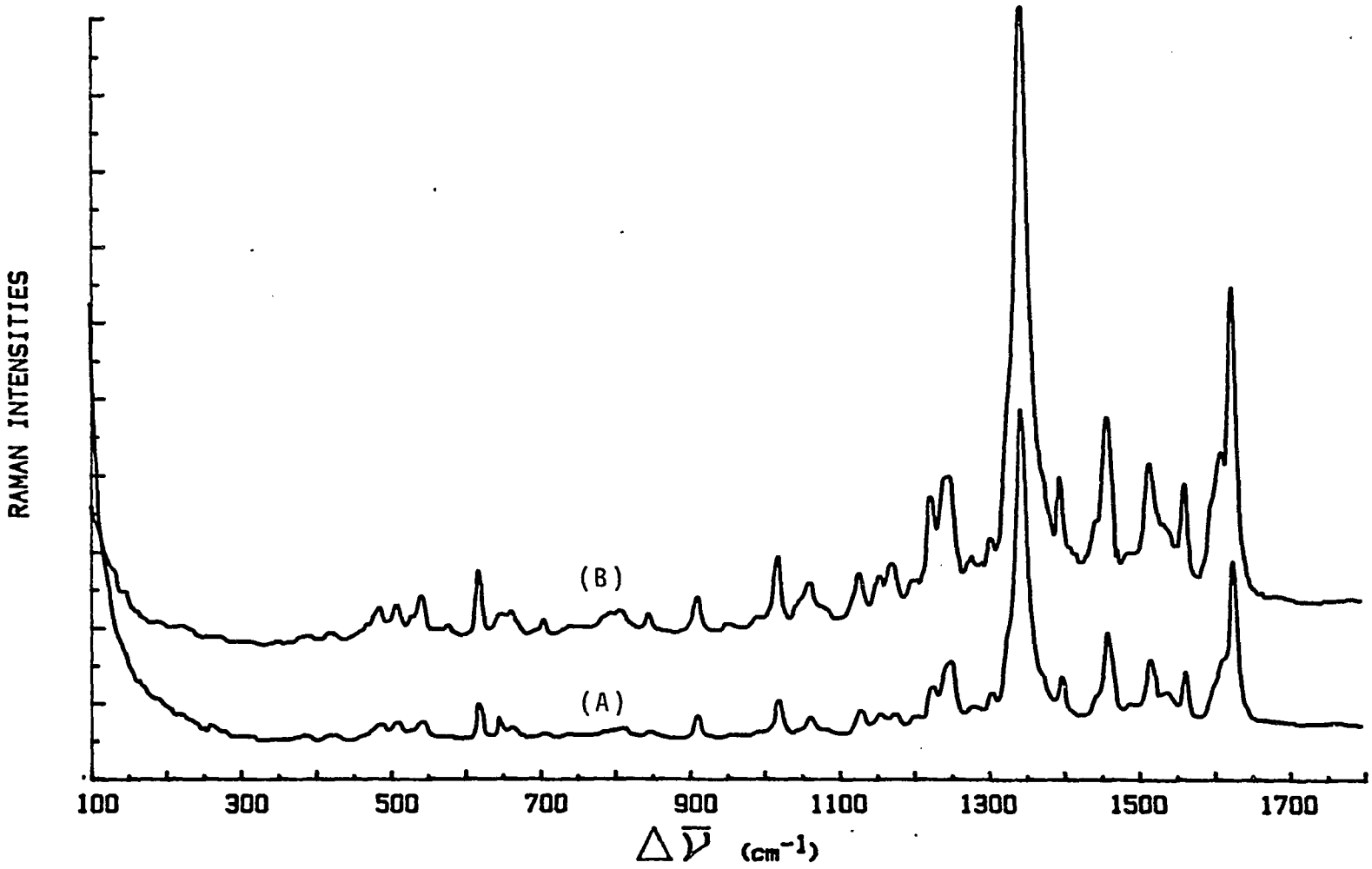

Fig. 5-18: Raman spectra of 2,4'-cyanine adsorbed on a silver electrode with (A) 0.1 M KCl and (B) 0.1 M KI as the supporting electrolytes, respectively; both excited by 488 nm radiation. Scale setting was 2.5 x 10^{+4} counts/sec in both cases.

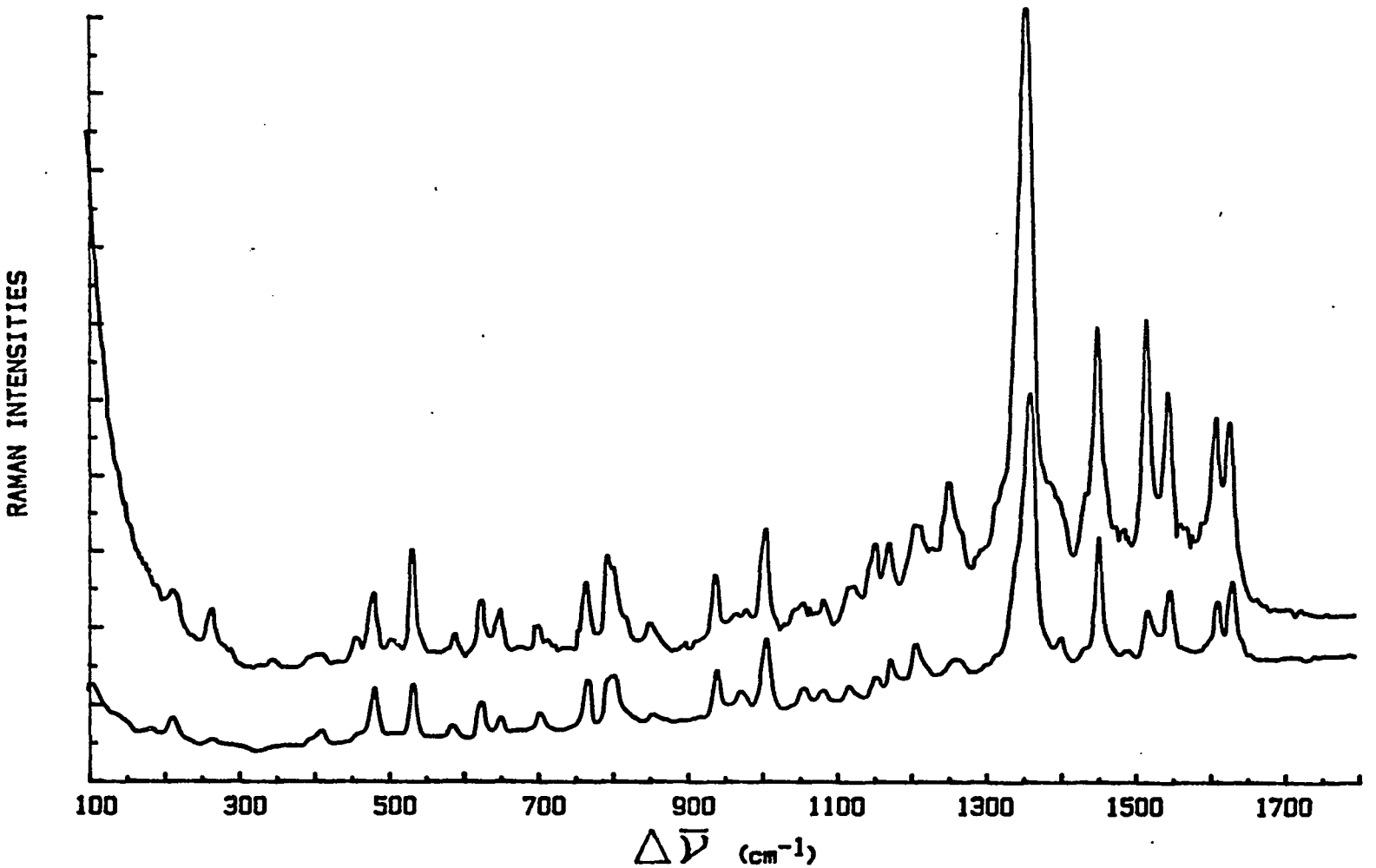

Fig. 5-19: Raman spectra of 4,4'-cyanine adsorbed on a silver electrode with (A) 0.1 M KCl and (B) 0.1 M KI as supporting electrolytes, respectively; both excited by 488 nm radiation. Scale setting was 2.5 x 10^{+4} counts/sec.

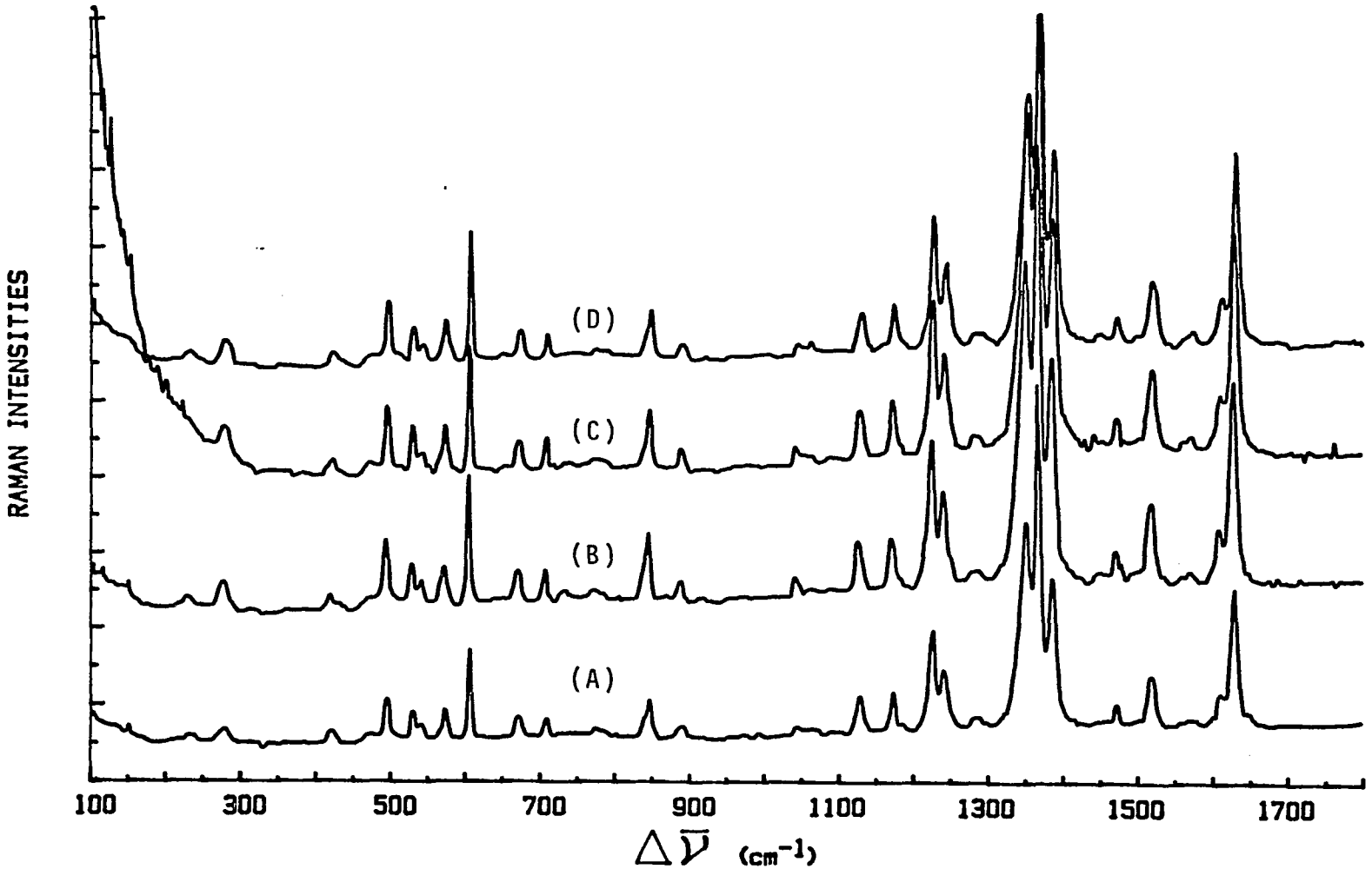

Fig. 5-20: Raman spectra of 2,2'-cyanine adsorbed on a silver electrode and excited by 488 nm radiation. The electrode was polished but treated differently: (A) no roughening, (B) chemical, (C) redox, (D) redox in the 0.08 M KI solution only. Scale setting was $1.1 \times 10^{+4}$ counts/sec.

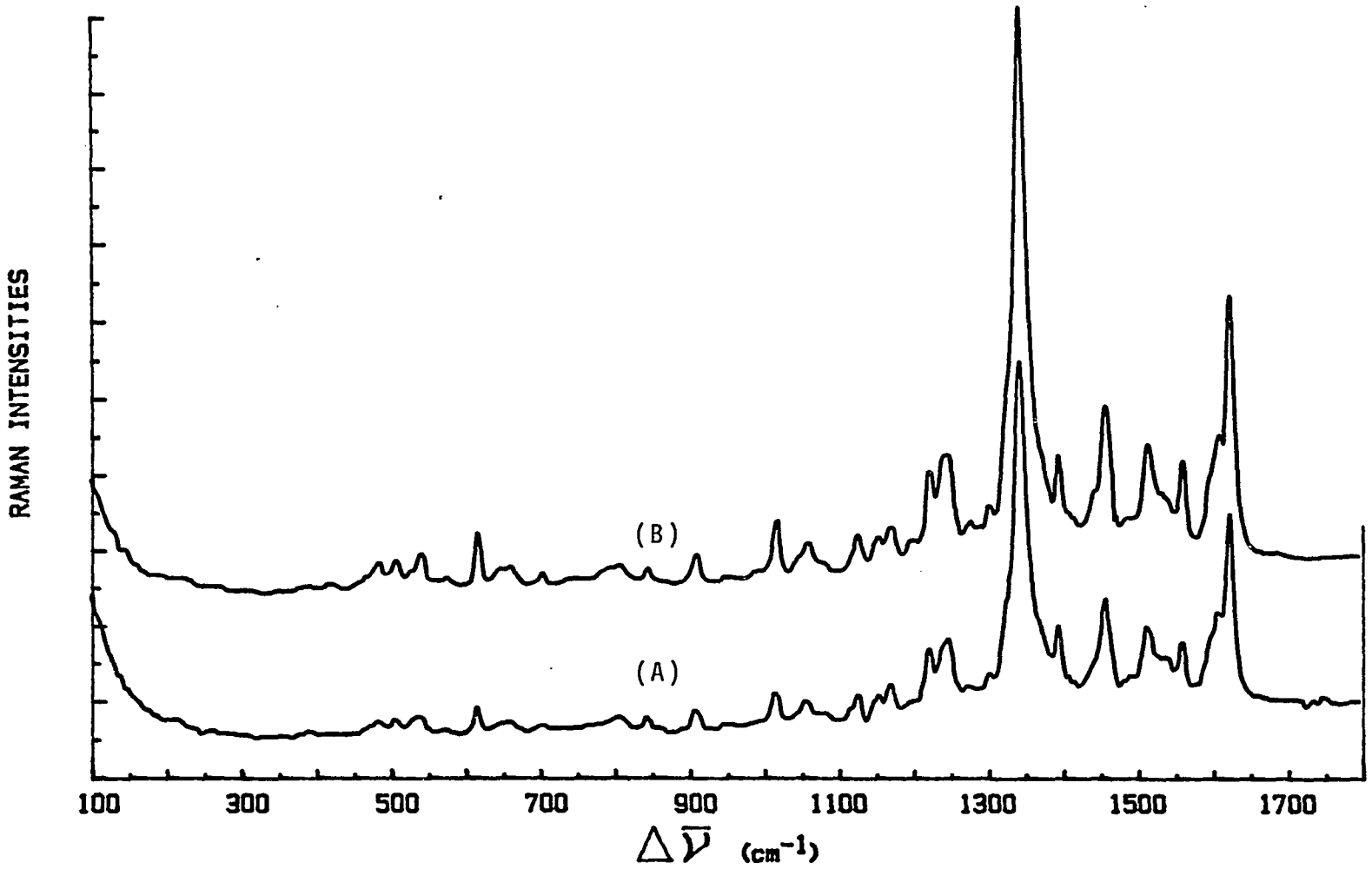

Fig. 5-21: Raman spectra of 2,4'-cyanine adsorbed on a silver electrode excited by 488 nm radiation, showing the effect of pretreatment: (A) chemical, (B) redox. Scale setting was 3 x 10^{+4} counts/sec.

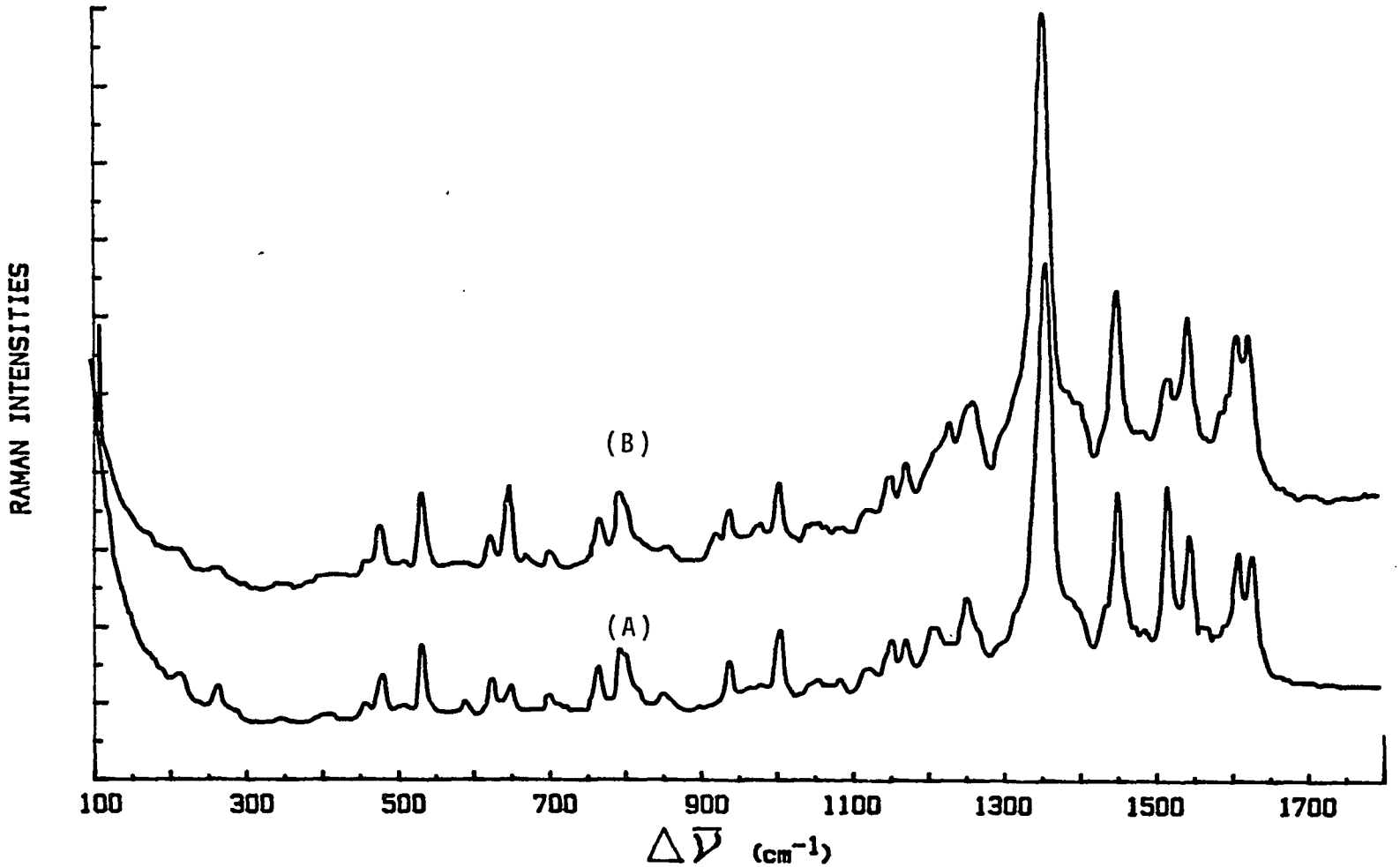

Fig. 5-22: Raman spectra of 4,4'-cyanine, adsorbed on a silver electrode excited by 488 nm radiation, showing the effect of pretreatment: (A) chemical, (B) redox. Scale setting was 3 x 10^{+4} counts/sec.

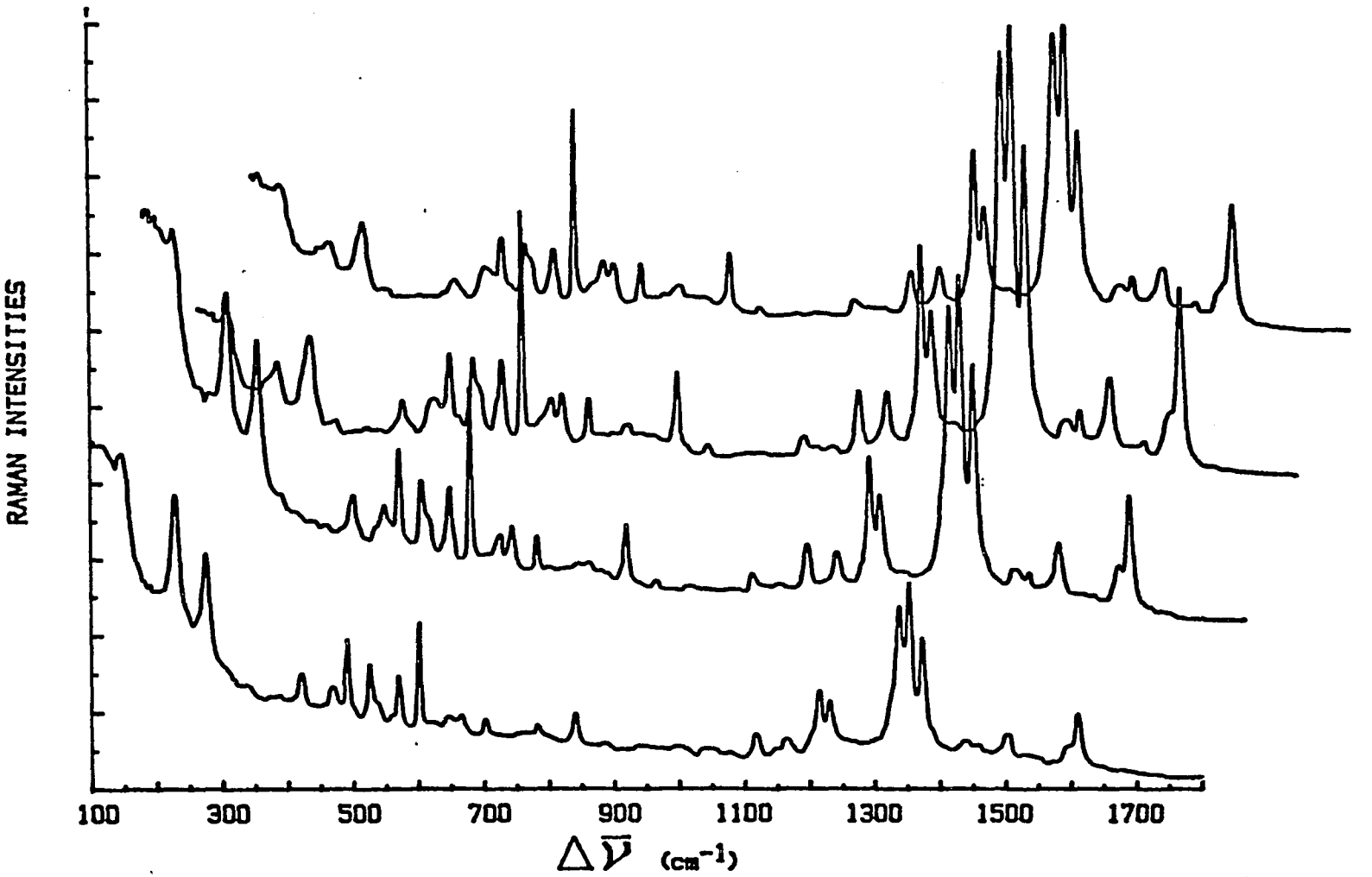

Fig. 5-23: Raman spectra of 2,2'-cyanine adsorbed on a silver electrode and excited by 583 nm radiation of 30 mW at the sample. The spectra are taken at potentials -0.8, -0.95, -1.1, and -1.2V, all vs. SCE, shown from bottom to top respectively. The scale setting was 3 x 10^{+4} counts/sec.

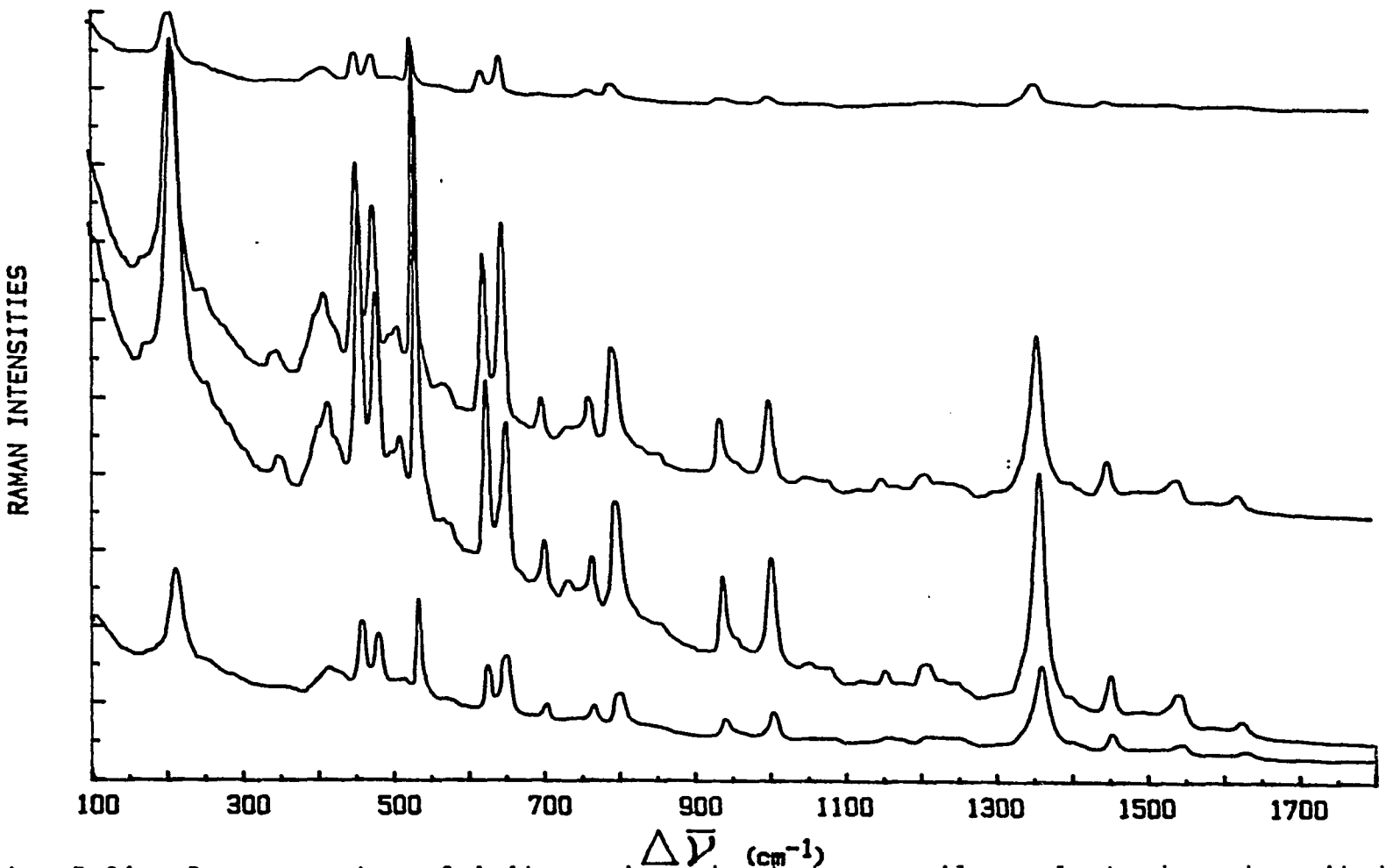

Fig. 5-24: Raman spectra of 4,4'-cyanine adsorbed on a silver electrode and excited by 647.1 nm radiation of 30 mW at the sample. Spectra show potential dependence at solution pH 7 for potentials -0.85, -0.95, -1.1 and -1.3V all vs. SCE, shown from bottom to top respectively. Scale setting was 4 x 10^{+4} counts/sec.

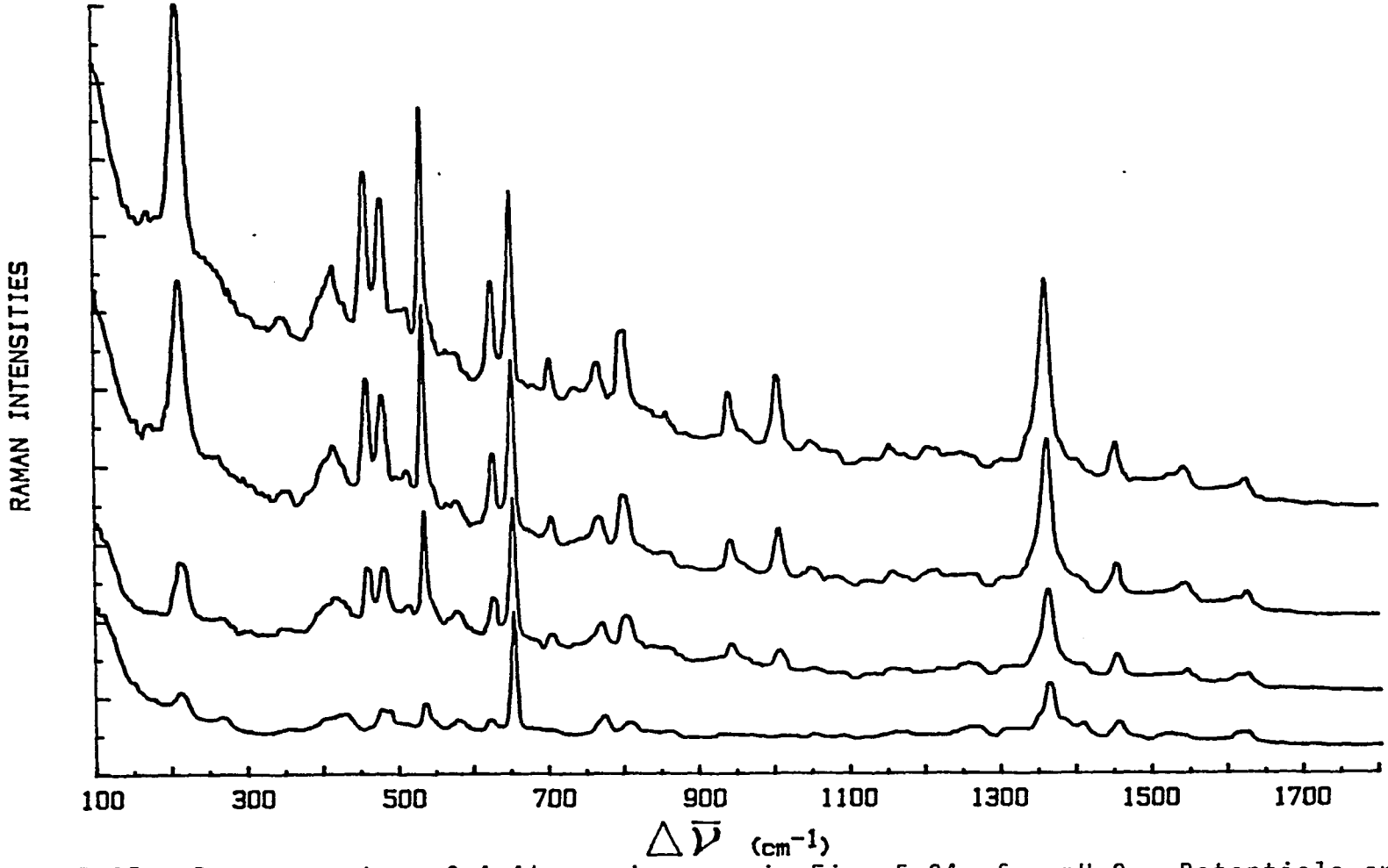

Fig. 5-25: Raman spectra of 4,4'-cyanine, as in Fig. 5-24, for pH 2. Potentials are -0.75, -0.85, -0.95, and -1.0V, all vs. SCE, shown from bottom to top respectively. Scale setting was 1.5 x 10^{+4} counts/sec.

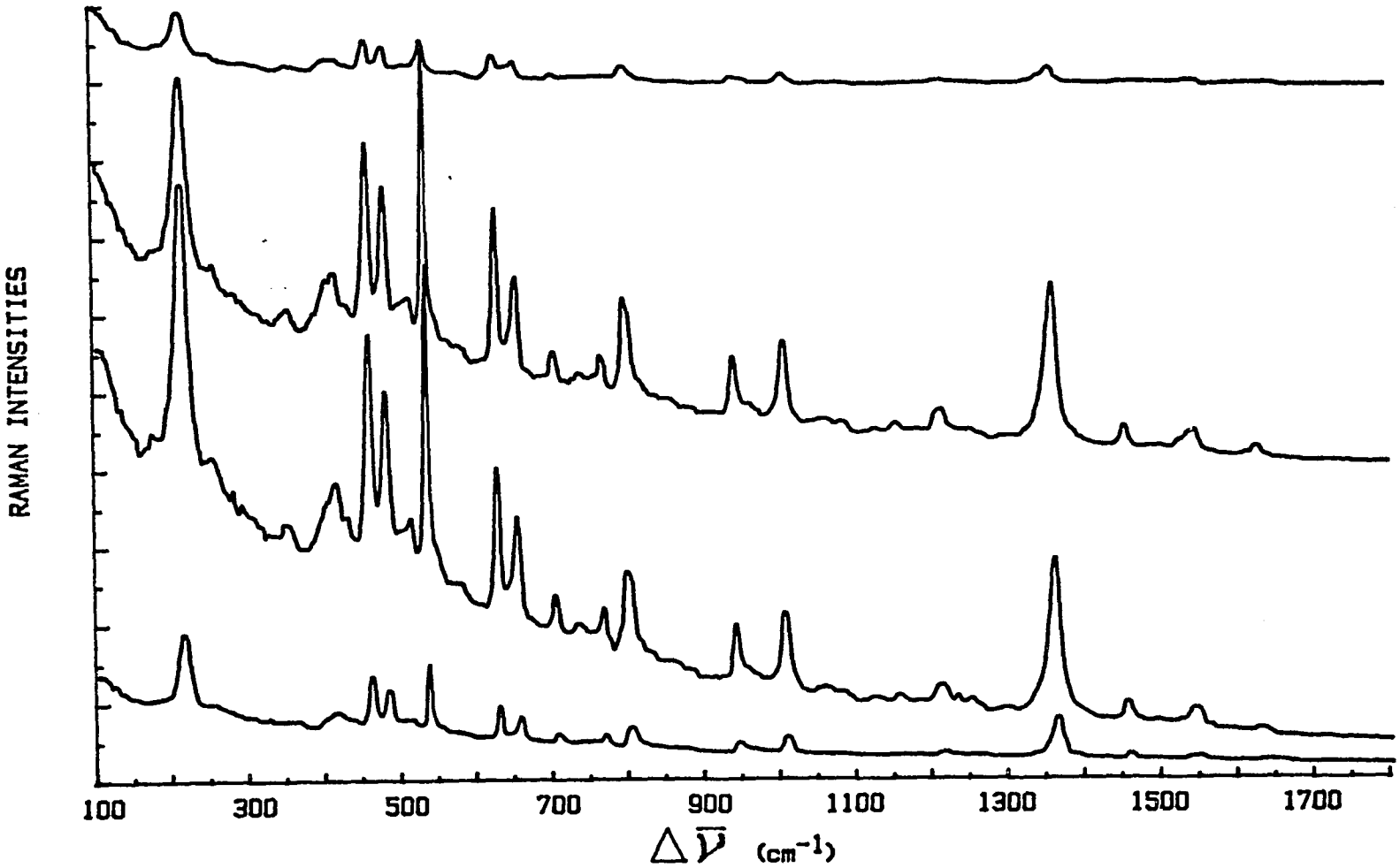

Fig. 5-26: Raman spectra of 4,4'-cyanine, as in Fig. 5-24, for pH 12. Potentials are -0.40, -0.70, -0.90 and -1.2V, all vs. SCE shown from bottom to top respectively. Scale factor was 1.5 x 10^{+4} counts/sec.

5.2.3 Raman Scattering by Molecular Excitonic Systems on Semiconductor Electrodes

The following spectra presented in Fig. 5-27 and Fig. 5-28, are samples of studies made of Raman scattering by the sensitizing dyes adsorbed on semiconductor electrodes. The two figures show results of samples adsorbed on ZnO electrodes and excited by off-resonant excitation wavelengths. Fig. 5-27 shows the results for 488 nm excitation of (A) 2,2'-cyanine and (B) 2,2'-carbocyanine, adsorbed on the ZnO semiconductor electrodes in the usual electrochemical system used for these investigations, which has already been described in the text. The electrodes were prepared as described in Chapter 4. The dye concentration in 0.4 M KI supporting electrolyte was 10^{-6} M in each case. The two spectra in Fig. 5-27 were given the same scale settng of $1 \times 10^{+4}$ counts/sec. The laser line power was 30 mW at the sample. Scanning was done when the cell was an open circuit.

Fig. 5-28 compares results obtained for adsorbed 2,2'-carbocyanine on a ZnO electrode, excited by (A) 488 nm and (B) 514.5 nm radiation. The scale setting for the two spectra was $1 \times 10^{+4}$ counts/sec and other conditions for obtaining the spectra were the same as described for those of Fig. 5-27.

These preliminary results are very interesting, showing the ZnO semiconductor electrode provides favorable surfaces for these cyanine dyes to form aggregates. Attempts were made to measure the photocurrent generated in the electrochemical cells involving these systems, the results will be the subject of a future publication.

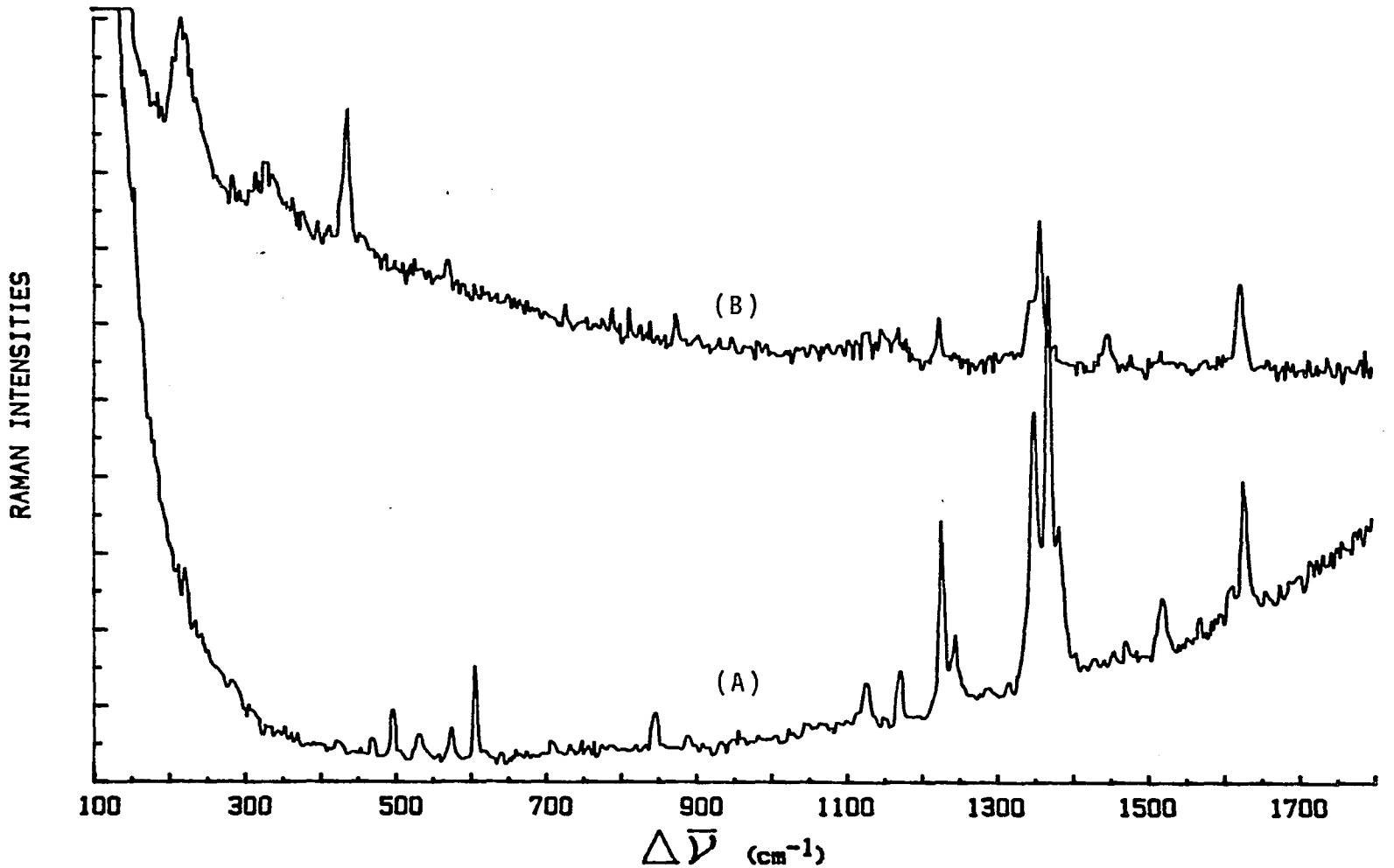

Fig. 5-27: Raman spectra of (A) 2,2'-cyanine (B) 2,2'-carbocyanine adsorbed on ZnO_{+4} semiconductor electrodes and excited by 488 nm radiation. Scale setting was 1 x 10^{+4} counts/sec.

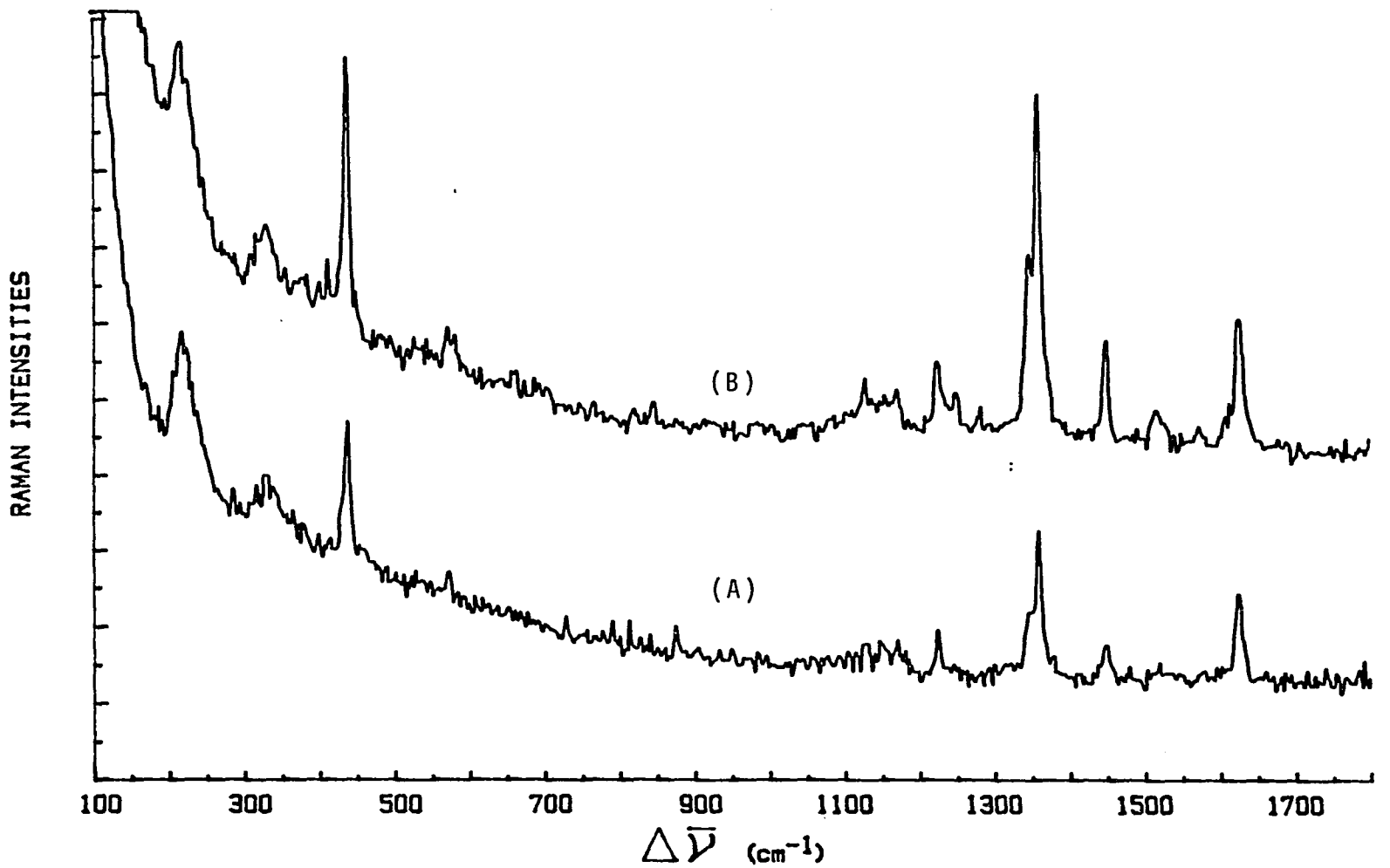

Fig. 5-28: Raman spectra of 2,2'-carbocyanine adsorbed on ZnO semiconductor electrode excited by (A) 488 nm and (B) 514.5 nm radiations respectively. Scale factor was $1 \times 10^{+4}$.

CHAPTER 6

DISCUSSION AND CONCLUSIONS

6.1 DISCUSSION OF RESULTS

6.1.1 Raman Scattering Involving Vibro-Exciton States

A. Importance of A-, B-, and C-Terms of the Polarizability

The graphical representation of the scattering process shown in Fig. 6-1, is helpful in assessing the meaning and relative importance of the various contributions (A, B, and C) to the polarizability that appear in the polarizability expression of Eq. (3.30). Similar illustrations have been used elsewhere (37,71) to account for the energy of the incident radiation and absorption resonances which are important factors in determining the magnitude of each of the contributions to the polarizability. The density-of-states for the exciton, arising from exciting a molecule in the adsorbed aggregate, is considered as having a distribution similar to that suggested in Fig. 6-1 (71). The effective energy spread of the exciton's density-of-states is diminished beyond the intrinsic width associated with the dipole-dipole interaction energy (248) by the smaller spread of states associated with allowed dipole transitions (which leads to the narrowness of aggregate bands in fluorescence and absorption spectroscopies (73,105) and by conservation of energy as regards to the incident photons.

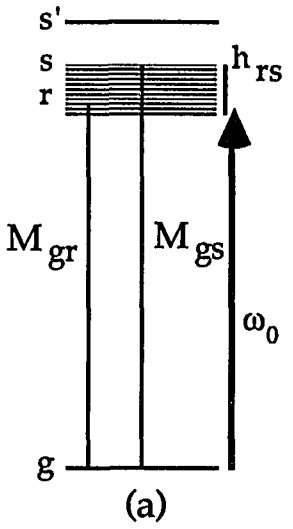

Corresponds to B-term of polarizability

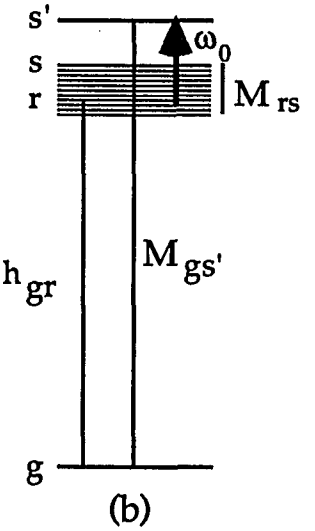

Corresponds to C-term of polarizability

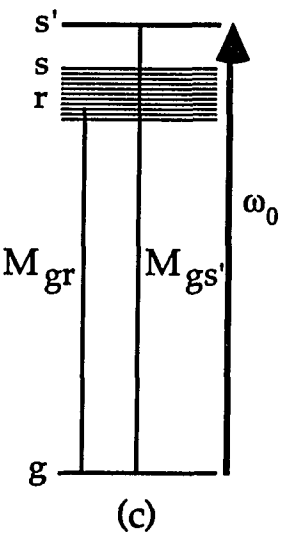

Corresponds to "dressing" a particular state

Fig. 6-1: Aggregation Enhanced Raman Scattering (AERS): Energy Level Scheme.

The excitonic states can also experience a "Stark-effect" due to the coupling between the permanent dipole moment of the aggregate and the applied potential in our electrochemical system; this should result in the possibility of tuning the vibro-excitonic states by the applied potential. This is incorporated in the scattering problem and is predicted by the theory through the dependence of E_s^o in Eq. (3.32) on potential. The relative importance of A, B, and C in the polarizability expression can then be assessed from the frequency dependent scattering schemes of Fig. 6-1 (71).

Fig. 6-1(a) represents the case where the incident radiation's energy is just sufficient to reach the lower states of the exciton band. For J-aggregate formation, the exciton band is of lower energy than the isolated molecule energy indicated by the symbol s'. This situation leads to electronic excitation from the ground state aggregate to the exciton, which is analogous to the molecule-to-metal excitation scheme used by Lombardi et al. (37), and gives importance to the B-term of the polarizability. Fig. 6-1(a) can also be applicable to the case where the incident radiation's energy is sufficient to raise electrons from the aggregate ground state to exciton states greater than those represented by the band center, yet still lower than the single molecule state s'. In this case $[M]^0_{g,r}$ corresponds to a transition dipole moment for excitation into a more highly excited vibro-exciton band, and different vibronic excitation with different matrix elements would be expected for the B-term. This latter point is made for the fact that a particular electronic distribution upon formation of the exciton will be reflected in the vibrational wave functions which are the eigenvalues of the nuclear motion in the field of the electrons.

The description of the C-term (Fig. 6-1(b)) shows the case of electron transfer from the exciton to other excited states (37). The C-term is considered to be less important than the B-term, in the present scattering problem, for two main reasons. First, the energy spacing $E_g^0 - E_t^0$ in the denominator of Eq. (3.33) (with $t \equiv s$), in general, will be greater than the energy difference $E_r^0 - E_s^0$ in the denominator of Eq. (3.32). Secondly, the excitonic state only exists once a single molecule in the aggregate has been excited--thus, a two photon process is necessitated by this scheme and is anticipated to have a small cross-section. Dye molecules, which have led to this particular scattering problem, function as spectral sensitizers where they absorb from their ground states and inject electrons into substrates from their excited states, suggesting that $[\mathbf{M}]^0_{t,r} = 0$. For the above reasons, of the Herzberg-Teller contributions, the B-term, but not the C-term, is expected to be important in the present scattering system.

When the exciting frequency is close to a "resonance", the A-term can be expected to become enhanced, and non-zero overlap integrals in Eq. (3.31) can lead to fundamental-, overtone-, and combination-bands, especially for totally symmetric vibrational modes (245,249). However, even though the excitation conditions may correspond to a resonance situation, both A and B, in general, can lead to the presence of vibrational bands in the Raman spectrum. For certain bands, in fact, contributions from the A-term may vanish. This latter situation is expected for the "strong-coupling case" for exciton formation (244), which corresponds to small barriers for the excitation leaving the isolated single molecule and "roaming" through the aggregate structure. In such a case the Born-Oppenheimer separability of intramolecular electronic and vibrational motions is necessary. Further,

since the excitation would be spread over many molecules, each individual molecule would have essentially the same electronic structure as a ground state molecule. It therefore follows, from the Franck-Condon principle, that the A-term would only be non-zero for upper state modes identical to ground state modes and would not contribute to the appearance of Raman bands resulting from the overlap of intramolecular ground and vibro-excitonic modes. The excited state lattice modes of the aggregate, resulting from the intermolecular potential function, can however be expected to give rise to non-zero overlap integral products with ground state intramolecular modes.

Under some other conditions the B-term can become dominant in determining Raman Bands. In the non-resonant Raman case where vibrational closure over the excited state vibrational modes relegates the A-term to make a contribution only to Rayleigh scattering, and for non-totally symmetric modes (in both the resonance and non-resonance cases) for which the A-term vanishes through symmetry, B-term alone contributes to Raman bands.

The B-term is allowed by intensity borrowing through the h_{rs}^{α} factor to contribute to Raman scattering, and, because of the explicit dependence of the factor h_{rs}^{α} on the vibrational mode (α), the B-term contributes only to intramolecular Raman modes.

Fig. 6-1(c) is the situation in which the frequency of the incident radiation is strongly resonant with the single molecule vibronic absorption. A highly perturbed electronic distribution is expected to be created in the aggregate in this case and the full complement of excitonic sub-bands allowed by conservation of energy. As a result, the A-term might be

expected to lead to overtone and combination bands in the Raman spectrum. Indeed, we have found this to be the case, with an extensive overtone/combination pattern. (Experimental results for 2,2'-cyanine and 4,4'-cyanine are presently being prepared for publication. In the former, excitation is at 514 nm, while, in the latter, 580 nm excitation is used.)

B. Association of Albrecht's A- and B-Terms with Specific Bands

In general, association of bands with the A and B terms depends on the scatterer. However, the excitation frequency dependence of Raman scattering by aggregated cyanines exhibits a behavior which is typified by that of 2,2'-cyanine. Thus, here we confine our discussion to 2,2'-cyanine but realize that other cyanines studied (4,4'-cyanine, 2,2'-carbocyanine, etc.) are subject to the same type of analysis.

Fig. 5-15 shows typical Raman spectra for aggregated 2,2'-cyanine excited by different excitation wavlengths. It is observed that off-resonance excitation, either of higher frequency than the single molecule state (ca. 520 nm) and aggregate state (ca. 575 nm), as the 488 nm excitation is, or of lower excitation frequency (e.g., 647 nm Krypton excitation) leads to spectra with the same bands in the region between 300 to 1700 cm^{-1}. These latter bands, though they have slightly different frequency dependent intensities for off-resonance excitation, are attributed to the B-term of the polarizability, and, as a result, are associated with intramolecular modes.

When 2,2'-cyanine was excited with 583 nm radiation (Fig. 5-15 (C)), which overlaps its J–aggregate absorption, two bands (4,4'-cyanine exhibits only one band upon excitation with 647 nm radiation as shown in Fig. 5-16(C)), broader than those attributed to the B–term, showed significant

intensity enhancements; also, all the B-term bands associated with non-resonant excitation appeared as well. In line with the discussion in subsection 6.1.1:A above, we attribute the two bands to the A-term of the polarizability to overlap of single molecule modes and aggregate (i.e., lattice) modes. In addition, we conclude that all B-term modes are most likely fundamentals, since with non-resonant excitation, these same modes, as a result of closure over excited state modes, must be fundamentals (in the harmonic oscillator approximation) (72).

Since A (Eq. (3.31)) and B (Eq. (3.32)) have the same excitation frequency dependence but A does not depend on the factor $E_r^0 - E_s^0$ which B has in its denominator, while in addition, all Raman intensities are proportional to the product of concentrations of scattering species, it follows that bands that depend only on A can be used as internal standards to isolate the $E_r^0 - E_s^0$ dependence of Raman bands that depend only on B. However, an additional frequency dependent factor $\nu_o\nu^3$, for photon counting measurements (249), where ν_o is the incident laser frequency and ν is the frequency of the Raman band, must also be taken into account.

The use of A only dependent bands as internal standards for Raman intensity versus potential measurements, as suggested here, makes possible a study that is impossible otherwise, and differs from the use normally made of internal standards (which are added scattering species) to normalize just the frequency dependence of Raman scatterers (250,251).

6.1.2 Aggregate Formation and Raman Scattering

Absorption spectroscopy for the sensitizing dyes has exhibited significant changes as a result of aggregation. The results show that ease of aggregation depends on the medium: surface-aggregation is promoted more on silver colloidal particles than on TiO_2 sols, and is more pronounced in the presence of KI than in the presence of the other halides. These deductions can be made from the intensity of the J-band that appears in the absorption spectra.

The observation that those media that promote aggregate formation by the sensitizing dyes also promote optimum Raman scattering by the dyes suggests a strong relationship between aggregation by these dyes and their Raman scattering. More excitingly, our finding is that only when J-aggregate absorption is present do the spectral sensitizer dyes exhibit intense Raman scattering.

The results also suggest that the particular substrate is not the most important factor in determining the Raman scattering efficiency of these dyes, rather surfaces are simply templates onto which aggregates form. The essential role played by the substrate in the aggregation enhanced Raman scattering by these dyes is thus different from that in SERS. In the former case the substrate serves to adsorb the sample but in the latter it participates in the enhancement mechanism in addition to enabling adsorbtion. This finding further suggests that in the enhanced Raman scattering by the dyes which form aggregates, the substrate role should depend only on the kind of the substrate but not necessarily on how it is pretreated. Results obtained in fact confirm this. Intense Raman scattering spectra were obtained from

smooth substrate surfaces as well as from roughened surfaces. Also different methods of pretreatment produce essentially the same result. The reason why the dyes give more intense Raman spectra on some substrates than on others can be attributed to purely interfacial phenomena involving interfacial energetics. Surfaces which provide better substrate-adsorbate (aggregate) systems (energetically) should promote more surface concentration of aggregates leading to more intense Raman scattering by these dyes.

The more intense Raman scattering by the dyes in electrochemical systems with KI as the supporting electrolyte as compared to the other halides can also be explained from an aggregation point of view. The absorption spectra of Fig 5-5 and Fig. 5-6 show intense J-bands for 2,2'-cyanine at various concentrations of KI and the dye respectively. The band intensity increases with an increase in concentration of either the KI or the dye at a fixed concentration of the other. We do not think the kind of mechanism operating here can be explained by the solubility effect (196) alone, for such unique behavior was not seen in the case of KBr and KCl. The explanation advanced here is that the iodide ion, having a lower charge to mass ratio, a property which makes it more polarizable than the other halide ions, plays an important role (through polarization) in helping orient the dipoles, making it energetically favorable for aggregation. Thus more aggregates are formed and their number and size should increase with the number of iodide ions and also with the number of the dye molecules. There could also be some contribution from changes in solvent properties caused by the added electrolyte (191,192) favoring aggregation. Once these

aggregates are formed they are then easily attracted to the substrate electrode surface.

The theory we advanced to explain the enhanced Raman scattering by the sensitizer dyes, applies to a finite aggregate structure consisting of N molecules. For the nonresonance case, B" (Eq. (3.35)) squared allows determination of an enhancement factor for the aggregated system as compared to a monomeric system. It is seen from Eq. (3.35) that the B" term, for large N, exhibits a factor of magnitude N, reflecting the summation over exciton states (72). Squaring, as required to determine the Raman intensity, one gets the factor $N^2\tilde{N}$ (appearing in the Raman equation) times other general terms; $\tilde{N}$ is the number of scattering centers (i.e. aggregates), hence $N\tilde{N}$ represents the number of molecules that scatter radiation. The additional factor of N thus represents an "intrinsic" enhancement factor due to the formation of an aggregate containing N molecules. An increase in the number of aggregates should therefore lead to an increase in Raman scattering intensity for these dyes. This is supported by the findings explained above.

The absence of the J-band in the absorption spectrum of cyanine taken in SiO_2 colloidal solution at pH 9 and the very weak Raman signals observed follow directly from the explanation given above. At such a pH, necessary to maintain the stability of the sol, the SiO_2 particles would be completely surrounded by the basic hydroxyl ions; and this could lead to insufficient attraction between the purely basic forms of the dye in such a medium to the sol particles. This, we think, could be a significant hindrance to adsorption and formation of aggregates on the substrate paticles.

Another observation in Raman scattering by the sensitizer dyes, which is a direct consequence of aggregation, is a significant fluorescence quenching from depletion of the monomer species when aggregates are formed. For surface Raman scattering by aggregated cyanine dyes, the implication is that SERS and SRRS by monomer species become more and more insignificant as aggregation proceeds.

6.1.3 pH Effect

Results obtained from pH dependent investigations of Raman scattering by the dyes on silver electrode can be attributed to two main factors, i.e. shift in absorption spectrum and aggregation,both of which affect the Raman scattering intensity. Results shown for 4,4'-cyanine on a silver electrode in an electrochemical system excited by 647.1 nm (near resonance) excitation wavelength, show that at pH 2, when the color of the solution disappeared as the result of protonation of the dye, spectra obtained at lower negative potentials (vs SCE) maintained on the substrate show very low intensity for the Raman bands. As the negative potential on the electrode is increased numerically, the bands, especially those which belong to fundamental modes involving the aggregate and which are found to be enhanced more through resonance, grow and become intense as compared to spectra of lower negative potentials of pH 7 and pH 12.

One explanation of the above observations is that at pH 2 there could be a lack of, or very little contribution from resonance Raman as a result of a possible shift in absorption spectrum (J-band) and high -ve potentials (vs SCE) were necessary to tune into resonance. The other explanation, based

on aggregation, is that pH affects the adsorption-desorption kinetics and at pH 2 there would be a little attraction between the dye and the electrode. Increase potentials allow attraction of dye molecules to form more aggregates on the electrode surface. Further experiments are necessary before a concrete conclusion can be drawn.

6.1.4 Excitation Wavelength Dependence

The various mechanisms which have been proposed for SERS include resonance Raman processes associated with excitation primarily on the silver surface (51,247,248) in which there is an optimum excitation wavelength which depends on the metal but is relatively insensitive to the adsorbate. Results obtained in the present studies (Figs. 5-15,5-16,5-17) cannot be explained upon this basis. In the case of these sensitizing dyes which form aggregates, the optimum excitation wavelength depends solely on the adsorbate molecules which play a dominant role in determing the resonance, as predicted by our theory, where greater variations are expected in the wavelength of the profile maximum for different adsorbates (245). As the optimum excitation wavelength which coincides with the J-aggregate absorption band of the adsorbate is approached, the A term in the expression becomes more important as in the resonance case. The theory also accounts well for the nonresonant enhancement mechanism where the B term becomes the dominant factor.

One of the main objectives of the studies presented in this text was to investigate the extent to which surface excitation profiles depend on the adsorbate. Excitation profiles were found not to depend on the degree or

method of roughness of the electrode surface. Such independence on roughness throws more light on the enhancement mechanism in the case of the aggregated dyes. In order to avoid the complication due to varying degrees of roughness in comparing the profiles for different adsorbates, the results shown were all for smooth electrodes.

It is clear, from the presence of a maximum in the Raman excitation profiles both for the electrode species reported in this text and for 2,2'-cyanine adsorbed on silver colloids studied previously but not reported here (awating publication), that the enhanced Raman scattering is, at least in part, a resonance phenomenon. The wavelength of this resonance maximum coincides with the absorption band of the J-aggregate of the dye, whereas in the case of molecules following SERS, this resonance maximum was found to coincide with the Mie extinction maximum for the metal particles, thus establishing the role of plasma in the latter case (51,236), which is the consequence of an electromagnetic field enhancement at the metal surface on resonance. In SERS the adsorbate molecules are not themselves involved in this resonance, and if what has been stated above were the only contribution to the Raman enhancement effect, the excitation profiles of all molecules on a given surface would be the same. It is not so for these dyes, as results obtained indicate. If there were any excitation profile contributions from field enhancement effects, they might be rather small and flat, and undetected in this wavelength region for these dyes which have their optimum resonance determined by aggregation and its absorption bands.

The A term of the theory, as developed in references (72) and (235), specialized to the aggregated molecule model in the resonance case is given

by Eq. (3.34); from which discussions in Ref. 245 derive the final expression as Eq. (3.35). In the present discussion, M is the dipole-dipole interaction energy for excitation on two adjacent molecules in the aggregate. It is clearly seen from the right hand side of the above equation that a resonance is predicted as the incident laser radiation frequency is tuned through the J aggregate absorption, and occurs when $\nu_{V}^{V''} - \nu_{0} = -2\,M/h$. It is to be noted that J-bands are generally narrow compared to monomer absorption bands, with a value of 150 cm^{-1} (~ 50 Å at 572 nm for 2,2'-cyanine) being typical.

The excitation profile results can now be seen to be in accord with the above proposal of the theory. The excitation wavelength-dependence of the enhanced Raman scattering as performed for these various adsorbates forming their J aggregate absorption bands at different places of the spectrum is thus an important measurement for testing the theory.

There are differences even between the excitation profiles of different bands of adsorbed dye and it is clearly necessary for such differences between the Raman excitation profiles for bands of the same adsorbate to be understood. The explanation from an aggregation point of view is that as the J aggregate band excitation wavelength is approached, those bands which are due to vibrational modes of the aggregate are enhanced more than those bands due to vibrational modes of single molecules. The studies reported have confirmed this remarkable result.

6.1.5 Surface Potential Dependence

Our theoretical formulation for enhanced Raman scattering by aggregated molecules is now applied to the enhanced signal versus potential issue. The Raman scattering problem of aggegated molecules with the vibro-excitonic states used as excited states, utilizing the Herzberg-Teller approach originally developed by Albrecht (221-223) is applied. The resultant polarizability expression indicates that certain bands may be used as internal Raman scattering standards, thereby isolating the static electric field functionality from the dependence on excitation frequency and surface concentration - we refer to bands corrected in such a fashion as being normalized. We also found that a resonance is predicted for normalized bands when exciton state band-edges are tuned into energy coincidence with the exciting radiation as a result of changes in the static electric field at the electrode surface. These conclusions explain the experimental results obtained through investigation of the potential dependence of Raman bands of aggregated 2,2'-cyanine and 4,4'-cyanine presented in Figs. 5-23 and 5-24. The experimental observations are consistent with the theory, once again strongly supporting the supposition that the phenomenon of enhanced Raman scattering of aggregated molecules is correctly described using vibro-excitonic states in the Raman scattering problem.

Intensity versus potential plots of some bands of 2,2'-cyanine excited by 583 nm radiation are shown in Fig. 6-2. Data plotted are results of experimental results of which samples are shown in Fig. 5-23, and have been corrected for background signal-defined by drawing a smooth curve beneath the spectra of Fig. 5-23 and subtracting. Fig. 6-3 shows similar plots

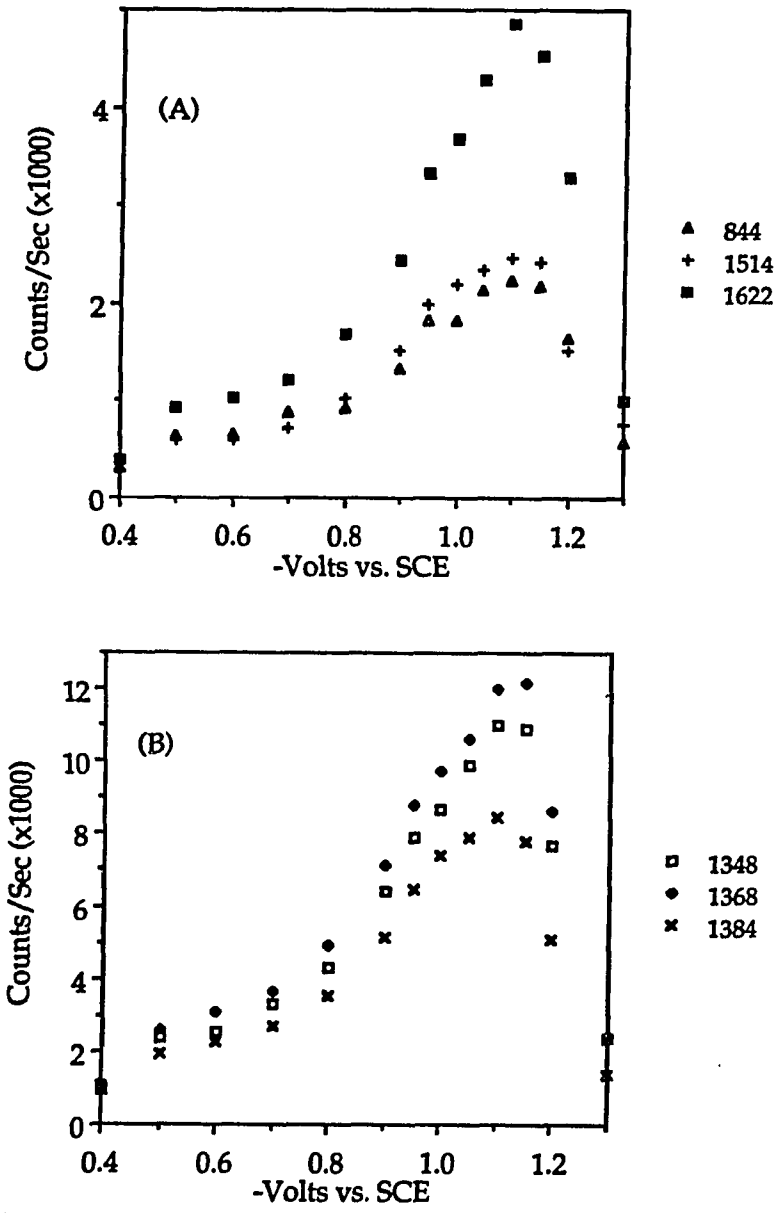

Fig. 6-2: Intensity versus potential plots for several bands of 2,2'-cyanine excited by 583 nm radiation. (A) Data for some of the weaker bands, (B) data for the stronger bands.

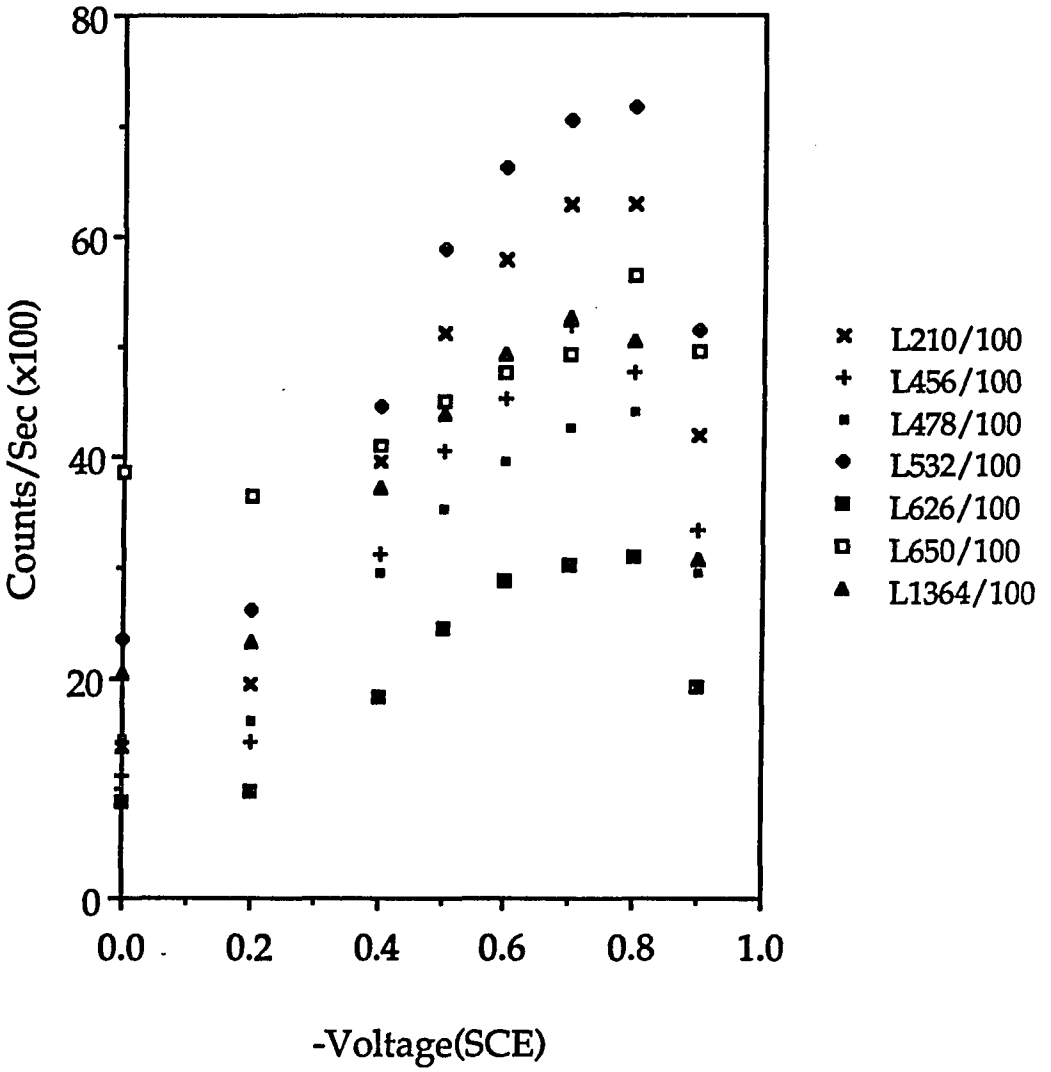

Fig. 6-3: Intensity versus potential plots for several bands of 4,4'-cyanine adsorbed on a silver electrode and excited by 647.1 nm radiation.

for 10^{-6} M 4,4'-cyanine in 0.1 M KCl, adsorbed on silver electrode and excited by 647 nm radiation.

Such plots of the data do not allow discrimation between models of the potential dependence of the Raman signal, but since our present theory is a quantum mechanical one, and our analysis procedure involves a ratioing of intensities associated with B and A terms of the polarizability, thereby factoring the potential dependent surface concentration and excitation frequency dependency, agreement with our model can be taken as strong affirmation of its theoretical concepts. For example, such disparate concepts as the adatom model (57,253) and that of Lombardi et al. (37) which involves a potential induced resonance with substrate states, predict the same type of behavior. In Fig. 6-4 for the same Raman bands of 2,2'-cyanine as used in Fig. 6-2, we show the residual potential dependencies of the relative intensities that result upon using the 274 cm^{-1} band (attributed to the A-term of the polarizability) as an internal standard and accounting for the frequency dependency of Raman intensities as discussed in section 6.1.1:B while Fig. 6-5 provides similarly treated data for 4,4'-cyanine using the 210 cm-1 band (see Fig. 5-24) as an internal standard.

We interpret the potential dependences shown in Fig. 6-2 and 6-3 as principally reflecting the increased aggregation on the surface induced at potentials more positive than the point-of-zero-charge (PZC), followed by a subsequent dissolution of adsorption sites as the substrate assumes a negative potential (55).

The potential dependence behavior for the intensity corrected bands shown in Fig. 6-4 and 6-5, in the present theoretical model, represent the residual tuning of the exciton state in relationship to the incident radiation.

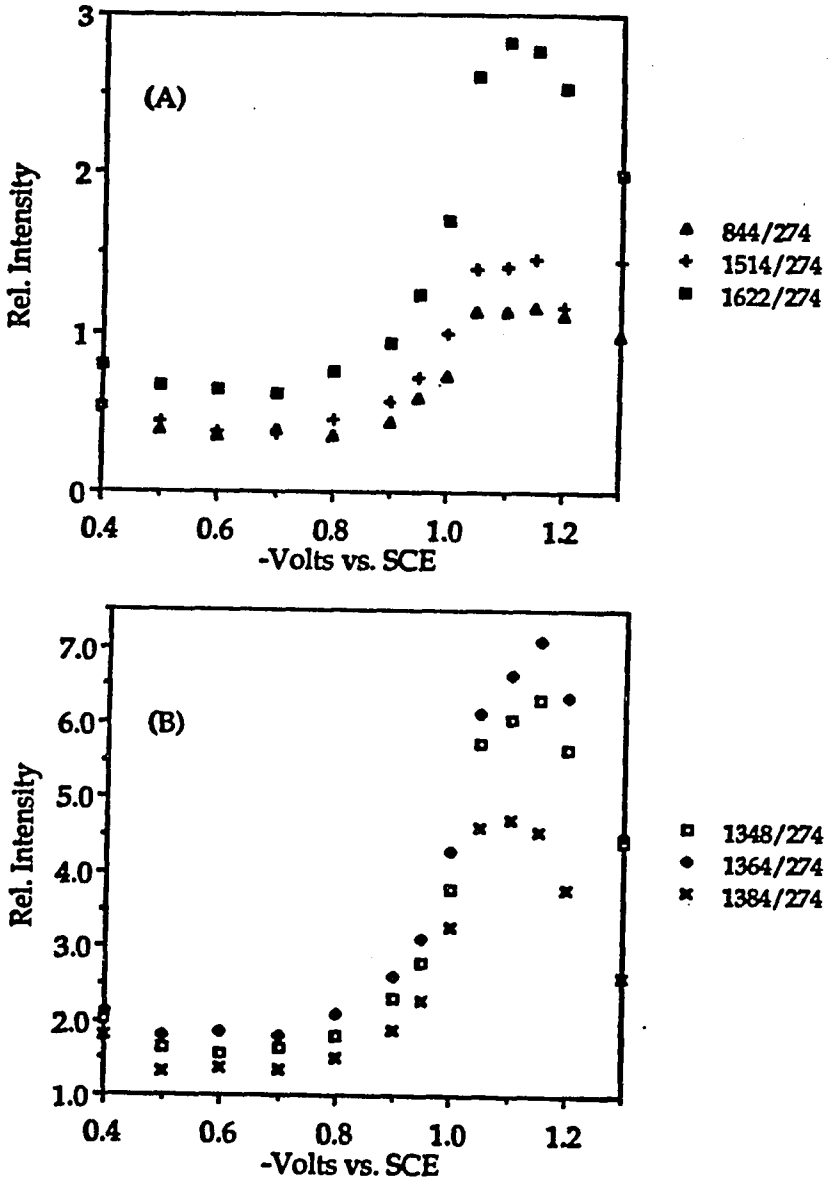

Fig. 6-4: Intensity versus potential plots for frequency and concentration normalized bands of 2,2'-cyanine excited by 583 nm radiation: (A) for the weaker and (B) for the stronger bands.

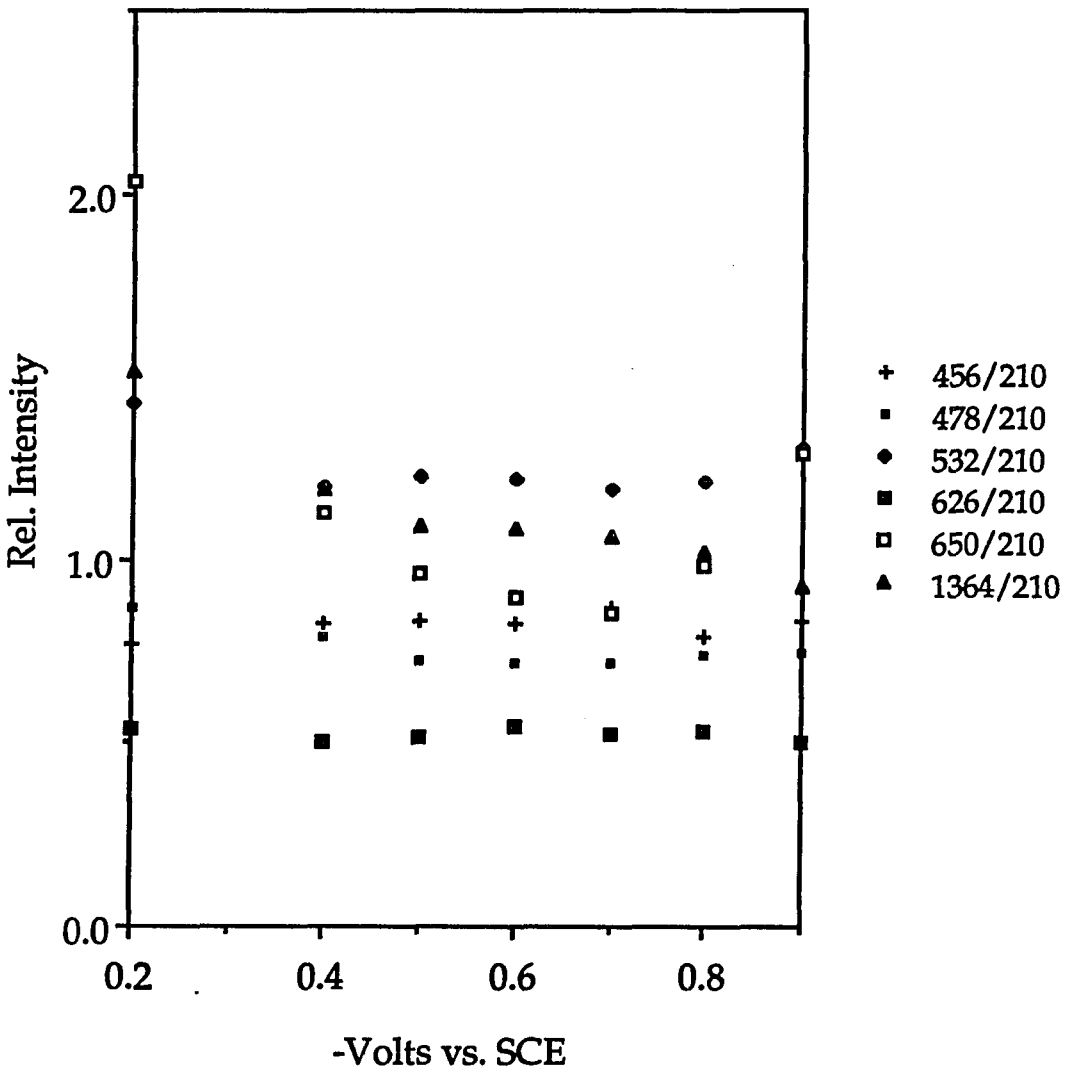

Fig. 6-5: Intensity versus potential plots for frequency and concentration normalized bands of 4,4'-cyanine excited by 647.1 nm radiation.

This latter assertion is based on the supposition that narrowband incident radiation will excite only a subset of the total number of exciton sub-bands that would be available if a single molecule in an N-molecule aggregate were fully excited to its first excited singlet level. An applied potential can then be expected to Stark shift the exciton bands, because of the expected large dipole-moment of the aggregate, creating a different subset of exciton sub-bands in resonance with the incident radiation. Since exciton sub-bands are equally spaced (at zero-applied electric field) with "allowed" transition dipole moments existing only for some, the subset excited by absorption of incident radiation would be part of the "allowed" constituency of exciton sub-bands. Tuning by varying the applied potential, in the above picture, would correspond to Stark-effect tuning of the subset of incident radiation created exciton bands through the range of allowed exciton substrates. We have, therefore, found that a Stark-effect shifting of the J aggregate band can explain the voltage dependence of excitation frequency and concentration normalized Raman band intensits for aggregated 2,2'-cyanine and 4,4'-cyanine (71).

A. Stark Effect

When a system is subjected to an electric field, the field acts as a pertubation on the electron distribution in the system leading to changes in the spectrum which may be observed. The system may be composed of atoms, molecules or aggregates of molecules and the changes in the spectrum, which are termed Stark effects can take various forms (e.g. splitting of bands, intensity changes, and energy or frequency changes), and can in turn be related to important atomic or molecular properties such as excited state dipole moments, polarizabilities and symmetry properties.

The application of Stark effects to high-resolution optical spectroscopy has been quite valuable and has given considerable insight into the electronic structure of several molecules (254-258). Some authors (259-261) have reviewed many of the earlier applications and results of the effect in optical spectroscopy. Resently Stark effect techniques have been used in Stark hole-burning spectroscopy to obtain highly accurate information for biologically important molecules (262).

When molecular wave functions are modified as a result of an applied Stark field, the dipole matrix elements and intensities of transitions are affected. If Ψ_1 and Ψ_2 are wave functions for two molecular energy levels when the electric field is zero, and $\Psi_1(F)$, $\Psi_2(F)$ their corresponding perturbed wave functions after an electric field is applied, and if F is not too large, the latter wave functions may be expanded in the form (263)

$$\Psi_1(F) = \Psi_1 + \sum_n{}' \; C_{1n}\Psi_n \qquad (6.1)$$

where $$C_{1n} = \frac{\mu_{1n}F}{E_1 - E_n}$$

μ_{1n} is the dipole matrix element between the unperturbed state 1 and n, E_1 and E_n are the energies of the two states. The summartion $\sum'$ is over all levels except level 1. If levels are degenerate so that $E_1 = E_n$, wave functions may be chosen to make $\mu_{1n} = 0$ so that the expression (6.1) has no divergent terms. $\Psi_2(F)$ is similarly

$$\Psi_2(F) = \Psi_2 + \sum_n{}' \; C_{2n}\Psi_n \qquad (6.2)$$

The transition probability between states 1 and 2 depends on the dipole matrix element between them,

$$\mu_{12}(F) = \int \psi_1^*(F)\mu_z\psi_2(F)d\tau \qquad (6.3)$$

using (6.1) and (6.2)

$$\mu_{12}(F) = \mu_{12} + \sum_n F\left(\frac{\mu_{1n}\mu_{n2}}{E_1 - E_n} + \frac{\mu_{2n}\mu_{n1}}{E_2 - E_n}\right) \qquad (6.4)$$

where μ_{12} is the matrix element for zero field. Expression (6.4) is accurate only when the wave functions are not greatly changed by the electric field, i.e. when $\mu F / (E_1 - E_n) \langle\langle 1$. F must be taken as positive, and the relative phases of the matrix elements are such that

$$\left|\mu_{12}(F)\right| = \left|\mu_{12}\right| + \sum_n{}' \left|\mu_{1n}\right|\left|\mu_{2n}\right| F\left(\frac{1}{E_1 - E_n} + \frac{1}{E_2 - E_n}\right) \qquad (6.5)$$

Since intensity is proportional to $|\mu|^2$, expression (6.5) allows an evaluation of band intensity changes due to mixing of electronic states. Thus, the effect may produce electronic states which are forbidden by orbital symmetry, and make allowed ones increase or decrease in optical density.

The Stark effect technique actually yields the change in the dipole moment ($\Delta\mu$) and polarizability ($\Delta\alpha$) during an electronic transition between the molecule's ground state and a particular excited state. Once these values are determined the excited state values are readily evaluated using the previously determined literature ground state values.

The change in dipole moment $\Delta\mu$ for a frequency shift $\Delta E / hc$

cm^{-1} and applied potential difference V(volt), is given by

$$|\Delta\mu| = 5.954 \times 10^{4} \left\{ \frac{D\Delta E / hc}{VL|\cos\theta|} \right\} \text{ debye} \qquad (6.6)$$

where D is the distance between electrodes, in cm, L is the Lorentz approximation for the local field and θ is the angle between the molecular dipole axis and the field direction.

B. Application of Stark Effect to the Results

The above concepts can be applied to the B-term to gain information concerning exciton parameters, such as permanent dipole moments and effective exciton band-edge energies. The analysis begins with the assumption that the product of transition moments and Herzberg-Teller constants for the B-term of Eq. (3.32) can be written as a constant times the density-of-states function of the exciton state. This assumption is the same as used by Lombardi *et al.* (37) in their treatment of metal conduction band states. As a result, the summation over exciton substates can be replaced by the integral

$$\int' \frac{\rho_s dE_s^0}{(E_1^0 - E_s^0)} \qquad (6.7)$$

with $E_1{}^0$ corresponding to the laser excitation energy (i.e., $E_1{}^0 = h\nu_0$), the prime specifying the absence of s = 1 from the sum, and ρ_s the density of states populated by the incident excitation. In accord with the discussion above, the density-of-states can be assumed to be a constant in the ranges $\left\{E_\ell^0 \le E_s^0 \le E_1^0 - \delta \text{ and } E_1^0 + \delta \le E_s^0 \le E_u^0\right\}$, with E_ℓ^0 and $E_u{}^0$ representing

the lower and upper effective band-edge limits, respectively, for the "allowed" exciton substates and δ a positive differential energy. The voltage dependent behavior of the B-term is determined by the logarithmic expression which results from the integration of the B-term under resonant excitation conditions (71):

$$\ln\left\{\left(E_{\ell}^{0} - E_{1}^{0}\right) / \left(E_{1}^{0} - E_{u}^{0}\right)\right\} \qquad (6.8)$$

Thus, resonances in the applied potential dependence occur when the "pumped" exciton substates of energy $E_1^0 = h\nu_0$, (with ν_0 the laser frequency) become the substates that define the effective band-edge energies E_{ℓ}^{0} and E_u^0. Hence, in general, we can expect two resonances in the plot of normalized band intensity versus potential. However, our studies to date have involved a metallic silver electrode and excitation frequencies which allow us to observe the resonance which occurs at negative potential, but not the resonance at more positive potential because of substrate oxidation.

We propose (among other things) that the voltage tuning is a Stark-effect tuning of E_u^0 into coincidence with the energy of the incident radiation (71). E_u^0 is taken as the active limiting energy because we envisage the exciton electric dipole moment as forming with positive charge density closest to the negative electrode, leading to the dipole pointing in the direction of the positive field. As a result, one gets a lowering of states with increasingly negative electrode potential as indicated by the Stark-effect energy relationship $\Delta E = \mu\xi$. The Stark-effect explanation appears reasonable as a simple calculation can support. This calculation starts from the realization that the potential gradient at the working electrode in our electrochemical cell likely ranges from 10^{+6} - 10^{+7} V/cm, while the electric

dipole moment of the excitonic state, because of its large spatial extent and delocalized electrons, should be substantially larger than the ground state electric dipole moment, probably by at least 1 Debye. With these parameters, the shift effected by the potential gradient can be calculated from the Stark conversion factor

$$5.954 \times 10^{4} \frac{D \cdot \frac{V}{cm}}{cm^{-1}} = 1 \qquad (6.9)$$

We find an energy shift of 168 cm^{-1} for a potential gradient of 10^{+7} V/cm and a conservative electric dipole moment increase of 1 D (for the excited aggregate relative to that of the ground state). This energy shift corresponds to a wavelength shift, centered on the incident excitation wavelengths (583 nm for 2,2'-cyanine and 647 nm for 4,4'-cyanine), of ca. ± 60 Å. This shift is of a magnitude that can tune the excitonic state of 2,2'-cyanine (with zero-applied potential state at 575 nm) through a resonance with the exciting radiation, but of insufficient magnitude for 4,4'-cyanine (with zero-applied potential state at 710 nm). Moreover, since E_u^0 is lowered as ξ becomes more negative, the original mismatch between the frequencies of the exciton band and the incident radiation (at 583 nm) for 2,2'-cyanine is diminished then increased, leading to a resonance maximum as shown in Fig. 6-4, while, the absence of residual tuning for 4,4'-cyanine, as shown in Fig. 6-5, is attributable to Stark shifting of its E_u^0 band to even longer wavelength with negative potential, thus not allowing for a resonance with the fixed incident excitation at 647 nm (264).

A possible use for the voltage resonance measurement is to determine relative dipole moment increases of excitonic states (above those of the ground states) for different cyanine dyes. This application necessitates that

only a narrow excitonic state sub-band region be excited, that the upper band-edge E_u^0 be identifiable, and that dipole moments be aligned in the field direction. With these conditions, the equation

$$E_u^0(0) - \mu \cdot \xi_{max} = E_1^0 \qquad (6.10)$$

applies for the different aggregates, where $E_u^0(0)$ is assumed constant and is the band-edge energy in the absence of an applied field, ξ_{max} is proportional to the voltage at which resonance occurs, and E_1^0 is the energy of the incident radiation. Relative μ's (for different aggregated molecules) can be determined by fitting respective data to Eq. (6.10) and taking a ratio of slopes.

6.2 CONCLUSIONS

The Raman scattering theories are discussed in general, and the vibro-exciton theory that we proposed for the aggregated dyes, presented and examined in detail. The key instrumental requirements for Raman spectroscopy are presented, and some experimental results obtained to date have been reviewed. A brief review of the photographic dyes has also been presented.

The experimental results, which have dealt with aggregated cyanine dye molecules adsorbed on substrates, have explained sufficiently well the various implications of the vibro-exciton theory. An intrinsic enhancement equal to the number of molecules in the aggregate, the excitation wavelength dependence of the Raman scattering, and the surface potential dependency of the Raman intensities are discussed. The rest of the results

presented helped to explain other things like the effect of the supporting electrolyte, effect of electrode pretreatment and pH dependence.

Results show that only when the J-aggregate absorption is present do the photographic sensitizer dyes exhibit intense Raman scattering spectra and that potential variation on the substrate electrode and pH of the solution have some effect on the intensity of Raman bands. There has been sufficient experimental evidence shown to conclude that an oxidation/reduction cycle or electrode surface roughening is not a prerequisite to observe enhanced Raman scattering by these dyes on surfaces. The substrate offers a surface upon which the dye molecules adsorb and aggregate.

The studies present surface Raman excitation profiles for some of the cyanine dyes adsorbed on silver electrodes over the visible range of excitation wavelengths. The profiles are maximum for excitation which is in resonance or near resonance to the absorption band of the J-aggregate of the adsorbate dye. The substrate and its roughening seem to have no effect. It is concluded that these findings are in line with the theory which predicts the position of the profile maxima and their dependence on the absorption band of the J-aggregate formed by these dyes. The shape of the Raman excitation profiles for the sensitizer dyes which form aggregates are, therefore, mainly determined by the profile for the absorption spectra of the aggregated dyes.

In another conclusion, we interpret our experiments to suggest that the potential dependence of enhanced Raman scattering by aggregated cyanine dye molecules can be explained by a Stark-effect shifting of

molecular exciton states. We have also ascertained that certain bands in the Raman spectrum are due to Franck-Condon overlap of intramolecular modes of the molecules in the aggregate with intermolecular lattice modes of the aggregate, and that such bands can be used as internal Raman standards to normalize surface concentrations. In addition, we have determined that it is not necessary to implicate the substrate states in a potential induced resonance scheme in which, for example, substrate states are tuned into resonance with exciton or single molecule states. The substantive agreement between theory and experiments for enhanced Raman scattering by aggregated molecules validates the utilization of molecular exciton states as excited states in the scattering problem.

Our studies suggest to us that Raman scattering by aggregate molecules on surfaces can provide a spectroscopic means of acquiring structural information for single molecules forming aggregates, and electron injection, dynamical information for aggregated structures; both types of determinations would not be complicated by strong substrate/molecule couplings.

Finally, for analytical purposes, the laser spectroscopic studies made on these dyes suggest that, use of the technique of Raman scattering by dyes that form aggregates, in their determination, offers many advantages in comparison with the commonly used methods which are mostly based on chromatography or visible absorption spectroscopy (265,266). It has been foound that for all the dyes considered, and the excitation sources used, an extreme off resonance excitation by 488 nm Ar^+-laser line even yields spectra of sufficient intensities that differ to the extent that they can be used as a fingerprint of the dye present. Taking the identification limit as being the

concentration for which at least five bands appear in the spectrum with a signal-to-noise ratio of at least 3, detection should be possible for solutions with a concentration of about 5 ppb or even less. The technique offers a potential for the characterization of raw or industrially processed dyes that form aggregates.

REFERENCES

(1) Vibrations at Surfaces; Cardoro, R., Gilles, J. M. , Lucus, A. A., Eds.; Plenum: New York, 1982.

(2) Bewick, A. J. Electroanal. Chem. 1983, 150, 481.

(3) Birke, R. L.; Lombardi, J. R.; Sanchez, L. A. In Electrochemical and Spectrochemical Studies of Biological Redox Componets; Kadish, H., Ed.; Amer. Chem. Society: Washington, D.C. 1982; Adv. Chem. Ser., No. 201, Chapter 4.

(4) Smekal, A. Naturwissenschaften 1923 11, 873.

(5) Raman, C. V. Nature 1928, 121, 619.

(6) Landsberg, G. S.; Mandelstam, L. Naturwissenschaften 1928, 16, 557; Compt. Rend. 1928, 187, 109.

(7) Gilson, T. R.; Hendra, P.J. Laser Raman Spectroscopy; Wiley: London, 1970.

(8) Tobin, M. C. In. Laser Raman Spectroscopy; Vol. 35; Elving, P. J., Kolthoff, I.M., Eds.; in Chemical Analysis, A. Series of Monographs on Anal. Chem. and its Applications; Wiley: New York, 1971.

(9) Grasselli, J. G.; Snavely, M. K.; Bulkin, B. J. Chemical Applications of Raman Spectroscopy; Wiley: New York, 1981.

(10) Raman Spectroscopy, Theory and Practice; Szymanski, H. A., Ed.; Plenum: New York, 1967; Vol. 1.

(11) Behringer, J. In Raman Spectroscopy, Theory and Practice; Szymanski, H. A., Ed.; Plenum: New York, 1967; Vol. 1, Chapter 6.

(12) Behringer, J. In Molecular Spectroscopy; Barrow, R. F., Long, D. A., Millen, D. J. Eds.; The Chem. Soc.: London, 1974; Vol. 2, p. 100.

(13) van Duyne, R.P. In Chemical Applications of Lasers; Moore, C. B., Ed.; Academic: New York, 1979; Vol. 4, Chapter 5.

(14) Shorygin, P.P.; Krushinsky, L.L. Dokl. Akad. Nauk SSRR 1960, 133, 337.

(15) Shorygin, P.P. Pure Appl. Chem., 1962, 4, 87.

(16) Herder, H.E. Anal. Chem. Ann. Revs. 1972, 44, 490R.

(17) Shorygin, P.P. In "Combination Scattering of Light and Conjugation"; Usp. Khim. 1971, 40, 604-739.

(18) Spiro, T. G. Acc. Chem. Res. 1974; Vol. 7, pp 339-344.

(19) Lewis, A.; Spoonhower, J.; Bogomolni, R. A.; Lozier, R. H.; Stoechenius, W. Proc. Nat. Acad. Sci. USA, 1974; Vol. 71, pp 4462-4466.

(20) Mendelsohn, R. Nature 1973, 243, 22.

(21) Mendelsohn, R.; Verma, A.L.; Bernstein, H. J.; Kates, M. Can. J. Biochem. 1974, 52, 774.

(22) Campion, A.; Terner, J.; El-Sayed, M.A. Nature 1977, 265, 659.

(23) Surface Enhanced Raman Spectroscopy; Furtak, T. E., Chang, R. , Eds.; Elsevier: Amsterdam, 1982.

(24) Fleischmann, M.; Hendra, P.J.; McQuillan, A. J. Chem. Soc., Chem. Commun. 1973, 80.

(25) Fleischmann, M.; Hendra, P. J.; McQuillan, A. J. Chem. Phys. Lett., 1974, 26, 163.

(26) Jeanmarie, D.L.; van Duyne, R.P. J. Electroanal. Chem. 1977, 84, 1.

(27) Albrecht, M. G.; Creighton, J. A. J. Am. Chem. Soc. 1977 99, 5215.

(28) Cooney, R. P.; Reid, E. S.; Fleischmann, M.; Hendra, P.J. J. Chem. Soc., Faraday Trans. 1, 1977, 73, 1691.

(29) Creighton, J. A.; Albrecht, M. G.; Hester, R. E.; Matthew, J. A. D. Chem. Phys. Lett. 1978, 55, 55.

(30) Pettinger, B.; Wenning, U.; Kolb, D. M. Ber. Bunsenges. Phys. Chem. 1978, 832, 1326.

(31) Furtak, T. E. Solid State Commun. 1978, 28, 903.

(32) Albrecht, M. G.; Evans, J. F.; Creighton, J. A. Surf. Sci. 1978, 75, L777.

(33) Birke, R. L.; Lombardi, J. R.; Gersten, J. I. Phys. Rev. Lett. 1979, 43, 71.

(34) Erdheim, G. R.; Birke, R. L.; Lombardi, J. R. Chem. Phys. Lett. 1980, 69, 495.

(35) Bunding, K. A; Lombardi, J. R.; Birke, R. L. Chem. Phys. 1980, 49, 153.

(36) Gu, B.; Akins, D. L. Chem. Phys. Lett. 1985, 113, 558.

(37) Lombardi, J. R.; Birke, R. L.; Lu, T; Xu, J. J. Chem. Phys. 1986, 84, 4174.

(38) Allen, C. S.; Schatz, G. C.; van Duyne, R. P. Chem. Phys. Lett. 1980 75, 201.

(39) Marinyuk, V. V.; Lazorenko-Manevich, R. M.; Kolotyrkin, Ya M. J. Electroanal. Chem. 1980, 110, 111.

(40) Pettinger, B.; Wenning, U.; Wetzel, H. Surf. Sci. 1980, 101, 409.

(41) Temperini, M. L.A.; Chagas, H. C.; Sala, O. Chem. Phys. Lett. 1981, 79, 75.

(42) Otto, A. Surf. Sci. 1978, 75, L392.

(43) Burstein, E.; Chen, C. Y.; Lundquist, S. Proc. U.S.-USSR Symp. Inelastic Light Scattering in Solids; Birman, J. L., Cummins, H. Z., Rebane, K. K., Eds.; Plenum: New York, 1979; p. 479.

(44) Smardzewski, R. R.; Colton, R. J.; Murday, J. S. Chem. Phys. Lett. 1979, 68, 53.

(45) Wood, T. H.; Klein, M. V. J. Vac. Sci. Technol. 1979, 16, 459.

(46) Seki, H.; Philpott, M. R. J. Chem. Phys. 1980, 73, 5376.

(47) Zwemer, D. A.; Shank, C. V.; Rowe, J. E. Chem Phys. Lett. 1980, 73, 201.

(48) Eesley, G. L. Phys. Rev. Lett. 1981, 81A, 193.

(49) Tsang, J. C.; Kirtley, J. R.; Bradley, J. A. Phys. Rev. Lett. 1979, 43, 772.

(50) Tsang, J. C.; Kirtley, J. R. Solid State Commun., 1979, 30, 617.

(51) Creighton, J. A.; Blatchford, C. G.; Albrecht, M. G. J. Chem. Soc.

Faraday Trans. 2, 1979, 75, 790.

(52) Lippitsch, M. E. Chem. Phys. Lett. 1980, 74, 125.

(53) Wetzel, H.; Gerischer, H. Chem. Phys. Lett. 1980, 76, 460.

(54) Akins, D. L. J. Colloid Interf. Sci. 1982, 90, 373.

(55) Li, X.; Gu, B.; Akins, D. L. Chem. Phys. Lett. 1984, 105, 263.

(56) Krasser, W. In Int. Conf. on Raman Spectrosocopy, Ottawa, Canada, 1980, p. 420.

(57) Otto, A. In Light Scattering in Solids; Cardona, M. Guntherode, G., Eds.; Springer: Berlin, 1983; Vol. 4.

(58) Chang, R. K.; Furtak, T. E. Surface Enhanced Scattering; Plenum: New York, 1982.

(59) Wang, D. S.; Chew, H.; Kerker, M. Appl. Opt. 1980, 19, 2256.

(60) Gersten, J. I.; Nitzan, A. J. Chem. Phys. 1980, 73, 3023.

(61) Gersten, J. I.; Birke, R. L.; Lombardi, J. R. Phys. Rev. Lett. 1979, 43, 147.

(62) Adrian, F. J. J. Chem. Phys. 1982, 77, 5302.

(63) Lippitsch, M. E. Phys. Rev., B. 1984, 29, 3101.

(64) Moskovits, M. J. Chem. Phys. 1982, 77, 4408.

(65) Schatz, G. C. Acc. Chem. Res. 1984, 17, 370.

(66) Blatchford, C.G.; Campbell, J. R.; Creighton, J. A. Surf. Sci. 1981, 108, 411.

(67) Otto, A.; Billman, J.; Eickmans, J.; Erturks, U.; Pettenkofer, C. Sur. Sci. 1984, 138, 319.

(68) Barz, F.; Gordon II, J. G; Philpott, M. R.; Weaver, M. J. Chem. Phys. Lett. 1982, 91, 291.

(69) Furtak, T. E.; Reyes, J. Surf. Sci. 1980, 93, 35.

(70) Weitz, A. A.; Garoff, S.; Gersten, J. I., Nitzan, A. J. Chem. Phys. 1983, 78, 5324.

(71) Akins, D. L.; Akpabli, C. K.; Li, X. "Surface Potential Dependenece of Enhanced Raman Bands of Aggregated Cyanine Dyes"; J. Phys. Chem. in press.

(72) Akins, D. L. J. Phys. Chem. 1986, 90, 1530.

(73) Herz, A. H. Adv. Colloid Interf. Sci. 1977, 8, 237.

(74) Maiman, T. H. Nature 1960, 187, 493.

(75) Hendra, P. J. In Laboratory Methods in Infrared Spectroscopy; Millerand, R. E., Stace, B. C., Eds.; Heyden: New York, 1972.

(76) Strommen, D. P.; Nakamoto K. Laboratory Raman Spectroscopy; Wiley: New York, 1984.

(77) Gold, H. S. Appl. Spectrosc. 1979, 33, 649.

(78) Shriver, D. F.; Dunn, J. B. R. Appl. Spectrosc. 1974 28, 319.

(79) Fastie, W. G. J. Opt. Soc. Amer. 1952, 42, 641 and 647.

(80) Smith, H. J.; Rodman, J. P. Appl. Optics 1963, 2, 181.

(81) Nakamura, J. K.; Schwarz, S. E. Appl. Optics 1968, 7, 1073.

(82) Kierstead, S. P. Natural Dyes; Bruce, Humphries: Boston, USA, 1950.

(83) Thurstan, V. The Uses of Vegetable Dyes; Dryad: Leicester, 1964.

(84) Perkin, W. H., In "Hofman Memorial Lecture"; J. Chem. Soc. 1896, 69, 603.

(85) Claxton, G. Benzoles: Production and Uses; National Benzole and Allied Products Association: London, 1961, p 91.

(86) Allen, R. L. M. Color Chemistry; In "Studies in Modern Chemistry"; Agosta, W. C., Nyholm, R. S, Eds.; Appleton-Century-Crofts: New York, 1971.

(87) Colour Index; The Society of Dyers and Colourists: Bradford,

England; The American Association of Textile Chemists and Colorist: Lowell, Mass., USA; 2nd ed., 1956 and Supplement, 1963.

(88) Colour Index; The Society of Dyers and Colourists; Bradford; The American Association of Textle Chemists and Colorists: North Carolina, USA; 3rd ed. 1971.

(89) Brooker, L. G. S. Rev. Mod. Phys. 1942, 14, 275.

(90) Brooker, L. G. S.; White, F. L.; Sprague, R. H.; Dent, Jr. S. G.; Van Zandt, G. Chem. Rev. 1947 41, 325.

(91) Brooker, L. G. S.; Simpson, W. T. Ann. Rev. Phys. Chem. 1951, 2, 121.

(92) Brooker, L. G. S.; Vittum, P. W. J. Photogr. Sci. 1957, 5, 71.

(93) Brooker, L. G. S. In Recent Progress in the Chemistry of Natural and Synthetic Coloring Matters; Gore, T. S., Joshi, B. S., Synthankar, S. V., Tilak, B. D., Eds.; Academic: New York, 1962, p 673.

(94) Brooker, L. G. S.; Van Lare, E. J. Encyclopedia of Chemical Technology; Wiley: New York, 1964; Vol. 5, p 763.

(95) Hamer, F. M. In The Chemistry of Heterocyclic Compounds, Vol. 18, The Cyanine Dyes and Related Compounds; Weissberger, A., Ed.; Interscience: New York, 1964.

(96) Kiprianov, A. I. Ukr. Khim. Zh. 1952, 18, 339; Chem. Abstr. 1955, 49, 984.

(97) Ficken, G. E. In The Chemistry of Synthetic Dyes; Venkataraman, K., Ed.; Academic: New York, 1971, Vol. 4, p 211.

(98) Sturmer, D. M. In The Chemistry of Heterocyclic Compounds; Weissberger A., Taylor, E.C., Eds.; John Wiley: New York, 1977, Vol. 30, p 441.

(99) Ninth Internat. Congr. of Sci. and App. Photogr.; Clerc, L. P., Ed.; Revue d'Optique Theor. Inst., Paris, 1936.

(100) Dye Sensitization: Bressanone, Italy; Semerano, G., Mazzucato, U., Berg, W. F., Meir, H., Eds.; Focal: New York, 1970.

(101) Photographic Sensitivity; Cambridge, England; Cox, R. I., Ed.; Academic: New York, 1973.

(102) "Vogel Centennial: Putney, Vermont"; published in Photogr. Sci. Eng. 1974, 18, 33, 165, 276, 410, 549, 610.

(103) Vogel, H. W. Ber. 1873, 6, 1302.

(104) Vogel, H. W. Ber. 1875, 8, 1635.

(105) Becquerel, E. Compt. Rend. 1874, 79, 185.

(106) Waterhouse, J., Phot. J., 1904, 44, 165.

(107) Miethe, A.; Book, G. Ber. 1904, 37, 2008.

(108) Meither, A.; Traube, A. Ger. Pat. 142 926, 1902.

(109) Homolka, B. Ger. 1905, 172, 118.

(110) Mees, C. E. K. The Theory of the Photographic Process; Macmillan: New York, 1942.

(111) Mees, C. E. K.; Wratten, S. H. Photo J. 1908, 48, 25.

(112) Mees, C. E. K. Phot. J. 1934, 74, 448; 1935, 75, 188.

(113) Mees, C. E. K. Proc. Roy Inst. Gt. Brit. 1936, 29, part 1, 136.

(114) Sturmer, D. M.; Heseltine, D. M. In The Theory of the Photographic Process; 4th ed.; James, T. H., Ed.; Macmillan: New York, 1977; Chapter 8.

(115) Vogel, H. W. Ber. 1874, 7, 976.

(116) Kendall, J.D. Chem. and Ind. (London), 1950, 121.

(117) Williams, C. H. G. Chem. News, 1859, 1, 15; 1860, 2, 219.

(118) Mills, W. H.; Wishart, R. S. J. Chem. Soc. 1920, 117, 579.

(119) Konig, W. Ber. 1922, 55, 3293.

(120) Kaufman, A.; Strubin, P. Ber. 1911 44, 690.

(121) Konig, W; J. Prakt Chem. 1912, 85, (2), 514; 86, 166.

(122) Fischer, O. J. Prakt. Chem. 1918, 98, 204.

(123) Mills, W. H.; Evans, P. E. J. Chem. Soc. 1920, 117 1035.

(124) Mills, W. H.; Pope, W. J. Photo. J. 1920, 60, 253.

(125) Mills, W. H. J. Chem. Soc. 1922, 121, 455.

(126) Konig, W. Ber. 1924, 57, 685.

(127) Konig, W.; Meier, W. J. Prakt. Chem. 1925, 109, 324.

(128) Piggott, H. A.; Rodd, E. H. Brit. 1929, 344, 409; 1930, 354, 898.

(129) Brooker, L. G. S.; Keyes, G. H.; Sprague, R. H.; VanDyke, R. H.; VanLare, E; VanZandt, G.; White, F. L. J. Am. Chem. Soc. 1951, 73, 5326.

(130) Brooker, L. G. S.; Keyes, G. H.; Sprague, R. H.; VanDyke, R. H.; VanLare E.; VanZandt, G.; White, F. L.; Cressman, H. W. J.; Dent, Jr. S. G. J. Am. Chem. Soc. 1951, 73, 5332.

(131) Brooker, L. G. S. Experientia Suppl. 1955, 2, 229.

(132) Mills, W. H.; Hamer, F. M. J. Chem. Soc. 1920, 117, 1550.

(133) Brooker, L. G. S. In The Theory of the Photographic Process; Mees, C. E. K., James, T. H. Eds.; Macmillian: New York, 1966 p 198.

(134) Brooker, L. G. S.; Keyes, G. H.; Williams, W. W. J. Am. Chem. Soc., 1942, 64, 199.

(135) Mills, W.; Raper, R. J. Chem. Soc. 1965, 2460.

(136) Brooker, L. G. S.; Dent, Jr., S. G.; Heseltine, D. W.; VanLare, E. J. Am. Chem. Soc., 1953, 75, 4335.

(137) Owen, J. R. Tetrahedron Lett. 1969, 2709; Eastman Org. Chem. Bull., 1971, 43 (3), 3.

(138) Dimroth, K.; Grief, N.; Klapproth, A. Justus Liebigs, Ann. Chem., 1975, 373.

(139) Huenig, S.; Woelff, E. Chimia Suppl., 1968, 33.

(140) Elwood, J. K. J. Org. Chem., 1973, 38, 2425.

(141) Reichardt, C.; Mormann, M. Chem. Ber. 1972, 105, 1815.

(142) Owen, J. R., Def. Publ. U.S. Pat. Off., 890 002, 1971.

(143) Rillaers, G. A.; Depoorter, H. Ger. Offen. Pat. 1 930 224, 1970.

(144) Collet, P.D.; Compere, M.A. Fr. Pat. 1 386 399, 1965.

(145) Jones, E. R. H.; Reed, K. J. Brit. Pat. 616 223, 1946.

(146) Goetze, J. Ber. Bunsenges. Phys. Chem. 1938, 71, 2289.

(147) Chapman, D. D.; Elwood, J. K.; Heseltine, D. W.; Hess, H.M.; Kurtz, D. W. J. Chem. Soc., Chem. Commun. 1974, 648.

(148) Prinzbach, H.; Futterer, E. In Advances in Heterocyclic Chemistry; Vol. 3; Katrizky, A. R., Boulton, A. J., Eds.; Academic: New York, 1964.

(149) Jakobi, H.; Kuhn, H. Z. Elektrochem., 1962, 66, 47.

(150) Doerr, F. Angew. Chem. Int. Ed. Engl. 1966, 5, 478.

(151) Peofilov, P. P. The Physical Basis for Polarized Emission; Consultant Bureau: New York, 1961.

(152) Bokinik, Y. I. Kino-Phot. Ind., 1933, 3, 84; Chem. Abstr. 1934, 28, 5353.

(153) Venkataraman, K. In The Chemistry of Syntheetic Dyes; Fieser, F., Fieser, M.; Eds.; Academic: New York, 1952; Vol. 2, Chapter 8.

(154) Leermakers, J. A.; Carroll, B. H.; Staud, C. J. J. Chem. Phys. 1937, 5, 878.

(155) Leermakers, J. A. J. Chem. Phys. 1937, 5, 889.

(156) Natanson, S. Nature 1937, 140, 197-198.

(157) Koslowsky R.; Mueller, O. Bibliography of Scientific and Industrial Reports; U.S. Dept. of Commerse, 1936, 8, 873; P.B. 70 053.

(158) Carroll, B. H.; West, W. Fundamental Mechanisms of Photographic Sensitivity; Butterworth: London, 1951, p 162.

(159) West, W.; Carroll, B. H.; Whitcomb, D. H. J. Phys. Chem. 1952, 56, 1054.

(160) Leermakers, J. A.; Carroll, B. H.; Staud, C. J. J. Chem. Phys. 1937, 5,

893.

(161) Sheppard, S. E.; Lambert, R. H.; Walker, R. D. J. Chem. Phys. 1939, 7, 265.

(162) Davey, E. P. Trans. Faraday Soc. 1940, 36, 323.

(163) Solov'ev, S. J. Phys. Chem. USSR 1945, 19, 451; Chem. Abstr. 1946, 40, 5653.

(164) West, W.; Carroll, B. H. J. Chem. Phys., 1951, 19, 417.

(165) Browning, C. H. Edinburgh Med. J. [N.S.], 1937, 44, 497.

(166) Browning, C. H.; Cohen, J. B.; Gulbransen, R. C. Zentr. 1922, III, 1381.

(167) Karwacki, L.; Biernacki, S. C. Zentr. 1925, II, 832.

(168) Brooker, L. G. S.; Sweet, L. A. Science 1947, 105, 496.

(169) Brooker, L. G. S.; Holcomb, W. F.; Banks, C. K.; Eastman Kodak Co. U.S. Pat. 2 472 565, 1949.

(170) Hamer, F. M. Chemistry and Industry 1947, 660.

(171) Heseltine, D. M.; Brooker, L. G. S.; Eastman Kodak Co. U.S. Pat. 2 895 955, 1959.

(172) Brooker, L. G. S.; Sprague, R. H.; Eastman Kodak Co., U.S., Pat. 2 268 798, 1942.

(173) Sprague, R. H.; Eastman Kodak Co. U.S. Pat. 2 571 775, 1951.

(174) Brooker, L. G. S.; Sprague, R. H.; Eastman Kodak Co. U.S. Pat. 2 298 731, 1942; 2 409 612, 1946.

(175) Snavely, B. B. In Org. Mol. Photophys.; Birks, J. B., Ed.; Wiley: London, 1973, Vol. 1, p 239.

(176) Schaefer, F. P. "Dye Lasers" In Topics in Appl. Phys.; Vol. 1, Springer-Verlag: New York, 1973; Top. Curr. Chem. 1976, 61, 1.

(177) Webb, J. P.; Webster, F. G.; Plourde, B. E. Eastman Org. Chem. Bull. 1974, 46(3), 1.

(178) Forster, Th. Fluoreszenz Organischer Vergindungen; Vandenhoeck and Ruprecht: Gottingen, 1951; p 254.

(179) Levinson, G. S.; Simpson, W. T.; Curtis, W. J. Am. Chem. Soc. 1957, 79, 4314.

(180) McRae, E. G.; Kasha, M. J. Chem. Phys. 1958, 28, 721.

(181) Kasha, M. Physical Processes in Radiation Biology; Academic: New York, 1964, p 17.

(182) Kasha, M.; Rawls, H.; El-Bayoumi, M. Molecular Spectrscopy, Proc. VIII European Congr. Molec. Spectroscopy; Butterworths: London, 1965, p 371.

(183) DeVoe, H. J. Chem. Phys. 1964 41, 393.

(184) Forster, Th. In Modern Quantum Chemistry; Sinanoglu, O. Ed.; Part III: Action of Light and Organic Crystals; Academic: New York, 1965, p 93.

(185) Frank, J.; Teller, E. J. Chem. Phys. 1938, 6, 861.

(186) Davydov, A. Theory of Molecular Excitons; trans. Kasha, M., Oppenheimer, M. McGraw-Hill: New York, 1962.

(187) McClure, D. Electronic Spectra of Molecules and Ions in Crystals; Academic: New York, 1959.

(188) Jelley, E. E. Nature 1936, 138, 1009; 1937,139, 631.

(189) Scheibe, G. Angew Chem., 1936, 49, 563.

(190) Scheibe, G.; Mareis, A.; Schiffmann, R. Z. Phys. Chem. B. 1941, 49, 324.

(191) Padday, J. F. Chem. Biol. Intercell. Matrix, Advan. Study Inst. 1970, 2, 1007; J. Phys. Chem. 1968, 72, 1259.

(192) Herz, A. H. Photogr. Sci. Eng. 1974, 18, 323.

(193) Dickinson, H. O. J. Photogr. Sci. 1954, 2, 50.

(194) Clementi, E.; Kasha, M. J. Chem. Phys. 1957, 26, 956.

(195) Emerson, E. S.; Conlin, M. A.; Rosenoff, A. E.; Norland, K. S.; Rodriguez, H.; Chin, D.; Bird, G. R. J. Phys. Chem., 1967, 71, 2397.

(196) Daltrozzo, E.; Scheibe, G.; Gschwind, K.; Haimerl, F. Photrogr. Sci. Eng., 1974 18, 441.

(197) West, W.; Pearce, S. J. Phys. Chem., 1965, 69, 1894.

(198) Brooker, L. G. S.; White, F. L.; Heseltine, D. W.; Keyes, G. H.; Dent, Jr. S. G.; Van Lare, E. J. J. Photogr. Sci. 1953, 1, 173.

(199) Steiger, R.; Kitzing, R.; Junod, P. J. Photogr. Sci. 1973, 21, 107.

(200) O'Brien, D. F. Photogr. Sci. Eng. 1974, 18, 16.

(201) Smith, D. L. Photogr. Sci. Eng. 1974, 18, 309.

(202) Rosenoff, A. E.; Walworth, V. K.; Bird, G. R. Photogr. Sci. Eng. 1970, 14, 328.

(203) Reich, C. Photogr. Sci. Eng. 1974, 18, 335.

(204) Yu, Z. X.; Lu, P. Y.; Alfano, R. R. Chem. Phys. 1983, 79, 289.

(205) Cooper, W. Photogr. Sci. Eng. 1973, 17, 217.

(206) Hada, H; Yonezawa, Y.; Inaba, H. Chem. Lett. 1980, 467.

(207) Natoli, L. M.; Ryan, M. A.; Spitler, M. T. J. Phys. Chem. 1985, 89, 1448.

(208) Kavassalis, C.; Spitler, M. T. J. Phys. Chem. 1983, 87, 3166.

(209) Broich, B.; Heiland, G. Surface Science, 1980, 92, 247.

(210) Kudo, K.; Moruzumi, T. Jap. J. Appl. Phys. 1980, 19 (11), 1683.

(211) Spitler, M. T. J. Chem. Ed. 1983, 60, (4), 330.

(212) Sonntag, L. P.; Spitler, M. T. J. Phys. Chem. 1985, 89, 1453.

(213) Cabannes, J.; Rocard, Y. J. Phys. Radium, 1929, 10, 52.

(214) Van Vleck, J. H. Proc. Natl. Acad. Sci. U.S. 1929, 15, 754.

(215) Placzek, G. "Rayleigh-Streuung und Raman-Effekt", In Handbuch der Radiologie; Marx, E., Ed.; Akad. Verlagsges: Leipzig, 1934; Vol. VI, Part 2, Ch. 3.

(216) Shorygin, P. P. "Combination Scattering of Light Near and Far From Rasonance"; In Uspekhl. fiz. Nauk, 1973, 109, 293-332.

(217) Behringer, J.; Brandmuller, J. Z. Elektrochem. 1956, 60, 643.

(218) Behringer, J. Z. Elektrochem. 1958, 62, 906.

(219) Eyring, H.; Walter, J.; Kimball, G. E. Quantum Chemistry; Wiley: New York 1944.

(220) Brandmuller, J.; Moser, H. Einfuhrung in die Raman Specktroskopie; Steinkopf Verlag: Darmstadt, 1962.

(221) Tang, J.; Albrecht, A. C. In Advances in Infrared and Raman Spectroscopy, Theory and Practice; Szymanski, H. A., Ed.; Plenum: New York, 1970; Vol. 2.

(222) Albrecht, A. C. J. Chem. Phys. 1960, 33, 156.

(223) Albrecht, A. C. J. Chem. Phys. 1961, 34, 1476.

(224) Bergman, G.; Heritage, J. P.; Pinczuk, A.; Worlock, J. M.; McFee, J. H. Chem. Phys. Lett. 1979, 68, 412.

(225) Rowe, J. E.; Shank, C. V.; Zwemer, D. A.; Murray, C. A. Phys. Rev. Lett. 1980, 44, 1770.

(226) Murray, C. A.; Alara, D. L.; Rhinewine, M. Phys. Rev. Lett. 1981, 46, 57.

(227) Weitz, A. A.; Gramila, T. J.; Genack, A. Z.; Gersten, J. I. Phys. Rev. Lett. 1980, 45, 355.

(228) DiLella, D. P.; Moskovits, M. J. Phys. Chem. 1981, 85, 2042.

(229) Abe, H.; Manzel, K.; Schulze, W.; Moskovits, M.; DiLella, D.P. J. Chem. Phys. 1981, 74, 792.

(230) Krasser, W.; Renouprez, A. J. Solid State Commun. 1982, 41, 231.

(231) Adrian, F. J. Chem. Phys. Lett. 1981, 78, 45.

(232) Kirtley, J. R.; Jha, S. S.; Tsang, J. C. Solid State Commun. 1980, 35, 509.

(233) McCall, L.; Platzmann, P. M. Phys. Rev. B 1980, 22, 1980, 1660.

(234) Persson, B. N. J. Chem. Phys. Lett., 1981, 82, 561.

(235) Campbell, J. R.; Creighton, J. A. J. Electroanal. Chem. 1983, 143, 353.

(236) Moskovits, M. J. Chem. Phys. 1978, 69, 4159.

(237) Siiman, O., Smith, R.; Blatchford, C.; Kerker, M. Langmuir, 1985, 1, 90.

(238) Efrima, S. J. Phys. Chem. 1985, 89, 2843.

(239) Yamada, H.; Amamiya, T.; Tsubomura, H. Chem. Phys. Lett. 1978, 56, 591.

(240) Mulliken, R. S. J. Am. Chem. Soc. 1952, 74, 811.

(241) Craig, D. P.; Thirunamachandron, R. Molecular Quantum Electrodynamics; Academic: New York, 1984.

(242) Fischer, G. Vibronic Coupling: The Interaction between the Electronic and Nuclear Motions; Academic: New York, 1984.

(243) Kasha, M. Rev. Mod. Phys. 1959, 31, 162.

(244) Kasha, M. Radiation Res. 1963, 20, 55.

(245) Akins, D. L.; Lombardi, J. R. Chem. Phys. Lett. 1987, 136, 495.

(246) Mullins, D. R.; Campion, A. J. Phys. Chem. 1984, 88, 8.

(247) Duonghong, D.; Ramsden, J.; Gratzel, M. J. Am. Chem. Soc. 1982, 104, 2977.

(248) McRae, E. G.; Kasha, M. In Physical Processes in Radiation Biology; Academic: New York, 1963; p 23.

(249) Hamaguchi, H. In Advances in Infrared and Raman Spectroscopy; Clark, R. J. H., Hester, R. E., Eds.; Wiley: New York, 1985; Vol. 12.

(250) Albrecht, A. C.; Hutley, M. C. J. Chem. Phys. 1971, 55, 4438.

(251) Dudik, J. M.; Johnson, C. R.; Asher, S. A. J. Chem. Phys. 1985, 82,

1732.

(252) Billman, J.; Kavacs, G.; Otto, A. Surface Sci. 1980, 92, 153.

(253) Weaver, M. J.; Barz, F.; Gordon II, J. G., ; Philpott, M. R. Surface Sci. 1983, 125, 409.

(254) Freeman, D. E.; Klemperer, W. J. Chem. Phys. 1966, 45, 52.

(255) Freeman, D. E.; Lombardi, J. R.; Klemperer, W. J. Chem. Phys. 1966, 45, 58.

(256) Lombardi, J. R. J. Chem. Phys. 1968, 48, 348; 1969, 50, 3780.

(257) Liptay, W. In Modern Quantum Chemistry III; Sinanoglu, O., Ed.; Academic: New York, 1965.

(258) Hochstrasser, R. M. ; Johnson, L. W.; Trommsdorff, H. P. Chem. Phys. Lett. 1973, 21, 251.

(259) Buckingham, A. D. In MTP International Review of Science, Physical Chemistry Series 1, Vol. 3, Spectroscopy; Ramsay, D. A. Buckingham, A. D., Eds.; Butterworths: London, 1972.

(260) Liptay, W. In Excited States; Lin, E. C., Ed.; Academic: New York, 1974.

(261) Hochstrasser, R. M. Acct. Chem. Res. 1973, 6, 263.

(262) Dicker, A. I. M.; Johnson, L. W.; Noort M.; van der Waals, J. H. Chem. Phys. Lett. 1983, 94, 14.

(263) Townes, C. H.; Schawlow, A. L. Microwave Spectroscopy; McGraw-Hill: New York, 1955.

(264) Li, X.; Akpabli, C. K.; Akins, D. L. Manuscript in preparation, 1988.

(265) Brown, C. W.; Lynch, P. F. J. Food Sci.1976, 41, 1231.

(266) Higuchi, S.; Tanaka, J.; Tanaka, S. J. Spect. Soc. Japan 1978, 27, 353.